

# RECLAMATION

*Managing Water in the West*

Technical Report: SRH-2015-5289-01

## Conceptual water budget analysis for screening agricultural and wetland water management projects



U.S. Department of the Interior  
Bureau of Reclamation  
Technical Service Center  
Denver, Colorado

March 2016

## **Mission Statements**

The mission of the U.S. Department of the Interior is to protect America's natural resources and heritage, honors our cultures and tribal communities, and supplies the energy to power our future.

The mission of the Bureau of Reclamation is to manage, develop, and protect water and related resources in an environmentally and economically sound manner in the interest of the American public.

**Technical Report No. SRH-2015-5289**

# **Conceptual water budget analysis for screening agricultural and wetland water management projects**

**Prepared by: (in alphabetic order):**

**Nigel Quinn, Ph.D., P.E., D.WRE, F.ASCE  
Mid-Pacific Region, Bureau of Reclamation, Sacramento, CA and  
HydroEcological Engineering Advanced Decision Support  
Berkeley National Laboratory, Berkeley, CA**

**Stanley Parrott, P.G., Geologist  
Mid-Pacific Region, Bureau of Reclamation, Sacramento CA**

**Megan Farley, Intern  
HydroEcological Engineering Advanced Decision Support  
Berkeley National Laboratory, Berkeley, CA**



**U.S. Department of the Interior  
Bureau of Reclamation  
Technical Service Center  
Denver, Colorado**

## **Mission Statement**

The U.S. Department of the Interior protects America's natural resources and heritage, honors our cultures and tribal communities, and supplies the energy to power our future.

The mission of the Bureau of Reclamation is to manage, develop, and protect water and related resources in an environmentally and economically sound manner in the interest of the American public.

REPORT DOCUMENTATION PAGE			Form Approved OMB No. 0704-0188		
T1. REPORT DATE MONTH YEAR	T2. REPORT TYPE Research		T3. DATES COVERED 7/1/15 – 3/31/16		
T4. TITLE AND SUBTITLE: Conceptual water budget analysis for screening agricultural and wetland water management projects			5a. CONTRACT NUMBER		
			5b. GRANT NUMBER		
			5c. PROGRAM ELEMENT NUMBER (S&T)		
6. AUTHOR(S) Nigel W.T. Quinn, Stanley (Chip) Parrott and Megan Farley			5d. PROJECT NUMBER SRH-2015-5289-01		
			5e. TASK NUMBER		
			5f. WORK UNIT NUMBER		
7. PERFORMING ORGANIZATION NAME(S) AND ADDRESS(ES) US Bureau of Reclamation, 2800 Cottage Way, Sacramento, CA 95825			8. PERFORMING ORGANIZATION REPORT NUMBER		
9. SPONSORING / MONITORING AGENCY NAME(S) AND ADDRESS(ES) Research and Development Office U.S. Department of the Interior, Bureau of Reclamation, PO Box 25007, Denver CO 80225-0007			10. SPONSOR/MONITOR'S ACRONYM(S) R&D: Research and Development Office BOR/USBR: Bureau of Reclamation DOI: Department of the Interior		
			11. SPONSOR/MONITOR'S REPORT NUMBER(S)		
12. DISTRIBUTION / AVAILABILITY STATEMENT Final report can be downloaded from Reclamation's website: <a href="https://www.usbr.gov/research/">https://www.usbr.gov/research/</a>					
13. SUPPLEMENTARY NOTES					
14. ABSTRACT (Maximum 200 words) This project examines the role of the conceptual model for analysis of complex water management decision making. The report is divided into 4 sections. The first section provides a detailed background of the hydrogeology of the region which is a necessary first step for conceptual model development. The second section describes the various types of models that can be applied to the problem – building any one of these model types is preceded by a conceptual model. The third section builds a conceptual model using the visualization capabilities of the Aquaveo GMS software. It walks the reader through the steps suggested by Aquaveo in the development of a conceptual groundwater flow model. The last section compares the results of two models that have different underlying conceptual models. The results highlight the importance of spending time to develop a realistic initial conceptual model.					
15. SUBJECT TERMS Conceptual model, hydrology, decision support					
16. SECURITY CLASSIFICATION OF: Open			17. LIMITATION OF ABSTRACT  U	18. NUMBER OF PAGES 107	19a. NAME OF RESPONSIBLE PERSON Nigel Quinn
a. REPORT U	b. ABSTRACT U	c. THIS PAGE U			19b. TELEPHONE NUMBER 916-978-5079



# PEER REVIEW DOCUMENTATION

## Project and Document Information

**Project Name :** Conceptual water budget analysis for screening agricultural and wetland water management projects

**WOID:** SRH-2015-5289

**Document Author(s):** Nigel Quinn, Stanley (Chip) Parrott, Megan Farley

**Document date:** 03/30/16

**Peer Reviewer:** Stanley (Chip) Parrott

## 1. Review Certification

**Peer Reviewer:** I have reviewed the assigned items/sections(s) noted for the above document and believe them to be in accordance with the project requirements, standards of the profession and Reclamation policy.

Reviewer Stanley E. Parrott Date reviewed 3-31-16  
(Signature)

# Acknowledgements

## Table of Contents

	Page
<b>1.0 Executive Summary</b> .....	1
<b>1.1 Introduction</b> .....	1
1.2 Context and problem .....	2
1.2.1 San Joaquin Basin hydrology.....	2
1.2.2 Regional Geology .....	2
1.2.3 Regional Hydrogeology .....	7
1.3 Irrigation and the Shallow Groundwater System.....	11
1.4 Regional Hydrogeochemistry .....	12
1.5 Irrigated Agriculture .....	12
<b>2.0 Modeling of Irrigated Land Use Systems</b> .....	20
2.1 Conceptual Models and Water Budgets.....	20
2.2 Mathematical Simulation models .....	22
2.3 Process-Oriented Models.....	23
2.4 Regional Simulation Models .....	23
2.5 Farm-Scale Models.....	24
2.6 Chemical Transport Models.....	25
2.7 Decision Support Models.....	27
2.8 Regional Planning Models .....	28
2.9 Expert Systems Models.....	29
<b>3.0 Developing a Regional Planning Conceptual Model Using GMS Software</b> ...	30
3.1 Problem Description .....	30
3.1.1 Basin Description.....	30
3.1.2 Regional Geology .....	31
3.1.3 Local Hydrogeology .....	34
3.1.4 Cone Penetrometer Logging .....	37
3.2 Conceptual Model Developemt .....	39
3.2.0 Getting Started .....	39
3.2.1 Importing the background image.....	39
3.2.2 Reading the image.....	40
3.2.3 Saving the project .....	40
3.2.4 Defining the units.....	40
3.2.5 Defining the boundary .....	40
3.2.6 Building the local source/sink coverage .....	42
3.2.7 Defining the boundary head arcs .....	43
3.2.8 Defining model layers.....	45
3.2.9 Locating the grid frame.....	45
3.2.10 Creating the grid.....	47
3.2.11 Creating the wells .....	48

3.2.12	Building the polygons .....	49
3.2.13	Defining the hydraulic conductivity .....	50
3.2.14	Initializing the MODFLOW data.....	50
3.2.15	Interpolating layer elevations .....	50
3.2.16	Converting the conceptual model .....	51
3.2.17	Checking the simulation .....	51
3.2.18	Saving the project .....	51
3.2.19	Running MODFLOW .....	51
3.2.20	Viewing the head contours .....	52
3.2.21	Viewing the water table in side view.....	54
3.3	Summary.....	55
4.0	Comparison of conceptual models of wetland hydrology using WARMF-SJR and CVHM .....	57
4.1	Introduction .....	57
4.2	Hypothesis .....	58
4.3	Model Theory .....	59
4.3.1	Central Valley Hydrologic Model (II) .....	59
4.3.2	Watershed Analysis Risk Management Framework.....	61
4.4	Procedure.....	63
4.5	Results .....	65
4.5.1	Central Valley Hydrologic Model (II) .....	65
4.5.2	Watershed Analysis Risk Management Framework.....	66
4.6	Discussion .....	68
4.7	Conclusions .....	69
5.0	References .....	70
5.1	Webography .....	74
<b>6.0</b>	<b>Annexes .....</b>	<b>76</b>
6.1	List of abbreviations and acronyms .....	76
 <b>APPENDICES</b>		
	Appendix A: Tables A1-A11 .....	78
	Appendix B : Figure B1-B23 .....	87

# Index of Figures

	Page
<b>Figure 1.</b> The San Joaquin Valley (from San Joaquin Valley Salinity Drainage Program 1990), with the focus subareas addressed in the 1990 drainage plan. ....	3
<b>Figure 2.</b> Surface drainage of the eastside San Joaquin Valley (DWR 2015) .....	5
<b>Figure 3.</b> Surface drainage of the west-side of the San Joaquin Valley.....	6
<b>Figure 4.</b> Alluvial fans of the West Side of the San Joaquin Valley.....	6
<b>Figure 5:</b> Different scale groundwater flow systems within a catchment.....	7
<b>Figure 6.</b> Idealized east - west geological cross sections across the western San Joaquin Valley .....	9
<b>Figure 7.</b> Water Table contours and extent of the artesian zone in the western San Joaquin Valley, 1908 .....	10
<b>Figure 8.</b> Land subsidence induced by groundwater pumpage in the western San Joaquin Valley, 1926-1972. ....	10
<b>Figure 9:</b> Water Table contours in October 1984 showing a groundwater divide caused by groundwater pumpage (From Belitz, 1990). ....	11
<b>Figure 10.</b> Generalized hydrogeologic cross section across the western San Joaquin Valley in 1984, showing vertical flow patterns and groundwater divide ....	13
<b>Figure 11.</b> General service areas of the San Joaquin Valley. ....	14
<b>Figure 12.</b> Nineteen large reservoirs of the San Joaquin River Basin:.....	15
<b>Figure 13.</b> Total water use by region in California. Agriculture is the dominant water use in the San Joaquin River Basin .....	16
<b>Figure 14.</b> Groundwater – surface water conceptual model diagram .....	22
<b>Figure 15.</b> Merced Groundwater Basin showing location of Stevinson and Merquin Water Districts located north-west of the 4-S Ranch ...	32
<b>Figure 16.</b> Wells and local conveyances affecting 4-S Ranch hydrology .....	33
<b>Figure 17.</b> Generalized cross-section of the San Joaquin River Basin in proximity to the 4-S Ranch. ....	34
<b>Figure 18</b> Generalized structural profile of sedimentary deposits and groundwater aquifers in the vicinity of the 4-S Ranch. ....	35
<b>Figure 19.</b> Soils map of the study area showing the 4-S Ranch and adjacent water districts .....	36
<b>Figure 20.</b> CPT log for production well no. 7 on the 4-S Ranch .....	38
<b>Figure 21.</b> Map of project area on east-side of the San Joaquin Basin near Stevinson ..	39
<b>Figure 22.</b> Creating arcs for boundaries and rivers, streams and bypasses .....	41
<b>Figure 23.</b> (a) Addition of new boundary condition arcs for the East-side canal and (b) the boundary of the 4-S Ranch property. ....	42
<b>Figure 24.</b> Defining the boundary properties along model arcs and at nodes converted from vertices. ....	44
<b>Figure 25.</b> Defining the grid frame and choosing a better model alignment.....	46

<b>Figure 26.</b>	Experimenting with the model mesh configuration to cover the project area. The grid frame was modified to allow surface hydrologic features to be extended to the grid and model boundary.	46
<b>Figure 27.</b>	Final model mesh showing the revised model boundary and new alignment.	48
<b>Figure 28.</b>	Two polygons were defined for the 4-S Ranch project area and the region outside from the 4-S Ranch boundary to the model boundary.	49
<b>Figure 29.</b>	Plan view of 4-S Ranch project area showing higher water tables away from the major conveyances which act as open drains	52
<b>Figure 30.</b>	Head contour map output of the steady-state conceptual model showing the influence of the pumped wells mostly along the alignment of the East-side canal	53
<b>Figure 31.</b>	Average annual pumping was increased from 30 gal/min to 90 gal/min at the wells in 4-S Ranch that are mostly along the alignment of the East-side Canal.	54
<b>Figure 32.</b>	Visualization of the project area using GMS 3-D projection tools.	55

**Index of Tables** .....

..... Page

Table 1. Irrigated Crop acreage ..... 17

Table 2. San Joaquin Basin agricultural water demand (acre-feet) ..... 18

Table 3. Salinity and drainage problems by major irrigated area .....19

# 1.0 Executive Summary

This report describes progress on a 1-year research project entitled, “Conceptual water budget analysis for screening agricultural and wetland water supply projects”. This title is slightly modified from the original title to reflect an emphasis on examining the conceptual design of existing models rather than just the development of new conceptual models. The project received additional support from the US Department of Energy SULI Program which sponsors undergraduate students interested in working on short term research projects at a National Laboratory.

## 1.1 Introduction

Fundamental to the analysis of water supply planning throughout Reclamation's service area is the development of a water budgets. Water budgets are merely a structured way of looking at all of the inflows and outflows to a three dimensional representation of the area (volume) of interest. The skill required to develop these budgets first involves determining the areal extent and depth of the 3-dimensional polygon that represents the project area in such a manner that it facilitates the collection of data. The establishment of reasonable boundary conditions and the estimation of major hydrologic inputs such as recharge, seepage and evapotranspiration follows. Where data aren't readily available past experience can help in the selection of numbers that are reasonable. The end result is a steady-state conceptual model which can be used to provide a screening level analysis of the potential impacts of new water projects and whether the new project is hydrologically sustainable. Steady-state conceptual models do not demand significant data and hence are relatively easy and inexpensive to develop. The concept of water balance is fundamental to the development of these models.

The same water balance methodologies and visualization frameworks can be applied to existing steady-state and transient models. These techniques can also be used to compare different model algorithms or formulations to describe watershed hydrology. The applications considered in this project apply specifically to irrigation or managed wetland hydrology. Several software products are available that can facilitate the development and visualization of conceptual surface and groundwater models. The USGS has developed MODFLOW postprocessing tools such as Zonebudget for groundwater conceptual model and water balance analysis and more recently the Farm management Process budget table which allows conceptual models of the crop root zone to be developed and compared. The California Department of Water Resources has developed their own version of MODFLOW Zonebudget called Z-budget. The groundwater components are similar between the two postprocessing tools as are the capabilities to define subareas for detailed water budget analysis. Other commercial products exist products such as Aquaveo's GMS software and Environmental Simulations Inc.'s Groundwater VISTAS software that allow MODFLOW models to be read into the model framework and which provide much greater options for output visualization and further data post-processing. In both cases the modeling frameworks allow models to be developed from scratch and can assist the model analyst in formulation of a preliminary steady-state conceptual model using available data. Both offer the visualization capability to facilitate conceptual model development. What is lacking in all instances is a

standardized methodology for developing reasonable assumptions and parameter estimates needed to construct these conceptual models. Good conceptual models are predicated upon a thorough understanding of the system and the surface and groundwater resources available. Hence the first chapter of this report develops and describes the hydrological context for conceptual modeling to begin. A literature review is the first step to developing this conceptual background and understanding.

## **1.2 Context and Problem**

### **1.2.1 San Joaquin Basin Hydrology**

The problems of irrigated agriculture in arid, drainage impaired basins around the world, share many characteristics. The west side of the San Joaquin Valley provides insights into how an age-old problem is addressed in a context of changing values and priorities, an increasingly complex regulatory environment, and the complication of a toxicity issue. The lessons learned in addressing this issues have applicability to similar situations worldwide. The models developed to allow growers and managers to better optimize their irrigation and drainage systems may be adapted and engineered for systems with like characteristics.

### **1.2.2 Regional Geology**

The San Joaquin River Basin (Figure 1) extends roughly NNW-SSE, descending from the foot of the Tehachapi Mountains, northwards to its confluence of the Sacramento River in the Sacramento-San Joaquin Delta. The Valley is about 250 miles long and about 50 miles wide, bounded on the east by the Sierra Nevada Mountains and on the west by the California Coast Ranges.

The major tributaries to the San Joaquin River that drain the east side of the San Joaquin Basin are the Fresno, Merced, Tuolumne and Stanislaus Rivers (Figure 1). The headwaters of these rivers contain water of high quality that are important in providing dilution to the San Joaquin River that receives drainage of poor quality from west side sources. Many surface water impoundments have been created by flood control and water supply dams on the tributaries of the San Joaquin River, including Millerton Lake (on the San Joaquin River), Hensley Lake (on the Fresno River), Lake McClure (on the Merced River), New Don Pedro Lake (on the Tuolumne River ) and the New Melones Lake (on the Stanislaus River). On the west side of the San Joaquin Basin, the major facility is the man-made San Luis Reservoir which is hydraulically connected to the California Aqueduct and Delta Mendota Canal and which provides off-stream storage for both the Central Valley Project and State Water Project. Prior to the construction of the CVP and the Delta Mendota Canal, San Joaquin River water was used to irrigate land on the west side of the San Joaquin Valley. The CVP provided for water released from Friant Dam to be diverted to the Tulare Basin through the Friant-Kern Canal and water from the Delta Mendota Canal was made available to these "exchange contractors" for irrigating ands formerly served by the San Joaquin River. The Mendota Pool is a CVP storage reservoir, located at the terminus of

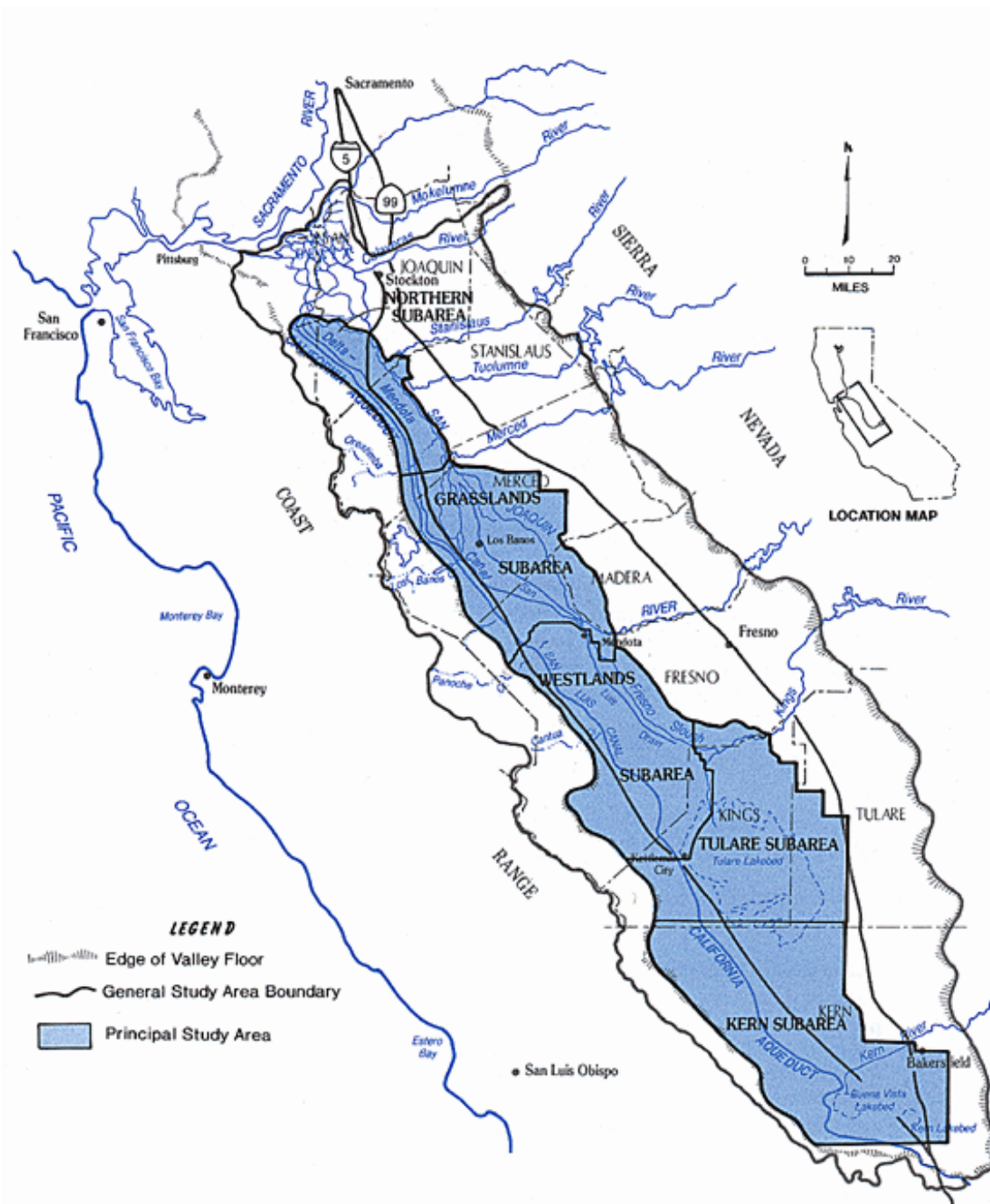


**Figure 1.** The San Joaquin Valley (from San Joaquin Valley Salinity Drainage Program 1990), with the focus subareas addressed in the 1990 drainage plan. The Northern and Grasslands subareas on the west-side discharge saline drainage to the San Joaquin River.

the Delta Mendota Canal, which provides water to a number of supply canals which take the water north to irrigation turnouts located along their length, irrigate land on the west side of the San

Joaquin Valley. The CVP provided for water released from Friant Dam to be diverted to the Tulare Basin through the Friant-Kern Canal and water from the Delta Mendota Canal was made available to these "exchange contractors" for irrigating and formerly served by the San Joaquin River. The Mendota Pool is a CVP storage reservoir, located at the terminus of the Delta Mendota Canal, which provides water to a number of supply canals which take the water north to irrigation turnouts located along their length.

Belitz (1988, 1990) provided an account of the state of the groundwater system as it existed at the turn of the century and how its character has changed to the present time due to intensive irrigated agriculture. Although his account addresses the central part of the west side, largely falling within the drainage areas of the Panoche Creek and Little Panoche Creek, the ideas presented can be applied reasonably to the entire west side of the Valley. Because the regional groundwater system is driven by gravity, physiography and geomorphology play a decisive role in determining its character. The west side is characterized by a fairly simple topographic pattern; an easterly sloping flank of the Coast Ranges extending for over 80 miles in the NNW-SSE direction (Figure 3). The distance from the boundary of the Valley deposits to the San Joaquin River is about 20 miles, but varies slightly. Over this distance, the elevation declines from about 600 ft msl (mean sea level) to about 160 feet msl. The upper slope (comprising alluvial fans), from 600 feet to about 300 feet, tends to be steeper than the lower slopes. Four intermittent streams (from south to north, Los Gatos Creek, Cantua Creek, Panoche Creek, and Little Panoche Creek) have well-developed alluvial fans (Figure 4).

Sediments of recent alluvium deposited by the action of these four streams cover much of the west side, from the flanks of the Coast Ranges to the vicinity of the river. On the upper slopes and in the prominent alluvial fans, the sediments tend to be coarse-grained, having been deposited by episodic, high-energy stream flows. In the inter-fan areas and in the lower slopes of the Valley, the sediments show a flood-plain depositional character and consist of fine-grained materials. Mass-wasting, mud flows and surge flows associated with the high energy sediment transport of ephemeral and intermittent streams appear to play a very important role in controlling the physical- as well as the chemical properties of the sediments.

Marine sediments, ranging in age from Jurassic to Miocene age are exposed along the ridge crest of the Coast Ranges (Presser et al., 1991). Two members of this sequence, the Moreno Formation (upper Cretaceous to Paleocene) and the Kreyenhagen Formation (Eocene to Oligocene) are exposed over a 20-mile stretch of the Moreno Ridge. Despite their limited extent, these formations play an important geochemical role because of their trace elements, including selenium, boron, and arsenic. Following the Miocene, during Pliocene and Pleistocene periods the marine conditions gave way to continental and lacustrine conditions. The Tulare formation of Pliocene to Pleistocene age underlies the alluvium over much of the west side.

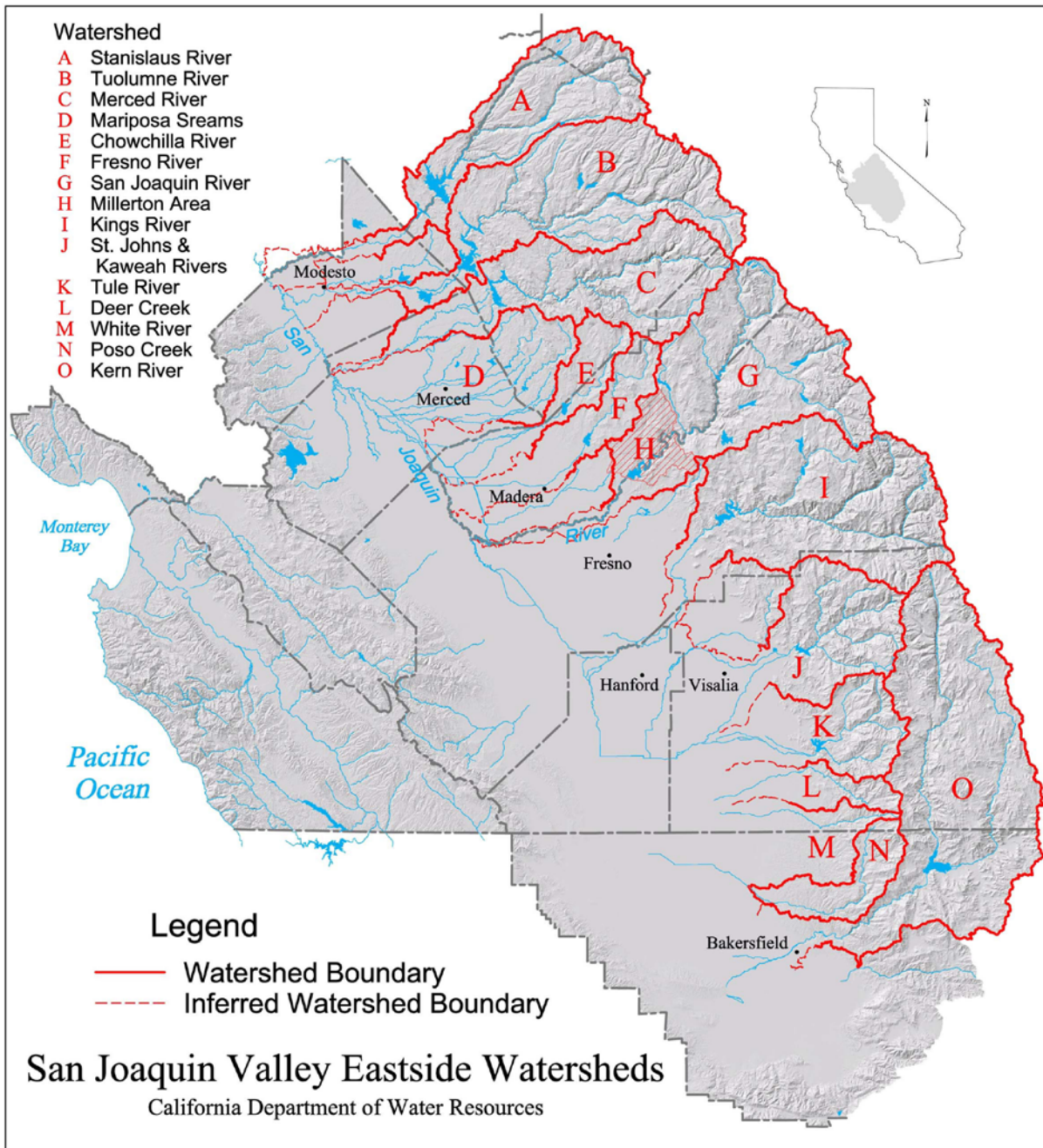


**Figure 2.** Surface drainage of the eastside San Joaquin Valley (DWR 2015)

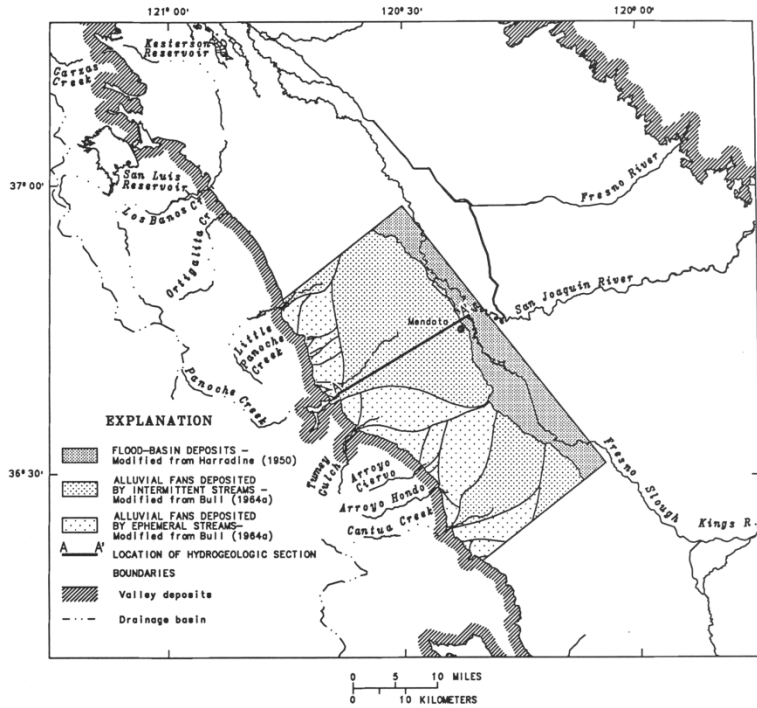


Figure 3. Surface drainage of the west-side of the San Joaquin Valley.

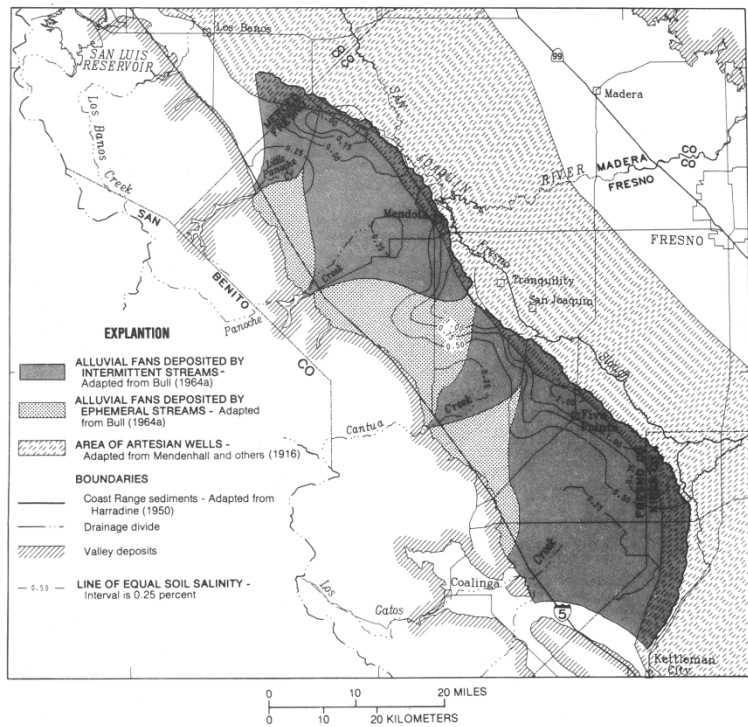
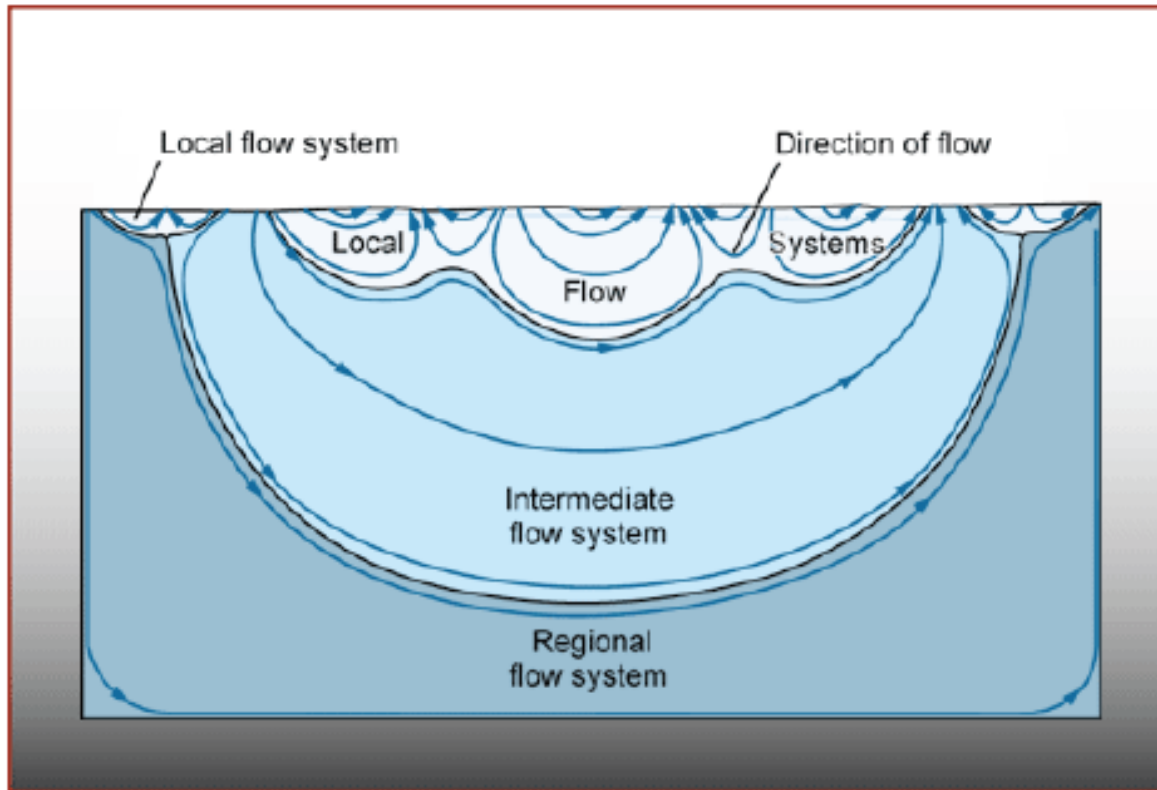


Figure 4. Alluvial fans of the West Side of the San Joaquin Valley.



**Figure 5:** Different scale groundwater flow systems within a catchment (Toth, 1963).

The Corcoran clay of the Tulare formation, approximately 100 feet thick, constitutes an extensive marker horizon beneath the west side. The alluvial sediments overlying the Corcoran clay decrease in thickness from a maximum of about 800 feet on the Valley margins to less than 100 feet in the vicinity of the San Joaquin River (Figure 6). In the valley trough, the coast range alluvium, characterized generally by fine-grained sediments, gives way to the alluvial Sierran sands derived from the Sierra Nevada Mountains. The coarser Sierran sands contain water with chemical characteristics distinct from the sediments of the Coast Ranges alluvium. The alluvial sediments overlying the Corcoran Clay are frequently referred to as the "semi-confined" zone.

### 1.2.3 Regional Hydrogeology

Consistent with the geology of the region, the Coast Ranges constitute the groundwater recharge area for the west side of the valley. At the turn of the century, before intense pumping commenced in the 1920s, the piezometric heads in the deep aquifers underlying the Valley floor reportedly resulted in free-flowing artesian wells along a long, narrow zone along the river (Figure 6). The physical disposition of the artesian zone, extending parallel to the trend of the Coast Ranges, is an indication that the regional groundwater system is driven by recharge from the Coast Ranges. Based on stable isotope data of water samples from wells located above and below the Corcoran clay, Dubrovsky et al. (1990) inferred that groundwater may also be leaking vertically through the Corcoran clay and recharging the deep aquifers, both due to pervasive flow through the formation

and due to the several hundred wells which are screened in horizons above and below the Clay.

The development of the west side of the San Joaquin Valley for irrigated agriculture and the advent of deep-well turbine pumps in the 1920s drastically changed the groundwater flow system. Groundwater became an important component of irrigation water and, responding to post-second-world-war boom in the economy, groundwater pumping increased by a factor of four, reaching a maximum of about a million acre-feet per year between 1950 and 1970. Most of this pumping was from the confined aquifer below the Corcoran Clay. Water tables dropped (Figure 7) and there was pervasive land subsidence on the west side (Figure 8) that increased cost of pumping called for a reduction in groundwater pumping and eventually led to the importation of surface water from the Delta and the construction of the CVP and SWP conveyance facilities.

Gronberg et al. (1990) produced a summary of the distribution of wells on the west side. Although nearly 6,000 wells are known to exist in the Valley, useable information is available only with respect to about 2,550. Nearly two-thirds of these wells are completed in the semi-confined zone overlying the Corcoran clay. Due to the general poor water quality within the shallow part of this zone (< 50ft from land surface), most of the wells in the shallow, upper portion are passive, observation wells. Production wells in the semi-confined zone are typically greater than 50 feet in depth. The Coast Range alluvium in the semi-confined zone generally contains fine-grained sediments. Because of the larger surface area of contact between water and solids in these sediments and longer residence times, these sediments tend to contain waters of poorer quality compared, for example, with waters of the Sierran Sands to the east of the San Joaquin River. Therefore, in the Valley trough and on the margins of the alluvial fans irrigation wells are screened in the Sierran Sand aquifer which contains coarser, cleaner sands and better quality water. Because of the reducing nature of these sands selenium fluxes are retarded and the mobile selenate form of selenium appears to be converted to reduced, less mobile species (selenite or elemental selenium). Hence selenium concentrations from pumped wells drawing from these sands tends to be low. Wells completed in the shallow semi-confined aquifer have screens that are typically a few meters in length.

Some 533 wells were screened in both the semi-confined zone and the confined zone allowing communication between confined and semi-confined aquifers. Although the volume of flow between the aquifers has yet to be quantified - some hydrogeologists believe that they may account for some of the variability in the groundwater flux across the Corcoran Clay over the west side of the San Joaquin Valley. Wells penetrating the confined zone below the Corcoran Clay are generally restricted to the upslope areas at the head of the alluvial fans beyond the extent of the Sierran sands. According to Gronberg et al. (1990), 410 wells tap the confined zone with open screen intervals in excess of 100 feet. Examination of water table data and potentiometric data for 1984 by Belitz (1988, 1990) showed the existence of a pronounced groundwater divide approximately midway between the Valley trough and the Coast Ranges. This divide shown in plan in Figure 9, and shown in cross-section in Figure 10, has most likely occurred due to overdraft of groundwater by pumping to the west and by leakage from the Aqueduct. Clearly the pre-development areal distribution of recharge and discharge areas of the west side has been significantly modified by the pumping, and has led to a very complex groundwater hydrology and

distribution of contaminants within the semi-confined aquifer.

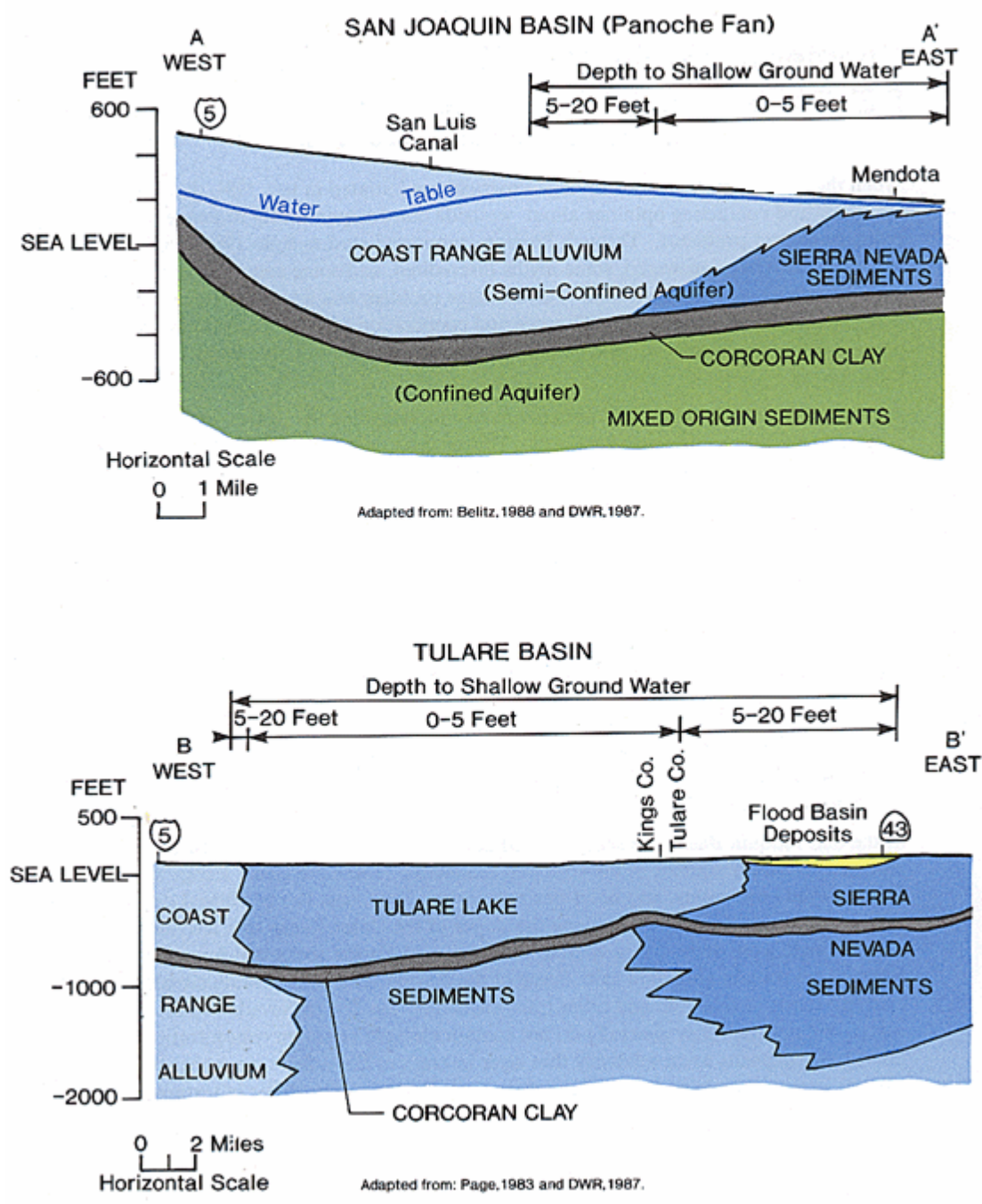


**Figure 6:** Idealized east - west geological cross sections across the western San Joaquin Valley (From Belitz, 1988 and DWR 1987).

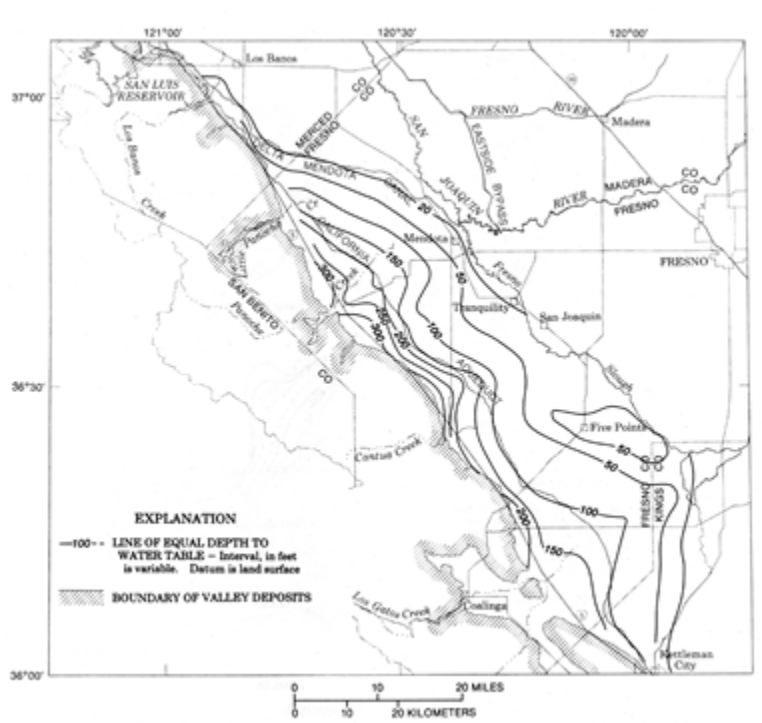


**Figure 7:** Water Table contours and extent of the artesian zone in the western San Joaquin Valley, 1908 (From Belitz, 1990).

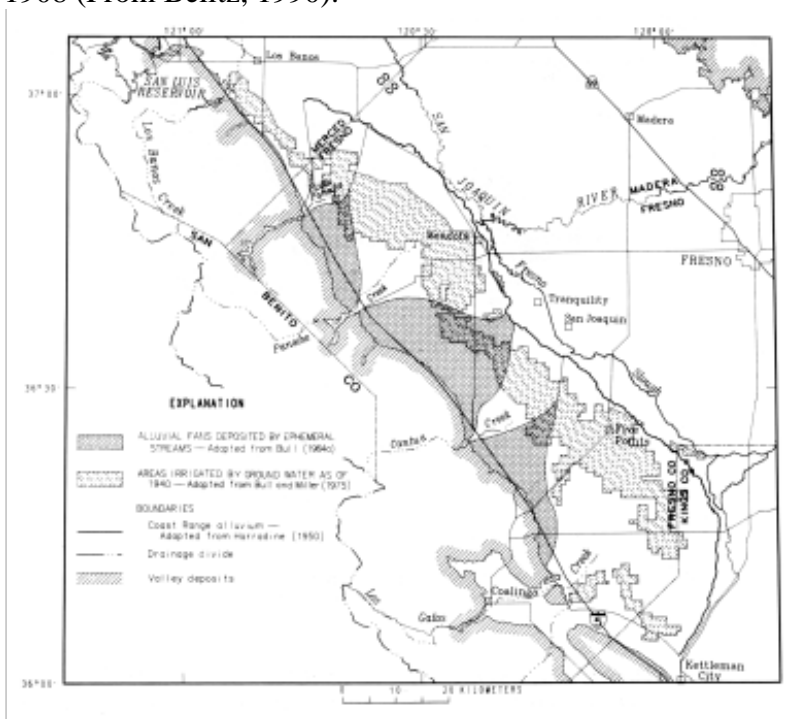


**Figure 8:** Land subsidence induced by groundwater pumpage in the western San Joaquin Valley, 1926-1972 (From Belitz, 1990).

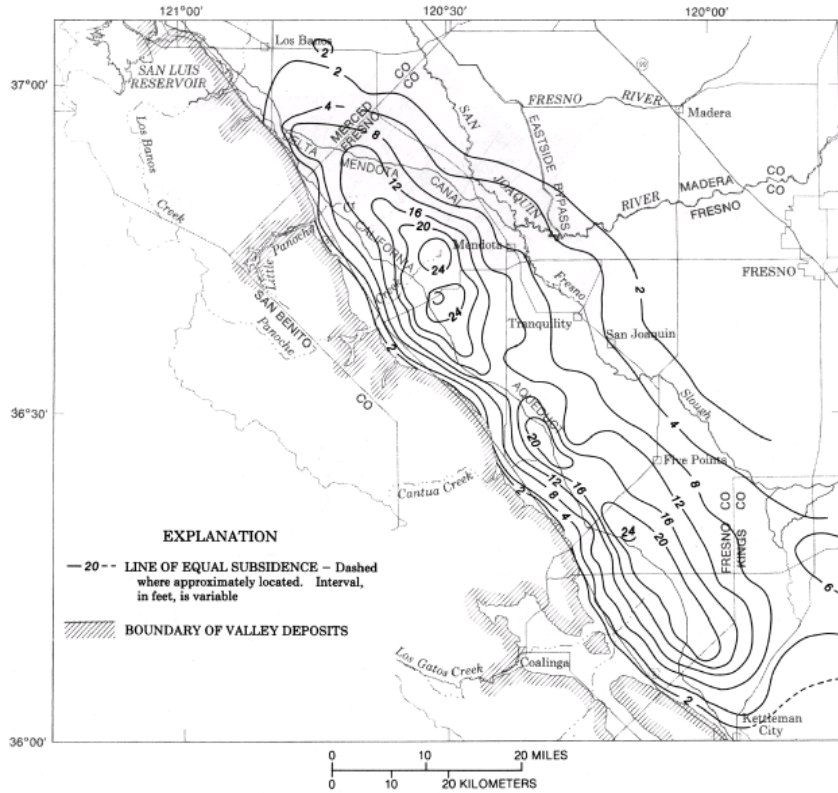


**Figure 9:** Water table contours in October 1984 showing a groundwater divide caused by groundwater pumpage (From Belitz, 1990).

### 1.3 Irrigation and the Shallow Groundwater System

Irrigated agriculture has been practiced on the west-side of the San Joaquin Valley for over a century and has interacted with and modified the pre-existing groundwater flow patterns, especially recharge-area and discharge-area relationships. Application of irrigation water causes water tables to rise in the shallow semiconfined aquifer, leading to an increase in the vertically downward movement of water. Because of the large areal extent of applied irrigation water on the west side, the resulting artificial recharge has significantly exceeded natural groundwater recharge by rainfall and stream flows. Williamson et. al. (1985) estimated that between 1961 and 1977 irrigation recharge was as much as 40 times that of the natural recharge.

Applied irrigation water directly affects the shallow groundwater system. In turn, the dynamics of water flow and water table fluctuations in the shallow aquifer are intimately related to local topographic variations. Very little attention has apparently been given by previous workers to understand such interactions on the basis of data from piezometer and tensiometer nests. Fio and Deverel (1991) studied, using nests of piezometers, the dynamic interactions between applied

irrigation water, two tile drains, the water table and the shallow aquifer at a site where drains had been in existence for 15 years. Their data, interpreted in conjunction with numerical simulations, suggest that the drains capture significant quantities of resident groundwater in the shallow semi-confined aquifer as well as deep percolation from the crop root zone immediately above the drain. Based on piezometer data down to a depth of 100 feet they inferred that the flow direction was upward at the site from about 50 feet below land surface and primarily downwards below 100 feet. That is, a horizontal groundwater divide seems to exist below 100 feet depth. It is not clear, however, whether the upward flow observed by them is a manifestation of the regional flow pattern. During periods of irrigation the gradient is reversed, causing the flow direction to change in the shallow zone, leading to downward migration of salts and soluble trace elements leached from the root zone. Grismer and Woodring (1987) investigated the importance of lateral flows to drains on the west side from the regional groundwater flow system and concluded that the problem has to be studied on the scale of a township (intermediate scale). They also found that the data required to support accurate simulation of the regional flow system, at this scale, were not available.

## **1.4 Regional Hydrogeochemistry**

The regional hydrogeochemistry of the San Joaquin Valley is governed by the regional groundwater flow system and by the character of the source rocks. According to Davis and Coplen (1989), the hydrogeochemistry of the west side can be understood in terms of two distinct geochemical units. The deep aquifers below the Corcoran Clay with thickness varying from 1000 ft to 2,500 ft contain very old waters (615,000 to 725,000 years before present). These sodium sulfate waters are thought to be mixtures of waters derived from the Sierra Nevada Mountains to the west as well as the Coast Ranges. Fairly well isolated by the poorly permeable Corcoran Clay, these waters are known to have a fairly uniform composition. The aquifers above the Corcoran Clay contain waters which are distinctly different in composition from that of the deeper aquifers. Much richer in mineral content, the waters of the shallow aquifers exhibit a great deal of spatial variability in chemical composition. As we shall see below, the waters of the shallow aquifers can be divided into Coast Range waters and Sierran waters. Groundwater in the Coast Ranges alluvium differs markedly from that in the Sierran sands. The former contains significant quantities of nitrate, boron and selenium while that in the latter is significantly higher in arsenic, molybdenum and manganese (Dubrovsky et al., 1990).

## **1.5 Irrigated Agriculture**

Historically, agriculture on the east side of the San Joaquin has been practiced on small holdings of less than 100 acres, whereas on the western side much of the land is owned by major corporations and holdings are much larger. The total irrigated area on the west side is about 2.3 million acres (Tanji, 1990), of which 0.89 million acres are affected by salinity and sodicity, 0.61 million acres by high water table and 0.93 million acres by poor groundwater quality. Cotton was the major crop grown (over 49% of the irrigated area) on the west side 20 years ago, with lesser areas planted with tomatoes and melons. Over the past 10 years there has been a dramatic increase

in the establishment of tree crops especially grapes, almonds and walnuts, even in some of the selenium impacted areas. Commodity prices and expected crop revenues have a significant impact on west side cropping practices; a trend is developing towards growing more fruits, nuts and vegetables in preference to cotton. Subsurface tile drains have been installed on nearly 135,000 acres of irrigated lands (Salinity and Drainage Task Force, 1992) to control seasonally high water tables and to dispose of salts flushed out from the root zone. A variety of irrigation methods are employed to manage irrigation, sustain soil fertility, and control crop pests: pre-planting irrigation, irrigation scheduling during the growing season, and crop rotations.

Administratively, the west side is divided into water (or irrigation) and drainage districts (Figure 11). Irrigation districts are typically those that deal with power as well as water resources. Westlands Water District is the largest water district on the west side and has no natural drainage outlet or an historic right to convey drainage water to the San Joaquin River. The San Luis Drain, with its terminus at Kesterson Reservoir, provided drainage relief to 5,300 acres of irrigated land within a 42,000 acre area in the north-east corner of Westlands Water District until 1986. Because of selenium (Se) toxicity, discharge of subsurface drain water from these 5,300 acres) of the Water District ceased in 1986.

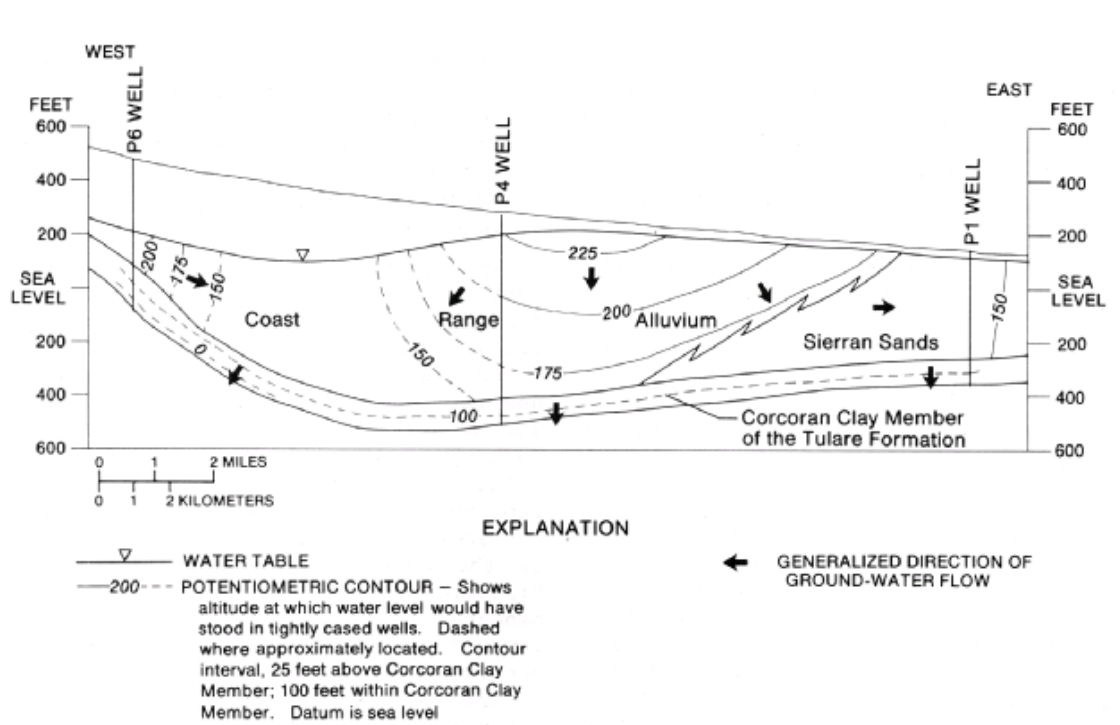


**Figure 10:** Generalized hydrogeologic cross section across the western San Joaquin Valley in 1984, showing vertical flow patterns and groundwater divide (From Belitz, 1990)

Although the on-farm tile drains in Westlands that discharged through subsurface collector drains into the San Luis Drain were plugged in early 1986, on-farm subsurface drains in water districts

north of Westlands in the Grasslands Basin continue to discharge salt- and selenium-contaminated drainage water to the San Joaquin River. These drains convey between 45,000 acre-feet and 75,000 acre-feet of combined surface and subsurface drainage water to the river annually, depending on annual precipitation and project water deliveries to agricultural contractors (San Joaquin Valley Drainage Program, 1990). These effluents contribute to the gradual increase of Se in the Bay. Therefore, it is necessary to evaluate the long-term changes in the Se content in the Bay and their relation to the disposal of drain waters into the San Joaquin River.

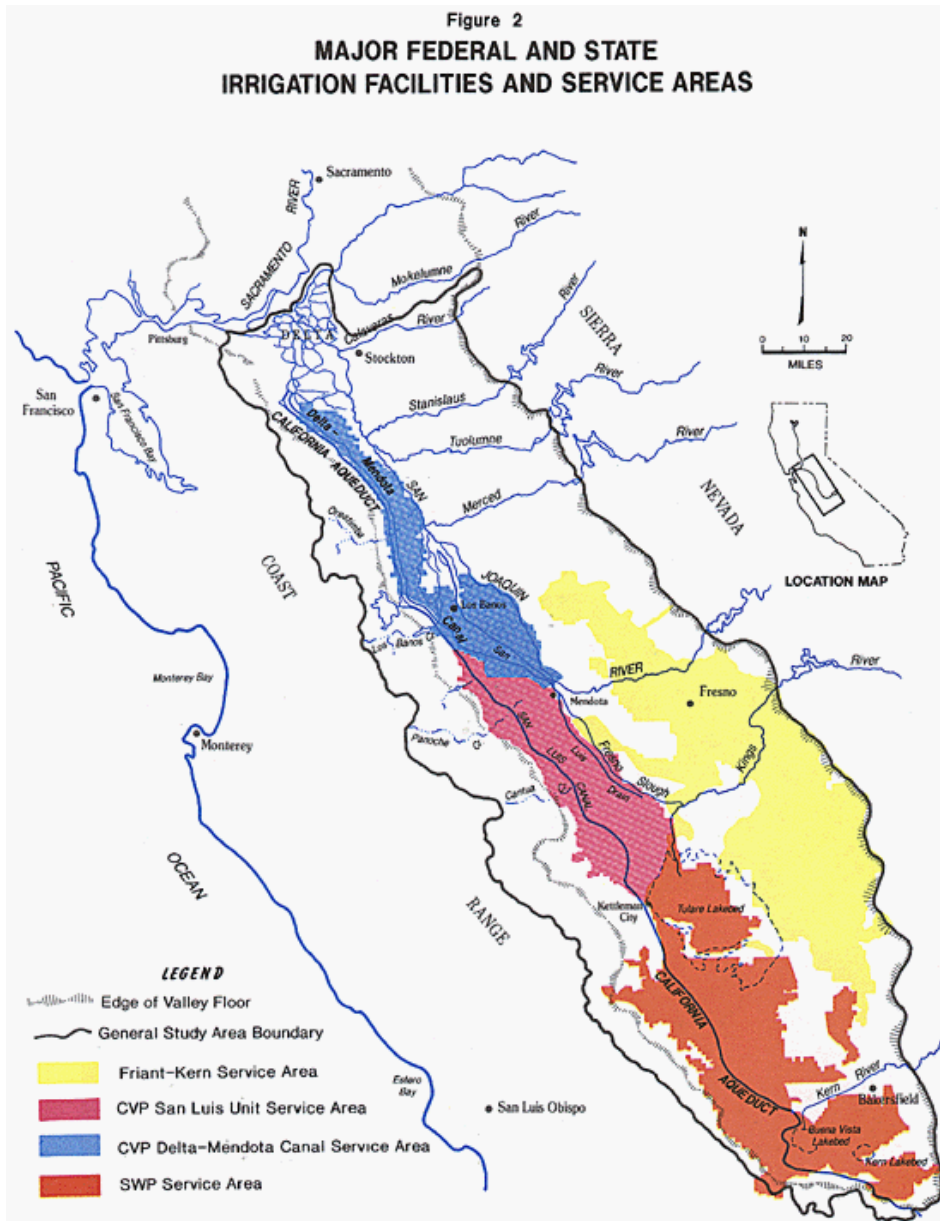
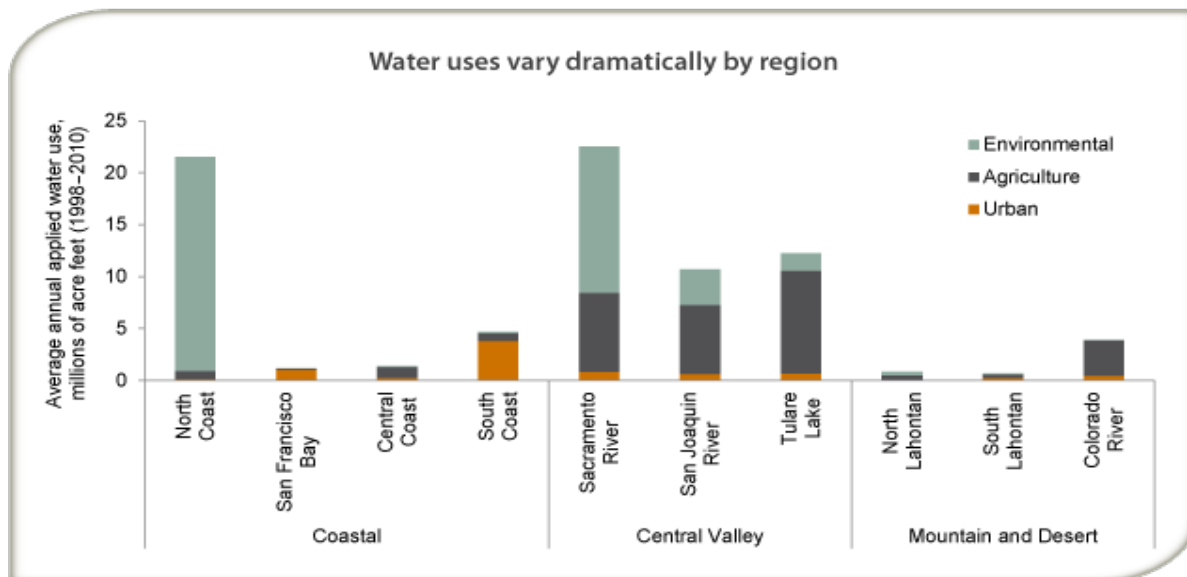


Figure 11. General service areas of the San Joaquin Valley. The Friant-Kern area receives CVP supplies from the San Joaquin River and the CVP Delta-Mendota Canal Service Area receives supplies from the Delta in-lieu of their historic supplies from the San Joaquin River.



Figure 12: Nineteen large reservoirs of the San Joaquin River Basin: (DWR 1987).

Irrigation development and the construction of east-side reservoirs combined with the importation of salts in irrigation diversions from the Delta have decreased the frequency and magnitude of flood flows which once performed a useful purpose by flushing salt from the San Joaquin Basin. Salts are accumulating in the soil or in the groundwater aquifers beneath agricultural land on the west side. The estimated net annual import over 1985-2005 has been modeled by Schoups et al (2005), who show a steady cumulative increase in net salt in San Joaquin Valley soils and groundwater, confirming Orlob's (1991) salinity model projection which showed net salt load imports to the valley. This long-term salt load imbalance will diminish irrigation sustainability. To address the salinization problem and drainage-related problems the following measures have been taken on the west side of the San Joaquin Valley.



Source: Department of Water Resources.

**Note:** Environmental includes water for “wild and scenic” rivers, required Delta outflow, instream flows, and managed wetlands. Urban includes residential, commercial, and industrial uses, and large landscapes. Agricultural includes water for crop production. Net water use—i.e. the volume consumed by people or plants, embodied in manufactured goods, evaporated, or discharged to saline waters—is lower. The figure excludes water used to recharge groundwater basins (3% for urban and 1% for agriculture on average), conveyance losses (2% for urban and 7% for agriculture), and water used for energy production (less than 2% of urban use). The North Lahontan region covers most of the northeastern Sierras; South Lahontan covers the eastern Sierras and high desert including Mono, Inyo, and parts of Kern, Los Angeles, and San Bernardino Counties; and the Colorado River region covers the southeastern portion of the state including Imperial, and parts of Riverside, San Bernardino, and San Diego Counties.

From: Just the Facts: Water Use in California, PPIC, 2014.

Figure 13: Total water use by region in California. Agriculture is the dominant water use in the San Joaquin River Basin.

- Reduction of deep percolation (the downward movement of water below the root zone, past drains to the local groundwater system) through the adoption of water conserving irrigation technologies and practices, better irrigation scheduling and changes in cropping practices.
- Reuse of drain water, through the use of salt-tolerant crops and agro-forestry.

- Manipulation of the water table to meet part of the crop evapotranspiration requirements.
- Conjunctive use of groundwater to meet a portion of crop needs.
- Improved instrumentation and monitoring systems to produce accurate and timely information and improve access to this information by growers.
- Development and installation of real-time monitoring systems to progressively evaluate changes in soil and water quality in the terrestrial and aquatic ecosystems over time.

Prior to the 1980's, local, state, and federal policy supported the development and expansion of agriculture in the valley. Since the 1983 selenium crisis, public perception of agriculture has changed and policies favoring agriculture have been re-evaluated and modified, reflecting a re-balancing of competing resource management objectives. Federal water contracts within the CVP have been re-evaluated, under the Central Valley Project Improvement Act (CVPIA PL 102-575 Title 34). The CVPIA seeks to redress the loss of wetland acreage that has occurred over the past century. The CVPIA mandates that 800,000 acre-feet of water, once allocated to agriculture, be re-designated for fish and wildlife purposes. Other re-allocations of water supply from agriculture and urban uses to environmental uses, including several settlements of water rights disputes, have further reduced the water available to support irrigated agriculture in the San Joaquin Valley.

Table 1: Irrigated Crop acreage

<b>San Joaquin Irrigated Crop acreage</b>				
Thousands of 4047m <sup>2</sup> or (acres)				
<b>Planning subarea</b>	<b>1990</b>	<b>2000</b>	<b>2010</b>	<b>2020</b>
Sierra Foothills	7	8	9	11
Eastern Valley Floor	273	272	271	269
Delta Service Area	277	276	273	271
Western Uplands	13	12	12	12
East Side Uplands	2	2	2	2
Valley East Side	1,003	985	965	950
Valley West Side	433	435	436	437
West Side Uplands	0	0	0	0
<b>TOTAL</b>	<b>2,008</b>	<b>1,990</b>	<b>1,968</b>	<b>1,952</b>

Source: Department of water resources, California, San Joaquin region

Over the past 20 years, the net water demand for agriculture has fluctuated in the region, mainly due to changing crop patterns, For instance, rice disappeared due to the recent water shortage near the city of Merced and has been replaced with sugar and cotton, which require far less water. There may be some minor scope for improvement in irrigation water use efficiencies; the use of low-volume irrigation system in new plantings of orchards is increasing the efficiency and reducing the overall use of water for irrigation. Table 2 shows agriculture water demands projected to 2020 (DWR, 2015).

Table 2: San Joaquin Basin agricultural water demand (acre-feet)

San Joaquin Agricultural Water Demand								
Thousands of 1233m <sup>3</sup> or (acre-feet)								
Planning subarea	1990		2000		2010		2020	
	Average	Drought	Average	Drought	Average	Drought	Average	Drought
<b>Sierra Foothills</b>								
Applied water demand	20	24	22	26	25	34	29	34
Net water demand	17	21	19	23	22	31	26	31
Depletion	15	17	16	19	20	25	21	25
<b>Eastern Valley Floor</b>								
Applied water demand	886	1,038	850	996	823	946	809	946
Net water demand	873	1,027	827	987	791	903	778	903
Depletion	639	749	630	737	621	717	614	717
<b>Delta Service Area</b>								
Applied water demand	739	830	719	805	694	774	681	755
Net water demand	690	772	673	749	650	721	639	705
Depletion	552	620	542	606	532	591	522	578
<b>Western Uplands</b>								
Applied water demand	40	47	38	44	36	42	34	40
Net water demand	43	49	40	46	38	44	37	42
Depletion	30	35	29	34	28	32	27	31
<b>East Side Uplands</b>								
Applied water demand	7	7	7	7	7	7	7	7
Net water demand	4	4	4	4	4	4	4	4
Depletion	4	4	4	4	4	4	4	4
<b>Valley East Side</b>								
Applied water demand	3,193	3,366	3,059	3,230	2,926	3,086	2,841	3,012
Net water demand	2,840	2,995	2,726	2,881	2,608	2,757	2,533	2,691
Depletion	2,340	2,468	2,271	2,398	2,200	2,326	2,138	2,269
<b>Valley West Side</b>								
Applied water demand	1,413	1,445	1,357	1,392	1,306	1,338	1,264	1,286
Net water demand	1,311	1,349	1,272	1,277	1,233	1,235	1,198	1,196
Depletion	1,139	1,171	1,113	1,111	1,085	1,082	1,057	1,054
<b>West Side Uplands</b>								
Applied water demand	0	0	0	0	0	0	0	0
Net water demand	0	0	0	0	0	0	0	0
Depletion	0	0	0	0	0	0	0	0
<b>TOTAL</b>								
Applied water demand	6,298	6,757	6,052	6,500	5,817	6,277	5,665	6,080
Net water demand	5,778	6,217	5,561	5,967	5,346	5,695	5,215	5,572
Depletion	4,719	5,064	4,605	4,909	4,490	4,777	4,383	4,678

Source: Department of water resources, California, San Joaquin region

Table 3: Salinity and drainage problems by major irrigated area

Location	Irrigated area	Salinity/ Sodicity soils*	High water table	Water quality
----- Millions of acres -----				
<b>San Joaquin Valley</b>	4.6	1.3	2.7	1.2
<b>Sacramento Valley</b>	0.8	0	<0.1	<0.1
<b>Imperial Valley</b>	8.9	0.4	0.2	0.2
<b>Other areas</b>	4.1	<0.1	<0.1	0.1
<b>Total</b>	25.3	1.9	1.6	2.3

Source: County Resource inventory 1982. U.S. Department of Agriculture Soil Conservation Services, Davis, California

\*Areas having and electrical conductivity of 4 ds/m (about 2,500 mg/L) or greater and/or exchangeable sodium percentage (ESP) values greater than 15 percent. Water table at a depth of 1.52m (5 feet) or less or at a depth that affects the growth of commonly grown crops. Includes parameters such as salinity or boron toxicity

Irrigated agriculture and farming practices also impact the salinity of groundwater - water quality generally declines over time (Suarez, 1989). High irrigation efficiencies may actually lead to higher concentrations of salt in deep percolation. Efficient irrigation methods are those with deep percolation of less than 10% of the irrigation applied water (Hanson et al., 2006). Doneen (1967) reported that in the San Joaquin Valley (SJV) the salinity of soils covered with native vegetation is generally lower than soils in irrigated areas.

Irrigation water normally contains from 0.06 to 3.95 tons per acre-ft of salt and crop requirements are between 2.03 to 3.05 acre-ft/acre to fulfill evaporation requirement. Thus, this amount of irrigation water may add approximately from 0.12 to 1.29 tons of salts/acre annually anywhere (Rhoades and Suarez, 1977). Groundwater can become degraded by salinity through irrigated agricultural practices by three process 1) salt concentrated is due to the uptake of water by plant, 2) salt moves down from the unsaturated zone into groundwater (saturated zone) because of leaching and mixing of subsurface saline water with higher quality groundwater and 3) enhanced percolation of saline water into the lower zone as a result of groundwater pumping for irrigation. (Suarez, 1989).

## **2. Modeling of Irrigated Land Use Systems**

This section covers the modeling of irrigated land use systems. This term applies both to irrigated agriculture as well as seasonally managed wetlands - which can be thought of as a special instance of irrigated agriculture similar to rice cultivation. In the San Joaquin Valley however most seasonally managed wetlands fall into three categories – wildlife refuges (State and Federal), privately owned duck clubs and land and cattle operations which combine duck hunting with beef cattle grazing in the early spring. Simulation of the hydrology of these systems requires a comprehensive understanding of the surface and groundwater resources of the Basin which contains the subarea for which the conceptual hydrology model is to be developed.

### **2.1 Conceptual Models and Water Budgets**

Conceptual models can take a variety of forms and are typically used to perform functions like : expressing relationships, exploring and testing ideas, checking inference and causality, identifying knowledge or data gaps, and synchronizing stakeholder mental models in order to build consensus (Argent, 2014). Conceptual models help to develop a stronger relationship between science and policy making – make the eventual outcomes potentially more useful to society. For stakeholder participatory planning and consensus building conceptual models are important to engage stakeholders and begin the process of consensus building. Conceptual models should be easy to understand by all (Voinov, 2008) since the overarching aim is to develop a common platform for understanding and learning about system.

The approach for developing conceptual models can be structured or unstructured – systems thinking often involves use of diagramming approaches to establish linkages between components of the system. Systems dynamics formalized by Forrester (1973) resolved systems into conceptual models consisting of stocks and flows with algorithms defining the rate at which stocks either increased or declined. These systems dynamics concepts are aligned with the principles of mass balance. The water balance (conservation of mass) is at the heart of every systems simulation model and the application of this concept to develop a steady-state representation of the system being analyzed forces the analyst to define and obtain estimates of the hydrologic inputs and outputs needed to create balance. Water and constituent mass balances are still considered essential building blocks in the development of systems understanding by stakeholders. The development of reliable stakeholder decision support systems –require identification, formalization and communication of elements or factors that are important to decision (Sojda, 2012). However different approaches may yield different conceptual models – models are not necessarily universal and may not be able to be reused. Building more complex conceptual models requires rules and syntax. In computer science knowledge engineering (Scott et al., 1991) separates the conceptual model building process from the formal coding of the relationship.

In the human psychology literature cognitive mapping is used to represent internal structures and beliefs to allow development of consensus view (Axelrod, 1976). Participatory modeling and decision making requires sharing of cognitive or mental models to achieve mutual learning and understanding (Guipponi and Sgobbi, 2007). A procedure known as fuzzy cognitive mapping uses

both qualitative and quantitative approaches for integrated modeling and scenario analysis (Koskom 1986; Kok, 2009 and Ozesmi and Ozesmi, 2004). Argent et al., (2014) propose eight principals of conceptual modeling best practices in support of decision support system development as follows :

1. *Use an open and transparent model development process*
2. *Encapsulate and communicate concepts effectively*
3. *Create robust and adaptable models*
4. *Use a formal approach to model representation*
5. *Test and re-test the models*
6. *Explore model behavior through scenarios*
7. *Ensure the model can be converted into an operational form*
8. *Maintaining a conceptual model can serve as representation of beliefs and can be a powerful communication tool*

The key tasks in conceptual model development lies in adequately defining the problem. This can be helped by creating a free-body diagram or cartoon of the system that is being analyzed. For groundwater models in particular it is important to define the bottom boundary of the “system” very carefully. For example water budgets constructed for the crop root zone will typically include terms such as upward capillary flow and tile drainage whereas water budgets for the shallow groundwater aquifer, that might extend from the ground surface to a depth of 50 ft – will not include these terms since they occur internally to the control volume being analyzed. Tools such as MODFLOW Zonebudget can be used to develop water budgets for multiple layers in the vertical profile as well as for subareas defined in 2-D space. These water budgets are perhaps the most direct way to present and validate groundwater conceptual models and this is the approach taken in the case study that will be presented in Chapter 4 of this report.

The next steps in conceptual model development are to take all information from site and use it to develop an analytical framework. The characteristics of this framework depend on the type of conceptual model being developed. In most cases the conceptual model is a precursor to numerical modelling. The conceptual model has further utility in helping the analyst to determine the data requirements of the numerical model and to plan the data gathering activity. With many model development enterprises there are different levels of availability and accessibility of site data.

There remains some ontological ambiguity within the published groundwater literature as to what constitutes a conceptual model. For example a random review of six journal papers that used the word “conceptual model” in the title – two were steady-state models (Leon and Ty, 2003; Minns, 1993), three described both steady-state and transient models (Singhal and Goyal, 2011; Yao et al., 2014; Willis, 2014) and one was a conceptual geology model which included analysis of the system hydrogeology. In Chapter 3 of this report the development of a steady-state (conceptual) groundwater model is described in detail using the GMS Groundwater Modeling System (GMS) modeling framework. Of the various conceptual model development software products reviewed – GMS is the easiest to follow and is best integrated with GIS software tools which makes watershed delineation and the recognition of surface water features within the watershed relatively easy. The application chosen for the test case is the 4-S Ranch hydrogeological investigation –

which was a subject of a proposal for long-term groundwater conjunctive use planning. In Chapter 4 two transient models of wetland hydrology are compared and the results of simulations made for the same area discussed.

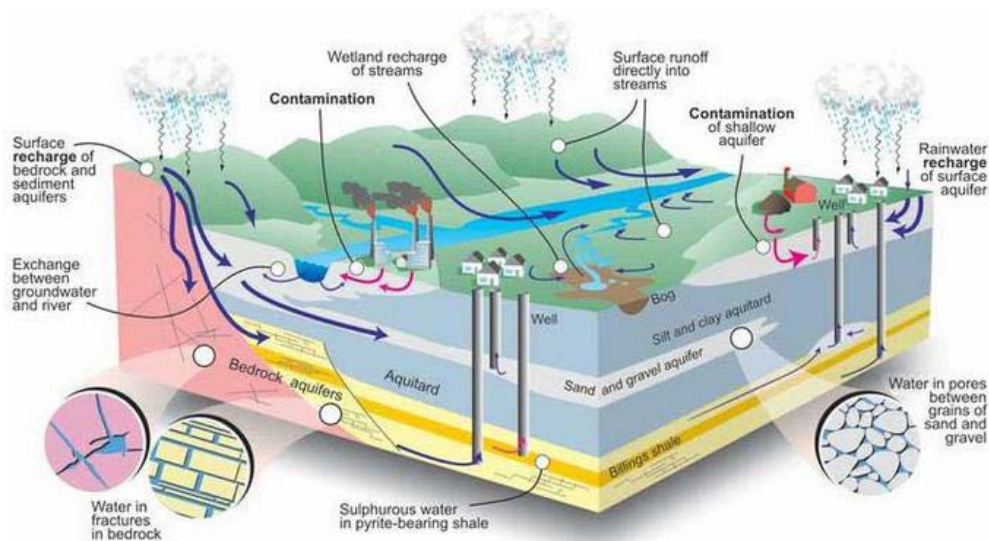


Figure 14. Groundwater – surface water conceptual model diagram.

The following section describes the types of simulation models for which conceptual models are an important precursor. In Chapter 4 two regional process models are compared – specifically targeting the conceptual wetland sub-models currently employed in both transient hydrologic models notably the WARMF-SJR (Watershed Analysis Risk Management Framework- San Joaquin River) and the CVHM (Central Valley Hydrologic Model). WARMF-SJR is a surface water quality model of the San Joaquin River Basin with rudimentary groundwater simulation capability – the code originally developed in the 1970’s to address acid-rain problems in forest ecosystems. The CVHM model is a three dimensional surface and groundwater flow model that includes the Farm Management Process (FMP) module. The FMP module is a data pre-processor that allows data inputs related to agricultural hydrology to be input into the model. The main objective of making this comparison is to demonstrate the importance of choosing the most appropriate conceptual model to simulate important processes.

## 2.2 Mathematical simulation models

To make rational decisions which might help achieve long-term sustainability of surface water and groundwater resources on the west-side of the San Joaquin Valley, the operation of this large, active, and variable system has to be continuously fine-tuned. Such a fine-tuning has to rely on two major efforts: monitoring and modeling. First, a complex and dynamic natural system continuously evolves. Some parameters of the system can only be estimated with adequate data in the time domain while other parameters may change with time. Therefore a network of monitoring

stations to continuously observe the hydrogeological and hydrogeochemical attributes of the system is an essential integral part of long-term planning for the west side. Second, on the side of interpretation and forecasting, it is essential that adequate interpretative tools are available to interpret the monitored data. At the present time, computer-based numerical models constitute the best interpretative tools for the purpose. Therefore, assembling a set of relevant computational tools is an issue of major importance. As we have seen, problems of interest vary in scale from that of a single farm to the Valley as a whole. In the time domain, the scale of interest may vary from a single irrigation event to several decades. On the small scale, process-oriented models for water movement, heat transport and reactive chemistry are important. On the largest scale, the operation of distribution networks plays a more important role than process-specific details. Yet small-scale and large-scale models must be compatible with each other. One way to achieve such an end is to think of a hierarchy of inter-related models, linking issues on all spatial and temporal scales. An integrative approach is needed since it is certain that models will assume an increased role in river basin planning activities in the future. Computer-based models can be divided into several groups: process-oriented models, optimization models, planning models and expert systems.

## **2.3 Process-Oriented Models**

Process-oriented models seek to analyze the interaction of fluid motion with plant roots and the atmosphere, the transport of heat and dissolved chemical components within the soil, and the chemical interactions that invariably take place between the aqueous phase and the solid phase. Because water ultimately governs the transport of chemical constituents and heat, modeling of water flow is a fundamental to all these models.

The equation governing transient flow of water in unsaturated-saturated, deformable media constitutes the basis for solving the solute transport problems, taking into account advective, dispersive and diffusive processes. Dynamic models combining fluid flow and solute transport, have been applied to study local, farm-level problems as well as regional-scale problems on the west side of the San Joaquin Valley. In addition, chemical reactions between mixing waters and between the aqueous and solid phases are governed by the equations of chemical thermodynamics.

## **2.4 Regional Simulation Models**

In order to gain an understanding of the regional groundwater flow conditions over the central part of the western San Joaquin Valley for developing drainage management strategies, Belitz et al. (1993) carried out three dimensional, transient groundwater flow simulations using a mathematical model. The simulated area covered 1,410 square kilometers (551 square miles), comprising 11 water districts. In this model, the semi-confined zone overlying the Corcoran Clay was divided vertically into five layers, of which the top two layers were assigned constant thicknesses while the remaining three were assigned spatially variable thicknesses. The confined aquifer was treated as a single layer. The low-permeability Corcoran Clay was represented through a "leakage" term governing the water transfer between the semi-confined zone and the confined aquifer. The

simulations accounted for aerially variable recharge rates to account for irrigation effects, pumping from wells, effects of subsurface drain systems and bare soil evaporation. In the horizontal plane, each grid block had an area of 2.56 square kilometers (1 square mile). The hydraulic properties of the materials (hydraulic conductivity, specific storage, porosity and specific yield) were initially assigned on the basis of lithology, data from laboratory tests and data gathered from hydraulic tests conducted in the field. Later, these values were fine-tuned through the model calibration process using field data gathered between 1972 and 1984 from specific sites. Having calibrated the model, Belitz and Phillips (1993, 1995) went on to apply the model to study the response of the system to alternate strategies of irrigation and drainage management. One finding of this study was that vertical flow predominates in the regional flow system. Based on this finding, the authors inferred that deliberate idling of lands or land retirement will have a noticeable impact only in the immediate vicinity of the land. This inference is at variance with the commonly held belief that upslope irrigators are contributors to down-slope drainage woes.

Belitz and Phillips (1993, 1995) examined alternate management strategies over a 50-year period, 1990-2040. If the status quo were to continue, they inferred that the area experiencing bare-soil evaporation will expand from about 575 square kilometers (224 square miles) to about 880 square kilometers (344 square miles) and the flow in the drains will increase from about 3,100 hectare-meter (25,000 acre-feet) to about 345 hectare-meter (28,000 acre-feet). Alternate simulations suggested that by reducing irrigation recharge by from 15 to 40 percent and by gradually increasing groundwater pumping, the area under bare soil evaporation could be reduced to about 200 square kilometers (78 square miles) and drainage flow reduced to about 1,000 hectare-meters (8,000 acre-feet). The authors estimated that some 50,000 hectare-meters (400,000 acre-feet) of water could be released for other beneficial use.

Using the regional model of Belitz and coworkers, Fio (1994) carried out sub-regional scale simulation of groundwater flow and drain interactions over an area largely defined by the boundaries of Panoche water district. Results generated from the regional model provided a basis for specifying the boundary conditions for these simulations. Attention was restricted to upper 26 meters (85 feet) of the semi-confined zone. This model generally confirmed the results of the regional model in regard to lateral flow but found instances where the vertical flow estimates of the regional model were at variance with field data.

## **2.5 Farm-Scale Models**

On the local scale, process-oriented mathematical models have been used for a variety of purposes including root zone water movement, water table fluctuations, evapotranspiration, efficiency of irrigation methods, and performance of drain systems. To study the dynamic interaction between the plants and the water table, Cardon and Letey (1992b) evaluated two types of plant-water uptake equations proposed in the literature (Nimah and Hanks, 1973; van Genuchten, 1987) and concluded that under saline conditions, typical of many parts of the west side, plant uptake models must give consideration to mechanical potentials (Darcy flow) as well as osmotic pressure variations, arising from spatial changes in salinity. Based on this finding, they coupled a form of van Genuchten's (1987) plant-water uptake model with a one-dimensional transient water and

solute transport model (Cardon and Letey, 1992c) to analyze crop yield under dynamic water flow conditions. The credibility of this model was tested by supplying it with detailed data from a well-controlled greenhouse experiment (Cardon and Letey, 1992c).

The efficiency of irrigation at the farm-level is dependent both on the method of irrigation (furrow or sprinkler irrigation) and the uniformity with which water is applied over the field. Using mathematical models restricted to saturated flow conditions, Ben-Asher and Ayars (1990) analyzed the effect of spatial non-uniformity in water application on deep seepage. An important issue addressed in the research was maximization of crop yield since non-uniform irrigation causes deep percolation in some parts of the field and under-irrigation in others. Ben Asher and Ayars (1990) found that more deep percolation resulted from non-uniform sprinkler irrigation than from uniform sprinkler applications.

Selenium data collected by Deverel and Fio (1991) in their study of the sources of drainage flow showed that upward-moving deeper groundwater contributed more to the annual selenium load to the particular drain lateral (332 kg) as compared to flow from the root zone above (68 kg). It is presumed that the selenium captured from the deepest aquifer originated from water that had deep percolated prior to the installation of the drains. Similarly from research conducted by Grismer (1989, 1993) "lateral flow" (or regional groundwater flow) is dynamically linked with the flow systems of the drains.

## 2.6 Chemical Transport Models

Although many of the process-oriented modeling efforts have been devoted to studying moisture movement and bulk salinity, the importance of understanding chemical reactions which occur between the numerous chemical species within an irrigated system has been recognized by many researchers. These interactions not only involve the mixing of waters of contrasting chemical quality (such as the imported irrigation water, the water in the root zone, and the groundwater) but also the interactions between the water and the solid phases of the soils and the sediments. The chemical interactions are further modified by evaporative concentration and dilution due to infiltration. These reactions result in profound modifications of the composition of the aqueous phase and the solid phase through precipitation, dissolution, adsorption and desorption. The quantitative analysis of these interactions involving several chemical species constitutes a computational complexity that is far more intensive than the task of modeling moisture movement. Therefore, the application of reactive chemical transport models to the resolution of problems in the west side has become possible only within the past few years, as a new generation of computer work-stations have become available.

Essentially the reactive chemical transport models needed for understanding the behavior of major ions (e.g. Ca, Mg, Na, K, Al, Fe, Si, SO<sub>4</sub>, Cl, HCO<sub>3</sub>) and trace elements (e.g. As, Mo, Se, B) are characterized by two attributes. The first is the chemical transformation of the species into various forms (valence states, complexes and minerals) and their addition or removal from the aqueous phase. The second is the transport of the multitude of chemical species by the flowing water. In addition, the chemical transformations are also influenced in a major way by mobile gases

(especially in the vadose zone), notably carbon dioxide and oxygen. The chemical transformations include redox reactions, hydrolysis, sorption and ion exchange. These processes are interlinked by the constraints of chemical thermodynamics (electrical neutrality, balance between electron donors and receptors and mass conservation). The transport of chemical species on the other hand, involves processes of advection, molecular diffusion and hydrodynamic dispersion. The task of reactive chemical transport modeling, therefore, entails the dynamic coupling of the transport modules with the various chemical reaction modules.

A quantitative understanding of the interactions between soil minerals and soil water is of fundamental importance for proper agricultural management. Therefore, even with the introduction of rudimentary computers in the early 1960s, soil scientists took the first steps toward applying the principles of equilibrium thermodynamics to interpret reactive chemical transport experiments on soils. Dutt (1962) and Dutt and Tanji (1962) pioneered the practical application of mathematical models for reactive chemical transport when they developed and validated a model for gypsum precipitation in the presence of exchangeable calcium and magnesium. Later, Tanji et al. (1972) applied a similar model to the study of the problem of land reclamation in the San Joaquin Valley. This model simulated, in a credible fashion, the effects of gypsum amendment on sodic soils at eight experimental field plots.

The availability of powerful computer work-stations has encouraged the development of a number of generic reactive chemical transport models for simulating the simultaneous migration of several chemical components in the presence of fluid-solid interactions involving redox reactions, ion-exchange processes and chemical kinetics. Among the generic models that have been available for analyzing fluid-solid interactions are, Felmy et al. (1984), Wolery (1979), Parkhurst et al. (1980) and Mattigod and Sposito (1979). Simunek and Suarez (1993) focused attention on modeling the role of carbon dioxide in controlling the chemistry of the vadose zone and hence, the yield of crops on irrigated lands. Their model couples the temperature-dependent production of carbon dioxide due to microbial action and root respiration and its subsequent transport by transient moisture movement in the unsaturated zone. Suarez and Simunek (1993) applied the model to data from field experiments and found reasonable agreement, thereby supporting model credibility.

The Watershed Analysis Risk Management Framework (WARMF) model is a GIS-based forecasting and simulation tool that utilizes meteorological, point source, air quality and historical data, observed hydrological inputs to simulate water quality and hydrology conditions (Herr et al., 2001) and can be used for short and range predication of water quality (Keller, 2007). WARMF contains five linked module as shown in Figure 12. (a) an Engineering module graphically represents the entire watershed and uses scientific data to simulate hydrology processes and water quality such as surface runoff and infiltration from catchment, river and reservoirs, (b) a Consensus module which serves as a road map for stakeholder to identify water quality and watershed management Strategies, (c) A TMDL module that calculates Total Maximum Daily loads (TMDL) from point and nonpoint sources and keeps track of violations of water quality objectives or criteria, (d) a Data Module that can produce time series plots of flow and water quality concentration data and as well as display data in tabular format for easy access and (e) A

Knowledge module which stores reference information and case studies to help in other WARMF model applications.

## 2.7 Decision Support Models

Process-based models can help evaluate how crop yield and salt-load generation will respond to various strategies of water application and drainage. We have also seen that activities such as leaching, aimed at increasing crop yield may conflict with protection of groundwater quality in the shallow groundwater aquifer in the long term. In addition, these competing objectives are also constrained by economic considerations of cost and benefit. To help make optimal decisions under these conditions, many researchers have applied linear and dynamic programming methods (Knapp and Wichelns, 1990). The decisions involved may apply to a single farm or group of farms and consist of identifying the optimal irrigation strategy, giving consideration to crop needs, salinity and the cost of production.

Optimization models constitute a primary the interface between science-based resource assessment on the hand and resource economics on the other. Agricultural resource economics and associated policy development constitute a very active field of inquiry in the social sciences (e.g. Carlson et al., 1993). Using the physical attributes of resource systems such as soil and water as the basis, researchers involved with economics and policy study how these resources will respond to various strategies of resource utilization and social behavior. Based on such analyses they proceed to understand how, through various strategies of marketing, regulation, incentives and taxation prevalent social behavior can be modified towards a sustained utilization of natural resources. In this context, optimization models constitute an analytical capable of quantifying the complex interactions of a multitude of variables.

At the farm level, the ideal is to consider several alternative strategies, evaluate the system response to each strategy based on relevant physical, chemical, and biological processes and automatically choose the particular strategy that is optimal in regard to crop productivity and environmental acceptability. The automatic choice of such a strategy is the goal of dynamic optimization. Unfortunately, such dynamic optimization is computationally intensive, but the feasibility of using dynamic optimization at the farm level over a sequence of years under different choices of crop rotation, spatial variability and investment in irrigation systems has been demonstrated by Knapp (1992a,b,c). However, as the system becomes complex in terms of interacting physical, chemical and biological processes, the dynamic optimization becomes more computationally impractical. In such cases, the optimization method can be used to screen various options, followed by the evaluation of selected options through detailed process-oriented simulation models already described (Knapp and Wichelns, 1990).

In a recent study, Dinar et al. (1993) attempted to provide a framework for policy analysis in regard to lands under irrigated agriculture in arid environments, using dynamic programming models as a quantitative tool of analysis. They applied such a model to conditions in evidence on the west side and used empirically observed input functions for crop-yield, salinity and drainage discharge.

The objective function in the model consisted of cost and revenue functions. By evaluating alternate strategies for drainage control, they inferred that direct drainage control policies were slightly more cost-effective than indirect control policies. This research also suggested that dynamic models may not always be necessary for this class of problem because under some scenarios, the system under study may rapidly converge to a steady state, eliminating the requirement that time be an independent variable.

The quantified modeling of the economic and social aspects of agricultural- and environmental resource utilization is a task of enormous complexity. On a local scale, at the level of a farmer, economic analysis concerns itself greatly with cost-benefit analysis. On a larger scale, as diverse users compete for available water, the allocation of water, especially during periods of drought becomes a very difficult task. One approach to overcome this difficulty is to let the market place decide the value each competing user attaches to its needs. For example, an agriculturist with appropriative water rights may trade water to an urban user. Nevertheless, as laid down in the amendment to California's Constitution in 1928, water has to be used for "reasonable and beneficial purposes". As a consequence, economic analysis needs to take into consideration the relative weights that have to be assigned to different segments of society which need water, such as, agriculture, fish and wild-life and urban communities. Clearly, determination of such weights transcends the gamut of the physical sciences.

## **2.8 Regional Planning Models**

A category of management models, distinctly different from the process-oriented models described above, is needed on the scale of the west side as a whole. Obviously, these models are broad in scope as they combine resource response with economic objectives. Two important consequences arise from this enlarged scope. First, the number of parameters to be considered becomes very large due to spatial variability of physical properties, spatial variability of agricultural activities, spatial distribution of economic parameters and so on. Secondly, physical and chemical processes which are defined on the micro scale become less and less meaningful and more difficult to scale up as the spatial scale becomes very large. Consequently, large scale management models have to restrict themselves fewer parameters, fashioned by combining groups of parameters into fewer lumped parameters, to simulate in a generalized fashion, the most important hydrologic, geochemical and agronomic processes and relationships.

These regional-scale models often use empirical relationships derived from smaller-scale, more detailed models, since models at the regional scale are usually difficult to calibrate and impossible to validate. These models are commonly used in planning studies which are concerned with comparisons of the effects of a potential future scenario with the effects of a no-action or base condition. Since the basis of these models is comparison rather than prediction, they play a useful role in basin planning as a means of evaluating alternate strategies. Two examples of planning models among the many models dealing with salinity are the SJVDP West side Agricultural Drainage Economics (WADE) Model (Hatchett et. al., 1989), and the Hydrosalinity Model (HYSAM), Aragues et. al (1990).

The WADE Model was used by the SJVDP to make projections of irrigation technology change and drainage production under a series of policy options and constraints on drainage loading to the San Joaquin River. The model used optimization to determine profit maximizing behavior based on crop revenues and the costs of agricultural production and drainage disposal. Decision variables included crop selection, water supply, irrigation technologies, drainage investment, groundwater pumping, drainage recycling, water transfers between regions and land use. The model divided the west side of the San Joaquin Valley into discrete cells of between 6800 hectares (15,000 acres) and 18,000 hectares (40,000 acres). Flow between adjacent cells was calibrated against the USGS regional groundwater flow model (Belitz et al. 1991) using a simple Darcy flow assumption and a horizontal conductance term. The WADE Model performed mass balance for flow and salts on the root zone, the shallow semi-confined aquifer, the deep semi-confined aquifer and the sub-Corcoran confined aquifer.

The HYSAM (Aragues et al., 1990) is a simple mass balance model for salt and water that can be applied to an area of any size on the west side of the San Joaquin Valley. Although designed for a single annual time step the model was subsequently adapted to perform sequential annual mass balances and thus simulate salinity transients on the shallow semi-confined aquifer.

## **2.9 Expert System Models**

To educate farmers and farm advisors on the effects of improved scheduling and water conservation practices, a graphics-driven expert system was developed for the California Department of Water Resources by California Polytechnic State University at San Luis Obispo. This computer program prompts the user for information on local climate, soil conditions, cropping practices, irrigation technologies employed and the manner in which these technologies are managed. The user then selects an irrigation application schedule and, using average California Irrigation Management Information System (CIMIS) data, the model plots water distribution uniformity and irrigation efficiency for each seasonal irrigation. In this way the user of the software can experiment with a wide range of management and irrigation options; testing new ideas and management strategies before committing to them in the field. The software is described by its developers as an expert system since it provides the user with recommendations based on his entered field, crop and climatic data and upon his answers to specific management questions posed by the computer program.

The advent of computer graphics and shell scripts for generating easily-understood user- interfaces has greatly enhanced the utility and usability of many simple models for the average computer-literate farmer that previously were strictly the domain of irrigation consultants and university researchers.

## **3.0 Development of a regional planning conceptual model using GMS software**

The conceptual model approach employed in GMS involves using the GIS mapping tools in the *GMS Map* module to develop a two dimensional map of the site being modeled. The location of sources/sinks, layer parameters such as hydraulic conductivity model boundaries, and all other data necessary for the simulation can be defined at the conceptual model level. Once this model is complete, the grid is generated and the conceptual model is converted to the grid model and all of the cell-by-cell assignments are performed automatically. The steps involved in performing a MODFLOW simulation using the conceptual model approach are described in this section.

### **3.1 Problem description**

The example problem focuses on long-term hydrogeological resources of the former 4-H Ranch site and the development of a preliminary conceptual model for this area. It should be understood that the conceptual model puts together the necessary information for the development of a groundwater simulation model – the final result is not a calibrated simulation model. Developing a calibrated simulation model would require a much greater commitment of time and additional data resources than were available through this Science and Technology Program-funded project.

The initial geology of the site was obtained from the Quinn, 2010 hydrogeological assessment report. – The boundary conditions of the site follow the legal boundary of the former Ranch as reported in the report entitled “Hydrogeologic Assessment of the 4-S Land and Cattle Company Ranch” (Quinn, 2006). There are two primary sediment layers. The upper layer will be modeled as an unconfined layer and the lower layer will be modeled as a confined layer. The boundary to the north will be a no-flow boundary and the remaining boundary will be a specified head boundary corresponding to the average stage of the rivers. We will assume the influx to the system is primarily through recharge due to rainfall. There are some creek beds in the area which are sometimes dry but occasionally flow due to influx from the groundwater. We will represent these creek beds using drains. There are also two production wells in the area that will be included in the model.

#### **3.1.1 Basin description**

The former 4-S Ranch lies within the Merced Groundwater Basin within western Merced County almost due west of the City of Merced and to the east of the San Joaquin River. Figure 15 shows the geographic extent of the Merced Groundwater Basin. The Merced Groundwater Basin is bounded by the Merced River on the north, the San Joaquin River to the west and the Chowchilla River on the south and contains over a great number of municipal, industrial, agricultural and domestic wells (Schmidt, 2005). Wells in the groundwater basin have been reported as having capacities ranging from 100 to 4,500 gallons per minute (DWR, 2003). The existing well field

within the former 4-S Ranch was most likely developed in the 1960's or early 1970's - these wells have capacities ranging from 434 to 1,946 gallons per minute.

### **3.1.2 Regional Geology**

The San Joaquin River Basin is a large structural trough filled with approximately 16,000 feet of eroded sediments from the granitic Sierra Nevada and the marine shales and siltstones of the Coast Range. These sediments derived from alluvial fans, rivers and shallow lakes that formed complex layered beds of various geologic materials that were later folded by landforming stresses in the earth's mantle. A generalized regional San Joaquin Valley cross-section is provided in Figure 16, derived from an hydrogeological assessment report by Bookman-Edmonston (2003) for the Stevinson and Merquin Water Districts. This report shows that only the upper 400 – 800 ft of the sedimentary material contains groundwater suitable for agricultural, domestic and industrial use and for managed wetlands. The regional geology of the groundwater system beneath the former 4-S Ranch is largely derived from this report and by a more recent report by Ken Schmidt and Associates (Schmidt, 2005). An earlier US Geological Survey report by Gary Balding and Ron Page (USGS, 1971) of aquifer and well water quality data within the Modesto and Merced area provides some of the background geology upon which these later reports are based.

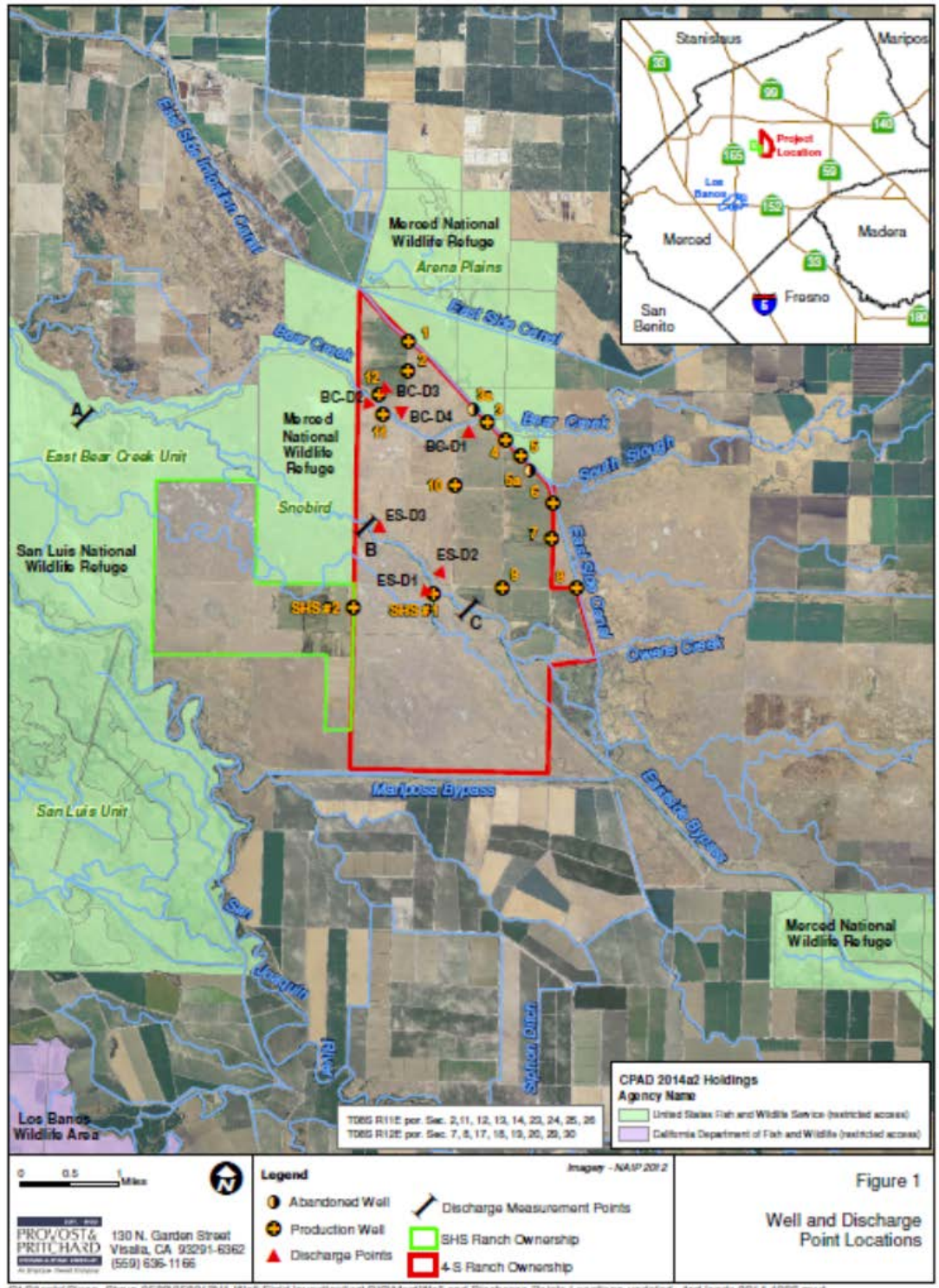
The upper 1,500 ft of sediments is comprised of both young and old alluvium, continental deposits and the Mehrten Formation (USGS, 1973). The Younger Alluvium consists of narrow bands of fine sand, sand and gravel with little or no hardpan and typically is found along river courses. This alluvial material ranges in thickness from 0 – 100 feet (USGS, 1973). The Older Alluvium is the more pervasive exposed structural unit in the vicinity of the 4-S Ranch and below the Stevinson and Merquin Water Districts, located less than 5 miles to the north-west. This structural unit comprises interbedded sand, silt, clay and gravel with some hardpan at shallower depths, and ranges in thickness from 400 to 700 ft below the land surface (Bookman-Edmonston, 2003). The bottom of the Older Alluvium is typically between 400 ft and 600 ft below sea level and is apparent in drillers logs as a transition from coarse grained to fine grained sediments (USGS, 1971, 1973).

Embedded within the Older Alluvium are a number of continuous lacustrine deposits of gray and blue silts, silty clays and clays that display low permeability and act as impermeable barriers to vertical groundwater movement. The most significant of these deposits is the Corcoran "E" Clay which is regionally extensive in the Valley trough between Tracy and Kern County and which pinches out close to the alignment of Highway 99 in the eastern San Joaquin Valley, north of Chowchilla and in the vicinity of Highway I-5 in the western San Joaquin Valley. In western Merced County the Corcoran Clay extends to Merced and Atwater and hence underlies the extent of the 4-S ranch. The Corcoran Clay is at its thickest in the Valley trough reaching thicknesses of 80-100 ft (Bookman-Edmonston, 2003). It is approximately 60 ft thick in the vicinity of the 4-S Ranch.



Figure 15. Merced Groundwater Basin showing location of Stevinson and Merquin Water Districts located north-west of the 4-S Ranch (Bookman-Edmonston, 2003).

The Continental Deposits are to be found beneath the Older Alluvium – the base of the Deposits extend to between 400 ft and 800 ft below sea level (Bookman-Edmonston, 2003). Water quality in the upper sections of the Continental Deposits is acceptable for many uses with an average electrical conductivity (EC) below 3,000 umhos/cm. The “base” of this fresh water – typically defined as the interface between water with an EC below 3000 uS/cm and poorer quality water – is not well defined and has been mapped by the USGS to be approximately 500 ft below mean sea level. Beneath the Continental Deposits lies the Mehrten Formation which is comprised of deposits of sandstone, tuff, siltstone, breccia, claystone and conglomerate often referred to by local drillers and “black sand and gravel” (Bookman-Edmonston, 2003; USGS, 1973). Although the depth of this formation is generally unknown because no wells have been sunk this deep, largely on account of abundant shallow water resources, it is an important aquifer in both the Sacramento and San Joaquin Valleys and has permitted well production between 1,500 and 3,500 gpm (Bookman-Edmonston, 2003).



01:Client:Soan\_Steve-3509:350912V1-Well Field Investigation\GIS\Map\Well and Discharge Points Locations-updatad2 - 1ad lands 2014-1022.mxd

Figure 16. Wells and local conveyances affecting 4-S Ranch hydrology.

### 3.13 Local hydrogeology

The local geology dictates the nature of the local groundwater system and can be derived from well driller's reports, geophysical logs, consultant reports and agency hydrogeological studies in the vicinity of the 4-S Ranch. Figure 17 is a generalized schematic of the aquifer system beneath the Stevinson and Merquin Water Districts, located approximately 3 miles north-west of the 4-S Ranch (Bookman-Edmonston, 2003). This same structural profile of the local geology can be applied to the 4-S Ranch, given the similar location of both the 4-S Ranch and the Stevinson and Merquin Water Districts, which lie in the discharge area close to the San Joaquin Valley trough, east and adjacent to the San Joaquin River. The distal end of the sedimentary deposits between major alluvial fans are characterized by having finer sediment texture and are often discharge zones where water originating from higher elevations on the east side of the San Joaquin Valley is forced under pressure upward through the near surface formations to discharge into sloughs and other surface drainages into the San Joaquin River. Past drainage problems in the Stevinson and Merquin Water Districts are well documented due to a heavy reliance on surface water for irrigation water supply.

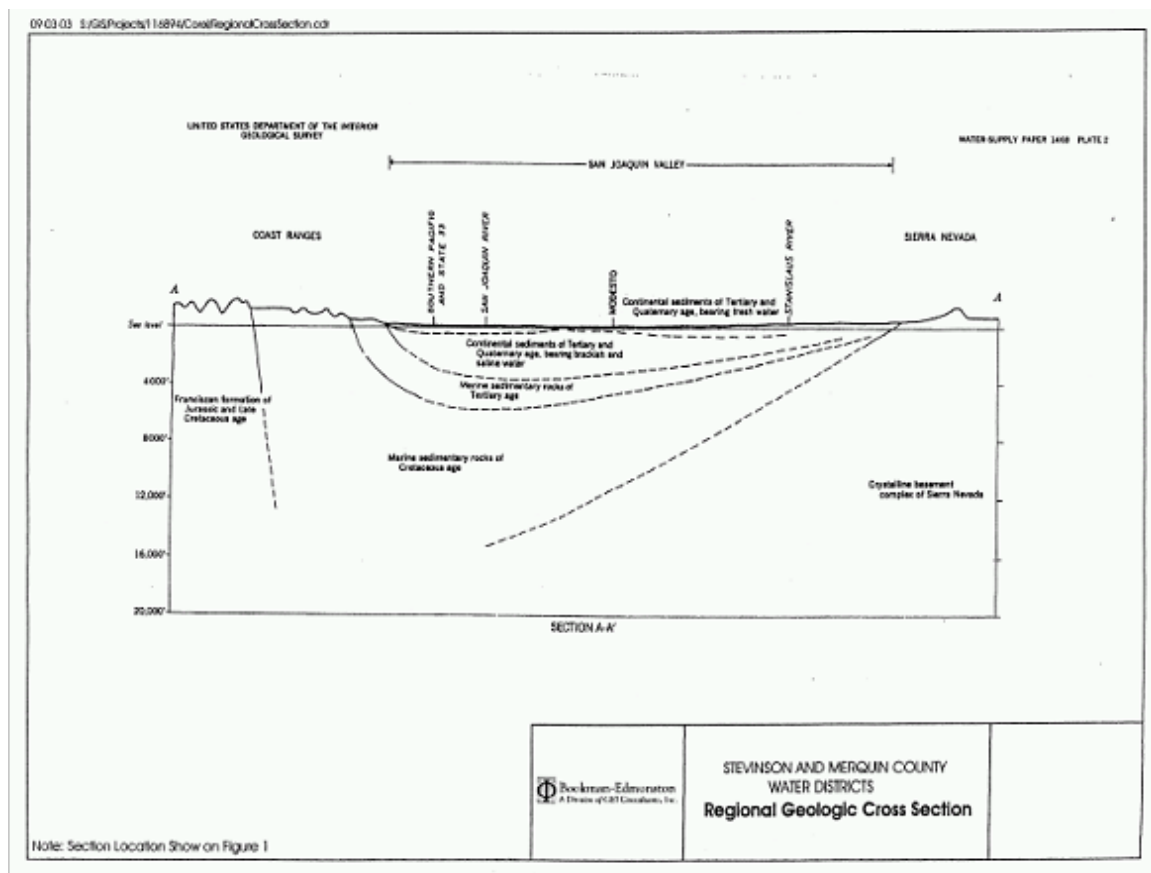


Figure 17. Generalized cross-section of the San Joaquin River Basin in proximity to the 4-S Ranch. (Bookman-Edmonston, 2003).

Figure 18 shows a depth profile of the major subsurface geologic units that are likely common to the 4-S Ranch property. Figure 18 is a generalized soils map for the study area obtained from the Natural Resource Conservation Service. Surface soils within the 4-S Ranch boundary are predominantly classified as Merced silt-loam. Both figures shows a shallow water table aquifer comprising of sandy-silt to silty sand sediments of Younger Alluvium that ranges between 50

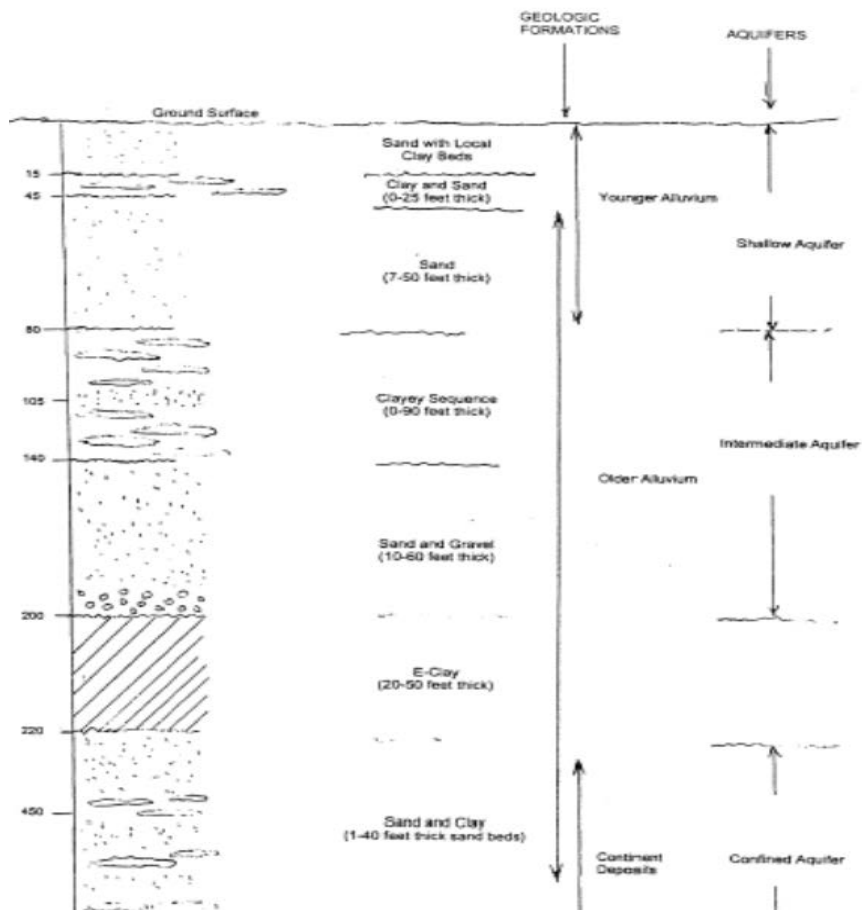
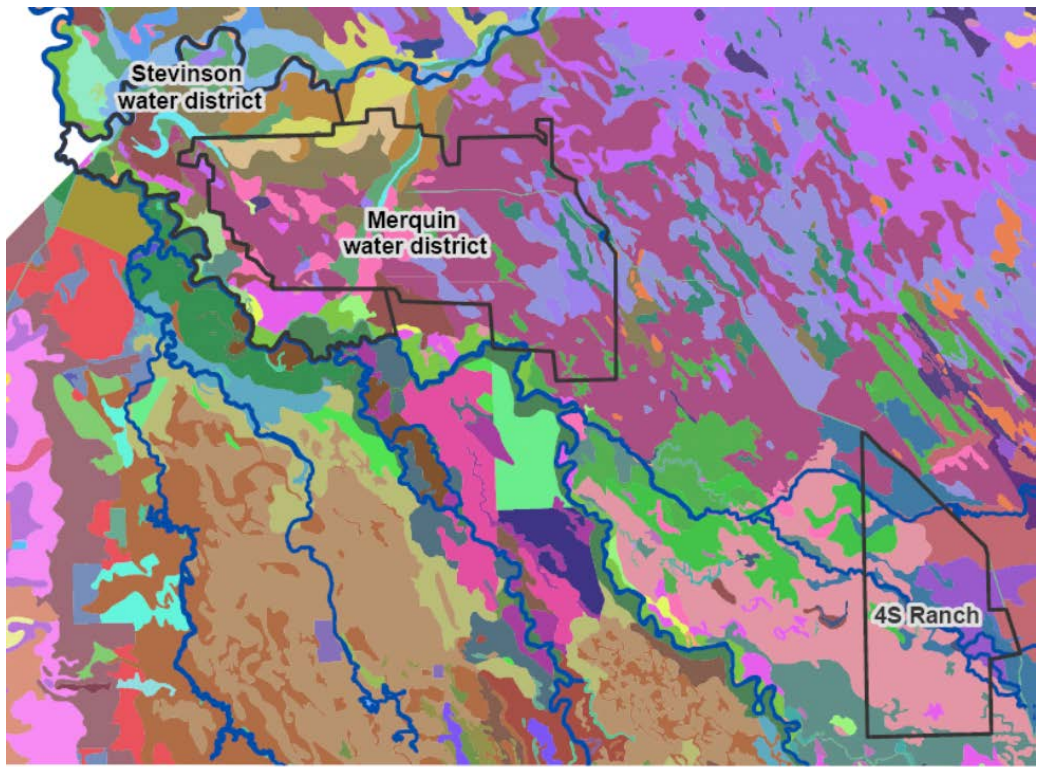


Figure 18. Generalized structural profile of sedimentary deposits and groundwater aquifers in the vicinity of the 4-S Ranch. (Source : Bookman-Edmonston, 2003).

and 100 ft in thickness and that is interfingered by a sequence of clay lenses that is sometimes referred to as the “A” clay. The “A” Clay in this vicinity occurs typically at depths of between 15 and 50 ft and may be up to 25 ft thick. This inter-fingering of deposits is typical of alluvial fans where meandering streams have changed course and clay beds have been eroded and replaced with sand. Beneath the shallow water table aquifer is a better defined series of discontinuous clay lenses that makes up the Older Alluvium. The “C” Clay is a layer within the Older Alluvium. This sequence of interbedded clay and sand layers is typically from 10 – 60 ft thick.



**Legend**

<ul style="list-style-type: none"> <li>Agrial clay loam</li> <li>Alos clay loam</li> <li>Atwater loamy sand</li> <li>Atwater sand</li> <li>Bapos-Arburua complex</li> <li>Bisgani clay loam</li> <li>Bisgani loamy sand</li> <li>Bolfar clay loam</li> <li>Britto clay loam</li> <li>Burchell silt loam</li> <li>Chinvar loam</li> <li>Columbia fine sandy loam</li> <li>Columbia loam</li> <li>Columbia soils</li> <li>Deldota clay</li> <li>Delhi loamy fine sand</li> <li>Delhi loamy sand</li> <li>Delhi sand</li> <li>Dello loamy fine sand</li> <li>Dello sand</li> <li>Dinuba sandy loam</li> <li>DosPalos clay</li> <li>DosPalos clay loam</li> <li>DosPalos-Bolfar complex</li> <li>Dosamigos clay</li> <li>Dosamigos clay loam</li> <li>Dune land</li> <li>Edminster loam</li> </ul>	<ul style="list-style-type: none"> <li>Edminster variant sand</li> <li>Edminster-Kesterson complex</li> <li>EINido clay loam</li> <li>EINido sandy loam</li> <li>Fluvaquents</li> <li>Foster fine sandy loam</li> <li>Fresno loam</li> <li>Grangeville fine sandy loam</li> <li>Grangeville loam</li> <li>Hanford fine sandy loam</li> <li>Hanford sandy loam</li> <li>Hilmar loamy sand</li> <li>Hilmar sand</li> <li>Kesterson loam</li> <li>Kesterson sandy loam</li> <li>Kesterson-Edminster complex</li> <li>Landlow clay</li> <li>Lewis clay</li> <li>Lewis silty clay loam</li> <li>Marcuse clay</li> <li>Marcuse silty clay</li> <li>Merced clay</li> <li>Merced clay loam</li> <li>Merced silt loam</li> <li>Pachappa fine sandy loam</li> <li>Pachappa sandy loam</li> <li>Palazzo sandy loam</li> <li>Pedcat clay loam</li> <li>Pedcat loam</li> </ul>	<ul style="list-style-type: none"> <li>Piper fine sandy loam</li> <li>Piper soils</li> <li>Raynor clay</li> <li>Riverwash</li> <li>Rossi clay</li> <li>Rossi clay loam</li> <li>SantaNela loam</li> <li>Stanislaus-DosAmigos-Urbar</li> <li>Temple clay loam</li> <li>Temple loam</li> <li>Traver fine sandy loam</li> <li>Triangle clay</li> <li>Tujunga loamy sand</li> <li>Tujunga sand</li> <li>Turlock loam</li> <li>Turlock sandy loam</li> <li>Turmount sandy loam</li> <li>Volta clay loam</li> <li>Waukena fine sandy loam</li> <li>Waukena loam</li> <li>Woo clay</li> <li>Woo clay loam</li> <li>Woo loam</li> <li>Woo-Urban complex</li> <li>water</li> <li>xerofluvents</li> </ul>
--	---	---

Figure 19. Soils map of the study area showing the 4-S Ranch and adjacent water districts.

### 3.14 Cone Penetrometer Logging

Cone Penetrometer Logging (CPT) was conducted at 4-S Ranch to develop a better understanding of the sedimentary geology of the semiconfined groundwater. During the CPT logging experiments, a conical-shaped probe instrumented with sensors was pushed into the ground up to depths of around 100 ft. The cone penetrometer used at 4-S Ranch contained sensors that continuously measured the friction sleeve, tip resistance, and electrical conductivity. A calibration curve was developed to convert bulk soil salinity measurements made with the CPT sensor to an equivalent soil solution salinity. Both Myron Inc. and YSI Inc. soil salinity sensors were used to develop this calibration curve. During the experiments it was noted that saturation occurred in the CPT electrode at bulk salinity concentrations above 600 mS/m – above this threshold the relationship between bulk salinity and EC became highly non-linear. Since the groundwater underlying much of the managed wetland area in the San Joaquin Valley has an EC below 9000 uS/cm – the non-linear portion of the calibration curve was eliminated and a best fit least squares calibration curve fitted.

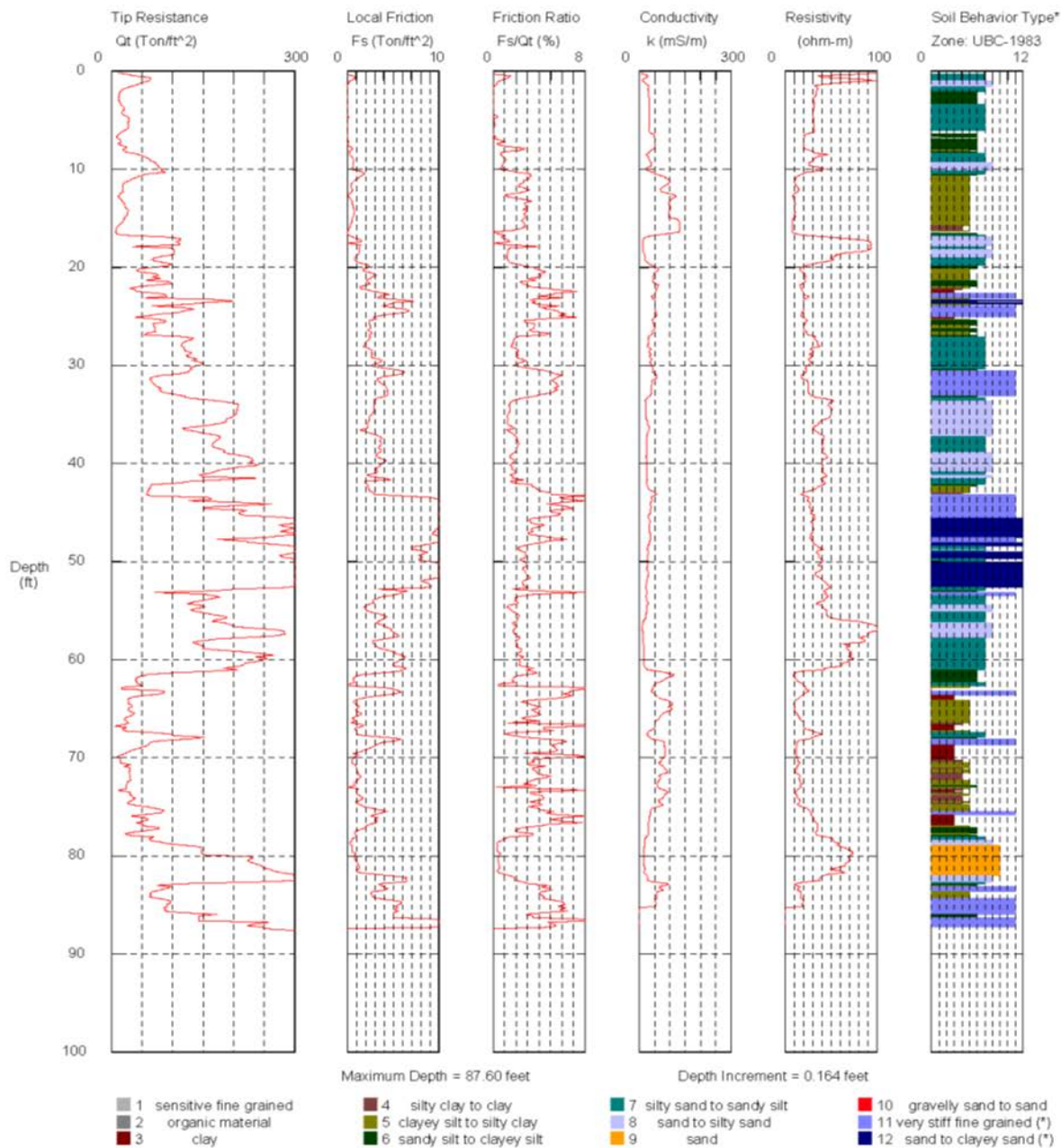
The best-fit equation was shown to be :  $EC (uS/cm) = 13.567 * \text{bulk salinity (mS/m)}$   
This equation has a regression coefficient of 0.9983

Plots of the sensor data with depth and the subsequent soil types determined from this data for a number of locations on the 4-S Ranch. The maximum depths of the CPT logs ranged from about 70 to 85 ft in the three locations. The general soil profile from the CPT logs is consistent with the upper half of the profile shown in Figure 18. We observed a clay and sand layer, followed by a sand layer, a clayey sequence and a sand layer. In Figure 20, where the CPT log was taken adjacent to production well 7, a similar stratigraphy is observed to the abandoned well, although these observations were more than 1 mile apart. The CPT log shows a larger fraction of finer grade material. Silty sands and intermediate sand-silty sands predominate over an aquifer that lies between 22 ft and 63 ft below the surface. The porosity and the specific yield of these aquifer materials are lower than that of sand. A clay aquitard, probably the “C” Clay, that is approximately 15 ft thick, lies immediately below the sand-silty sand aquifer. Bulk salinity concentrations are high in the vadose zone but diminishes to under 50 mS/m (680 uS/cm) until a depth of 62 ft below where the concentration increases to 150 mS/m (2,035 uS/cm).

# Bureau of Reclamation

Operator: TONY SHANAHAN  
 Sounding: 4SRA02  
 Cone Used: 351 TC

CPT Date/Time: 08-23-05 11:07  
 Location: FOUR S RANCH  
 Job Number: FOUR S RANCH



\*Soil behavior type and SPT based on data from UBC-1983

Figure 20. CPT log for production well no. 7 on the 4-S Ranch.

## 3.2 Conceptual model development

The conceptual modeling approach has many advantages – most significant is that the model itself and transient parameters such as well pumping rates can also be assigned independently of model discretization. Since the conceptual model is defined independently of the spatial and temporal discretization of the numerical model, the conceptual model can be easily modified and a new numerical model quickly generated. This allows the modeler to evaluate numerous alternative conceptual models in the space of time normally required to evaluate one, resulting in a more accurate and efficient modeling process. An additional advantage of storing attributes with feature objects in the application of boundary conditions to the grid cells is that it reduces inherent model instability. Using GMS to interpolate values at locations along a linear boundary condition such as a river insures that there will be no abrupt changes from cell to cell- thus minimizing the potential stair-step effect. It also produces a model with boundary conditions that more accurately represent real world conditions.

### 3.2.0 Getting started

Launch GMS. Select the *File / New* command to ensure that the program settings are restored to their default state.

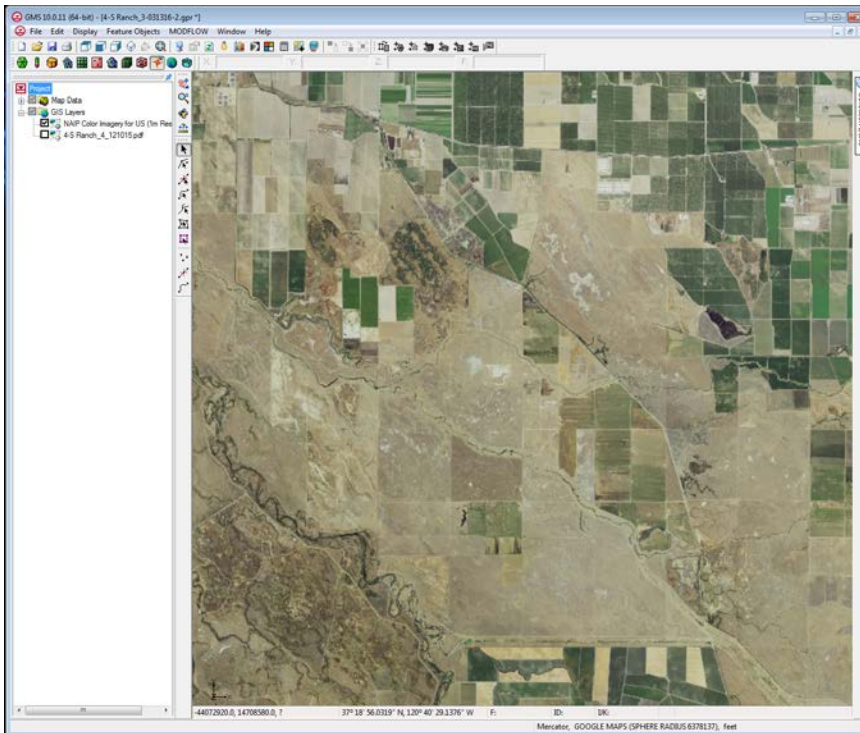


Figure 21. Map of project area on east-side of the San Joaquin Basin near Stevinson.

### 3.2.1 Importing the Background Image

The first step in setting up the simulation is to import a digital image of the site being modeled. In this case an image was created by searching online for appropriate color imagery – the most suitable was NAIP Color Imagery for US (1m Resolution) which appears below in Figure 20. The image was imported to GMS, registered and a project file was saved to **4-S\_Ranch.gpr** within a directory that was named **MODFLOW**. To read in the image, we open the project file. Once the image is imported to GMS, it can be displayed in the background as a guide for on screen digitizing and placement of model features.

### 3.2.2 Reading the Image

To import the image:

1. Select the *Open* button .
2. Locate and open the directory **MODFLOW/4-S\_Ranch.gpr**.
3. Open the file entitled **4-S\_Ranch.gpr**.

All other objects in GMS are drawn on top of the image. The image only appears in plan view. Other images can be added to the same folder.

### 3.2.3 Saving the Project

Before making any further changes, the project should be saved. Every so often it is useful to save the file under a new name, especially if significant work has been performed. This enables you to return to a previous .gpr file if mistakes have been made. The GMS software does not have an UNDO command.

1. Select the *File | Save As* command.
2. Save the project with the name **4-S\_Ranch**.

Hit the save button periodically as you develop your model.

### 3.2.4 Defining the Units

We need to define the units used in the conceptual model. The units we choose will be applied to edit fields in the GMS interface to remind the user of the proper units for each parameter.

1. Select the *Edit | Units* command.
2. For *Length*, select **ft** (for feet). For *Time*, select **d** (for days). Ignore the other units since they are not used for flow simulations.
3. Select the *OK* button.

### 3.2.5 Defining the Boundary

The first step is to define the outer boundary of the model domain as a “coverage”. This is done by creating an arc which forms a closed loop around the project area. In this application separate coverages were developed for each model boundary feature such as the San Joaquin River, the 4-S Ranch boundary, Bear Creek, the East-side Bypass and Mariposa Bypass. Similarly separate coverages were developed to define recharge zones, zones of hydraulic conductivity and evapotranspiration. Some of these objects could not be included in a single coverage because polygons within a coverage are not allowed to overlap. Coverages are managed on the GMS interface using the Project Explorer and appear below conceptual models. When GMS is first launched, no coverage exists until the user creates *feature objects* and then a new coverage is

created. One coverage at a time can be selected as the "active" coverage. New feature objects can be added to the active coverage and only objects in the active coverage can be edited. The active coverage is displayed with a color icon and bold text. The visibility of a coverage is controlled using the check box next to the coverage in the Project Explorer. A new coverage can be created by right-clicking on a folder or conceptual model and selecting the **New Coverage** command in the pop-up menu.

### 3.2.5.1 Create the Coverage

1. In the *Project Explorer* right-click on the empty space and then, from the pop-up menu, select the *New Conceptual Model* command.
2. For the *Name*, enter **4-S\_Ranch**. For the *Model*, select **MODFLOW**.
3. Click *OK*.
4. Right-click on the **4-S Ranch** conceptual model and select the *New Coverage* command from the pop-up menu.
5. Change the *Coverage name* to **Boundary**. Change the *Default elevation* to **30ft**. Change the *Default layer range* to go from **1** to **8**, then Click *OK*.

### 3.2.5.2 Create Coverage Arcs for Boundary Features, Rivers, Streams, Bypasses

1. Select the *Create Arc* tool .
2. Begin each arc by clicking once on the left (west) side of the model (Figure 22).
3. Create the arcs by proceeding around the boundary of the site in a counterclockwise direction and clicking on a sequence of points around the boundary. The boundary on the south-east side of ends at the San Joaquin River. Also digitize the **4-S Ranch** boundary.
4. To end the arc, click on the point where you began. If you wish to back up a point or two, press the *Backspace* key. If you wish to abort the arc and start over, press the *ESC* key.

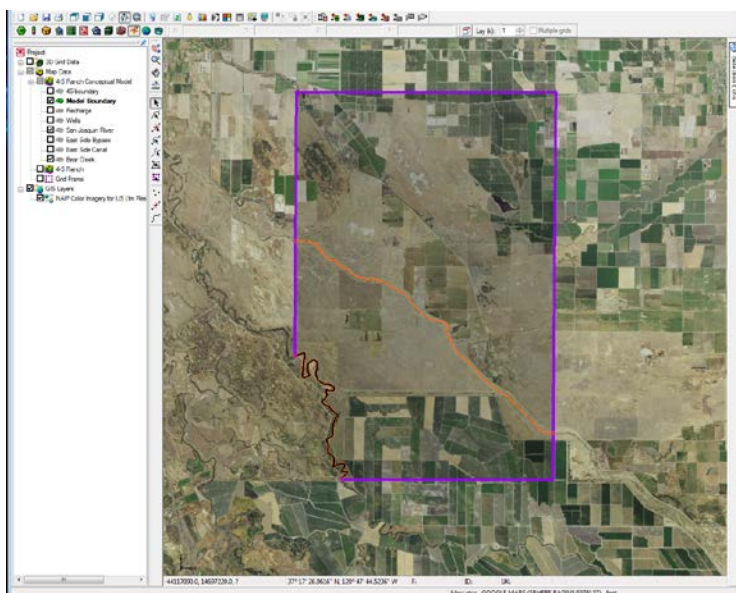


Figure 22. Creating arcs for boundaries and rivers, streams and bypasses.

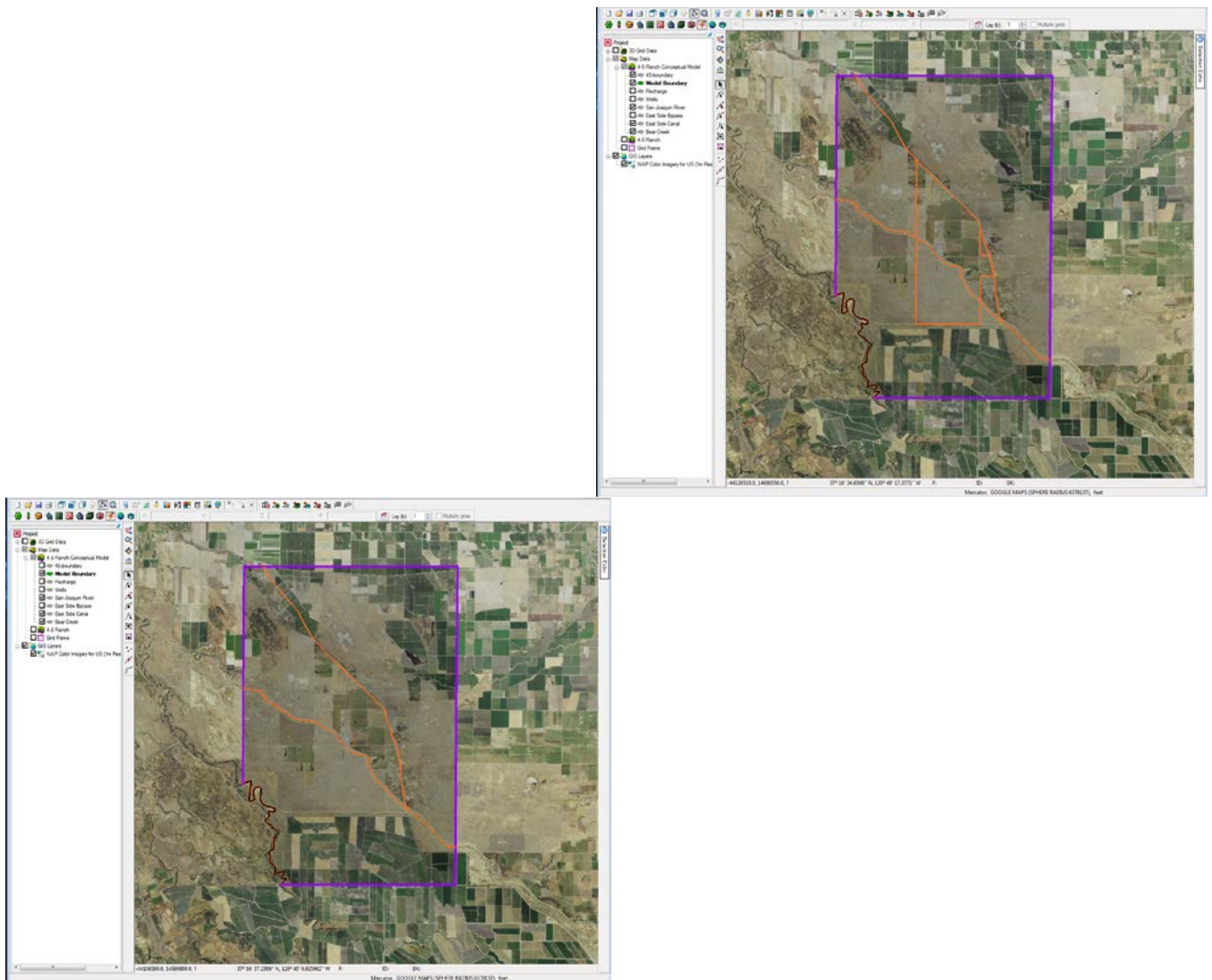


Figure 23. (a) Addition of new boundary condition arcs for the East-side canal and (b) the boundary of the 4-S Ranch property.

### 3.2.6 Building the Local Source/Sink Coverage

The next step in building the conceptual model is to construct the local sources/sinks coverages. These coverages define the boundary of the region being modeled and the local sources/sinks including wells, rivers, drains, and general head boundaries. The properties which can be assigned to the feature objects in a coverage depend on the conceptual model and the options set in the Coverage Setup dialog. Before creating the feature objects, we change the options in the Coverage Setup dialog.

1. Right-click on the **Boundary** coverage and select the *Duplicate* command from the pop-up menu. Change the new coverage name to add remaining boundary features including the **Mariposa Bypass**, the **East-side Canal**, the **East-side Bypass** and (added later) **Bear Creek**.

The **East-side Bypass** is digitized as a river in GMS since this feature can fill with water during wet years when excess flow can be diverted along its length to avoid flooding on the west-side of the San Joaquin Basin between Mendota and the Hwy 152 bridge.

2. Right-click on the each coverage in turn and select the *Coverage Setup* command from the pop-up menu.
3. Make sure the *Use to define model boundary (active area)* option is on.
4. In the list of *Sources/Sinks/BCs*, turn ON the following options for the above features.
  - *River*
5. For the boundary arc select the *Coverage Setup* command from the pop-up menu.
6. In the list of *Sources/Sinks/BCs*, turn ON the following options for the above features.
  - *General Head Boundary*
7. Click OK.
8. The **San Joaquin River** is digitized as a separate arc (shown red in Figure 22). Note that in GMS rivers and boundary condition arcs are ascribed different default colors to tell them apart. Follow the map in small arc increments – double-clicking to end the arc at the point the River meets the western boundary of the project area.
9. Right-click on the **San Joaquin River** and select the *Coverage Setup* command from the pop-up menu.
10. In the list of *Sources/Sinks/BCs*, turn ON the following options:
  - River
  - General head boundary
15. The elevations for the other boundary arcs – Bear Creek, East-side Canal, East-side Bypass and Mariposa Bypass are defined as *Rivers* and attributes are specified by right-clicking on each node where the feature crosses either another boundary arc or the model boundary and defining the *head stage* and *bottom elevation* in the *attribute table*. The following elevations for the upstream and downstream ends of each boundary arc are provided below:

	Upper elevation	Lower elevation	Depth to canal bottom
Bear Creek	18ft	18ft	10ft
East-side Bypass	10ft	9ft	2ft
East-side Canal	26ft	25ft	10ft
Mariposa Bypass	10ft	9ft	2ft

The San Joaquin River is defined both as a River and a boundary arc and only a top elevation is required. This is set to 10ft.

San Joaquin River	10ft	10ft
-------------------	------	------

The hydraulic conductivity of the bottom layer of each river is set to 7.5 ft<sup>2</sup>/day-ft except for the San Joaquin River which is assigned a value of 25 ft<sup>2</sup>/day-ft. When used as boundary condition, as in the current application – the hydraulic conductivity is not important.

### 3.2.7 Defining the Boundary Head Arcs

The next step is to define the head boundaries along the northern, part of the southern and western and eastern sides of the model. Before doing this, however, we must first split the arc we just created into three arcs. One arc will define the general head boundary along the top of the boundary outline in Figure 24 and the other two arcs will define the general head boundaries along the sides. An arc is split by selecting one or more vertices on the arc and converting the vertices to nodes.

1. Select the *Select Vertices* tool .
2. Select all the vertices shown in Figure 24. The first vertex is located at the junction of the boundary and the San Joaquin River. To select multiple vertices at once, select the first vertex and then hold down the *Shift* key while selecting the other vertices.
3. Right-click on one of the selected vertices and select *Vertex -> Node* command. Now that we have defined the three arcs, we will specify the arcs on the San Joaquin River and model boundary as general head boundaries. The general head boundary allows two way flow in and out of the model using the gradient between the cells at the boundary and adjacent cells within the model domain. If we were using heads from another model such as CVHM-2 (Faunt et al. 2010) we could use the specified head boundary condition for this steady state model and transient heads form the same model if the current steady-state model was further developed into a transient model.
4. Select the *Select Arcs* tool .
5. Select the boundary arcs on all sides of the model by selecting one arc and holding down the *Shift* key while selecting the other arc.
6. Right-click on one of the selected arcs and select the *Attribute Table* command from the pop-up menu.
7. Find the spreadsheet cell corresponding to the *All* row and the *Type* column. In this cell, select the **general head boundary** type. This will change the types for both arcs. (Note that if the user might want to change to a specified head boundary type later – both **specified head** and **general head** boundary types can be chosen.
8. Select the *OK* button.
9. Click anywhere on the model other than on the arcs to unselect them. Note that the color of the arcs has changed indicating the type of the arc (i.e. boundary, river etc.).

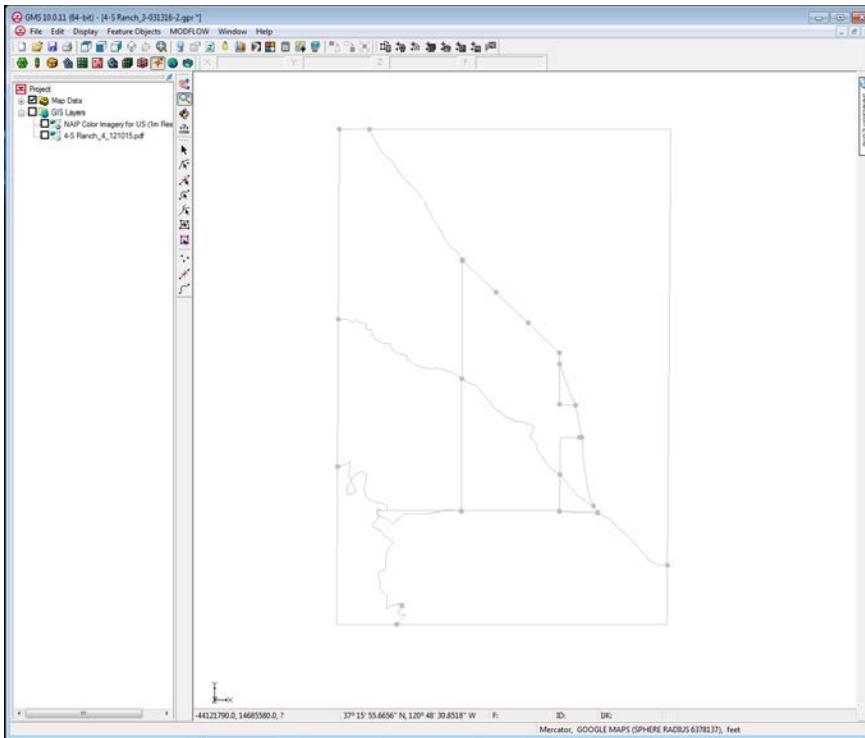


Figure 24. Defining the boundary properties along model arcs and at nodes converted from vertices.

The next step is to define the head at the nodes at the ends of the arcs. The head along a general head or specified head arc is assumed to vary linearly along the length of the arc.

10. Select the *Select Points/Nodes* tool .
11. Double click on the node on the west (top left) end of the arc on the northern (top) boundary.
12. Enter a constant value of **12ft** for the *Head-Stage*.
13. Select the *OK* button.
14. In a similar fashion, assign a value of **16ft** to the node at the top right corner of the model boundary and a value of the **15ft** to the node at the lower right corner of the model boundary.

### 3.2.8 Defining model layers

To create the layer coverage we begin by copying the first boundary coverage that we can further refine.

1. Right-click on the **Boundary** coverage and select the *Duplicate* command from the pop-up menu.
2. Change the name of the new coverage to **Layer 1**.
3. Right-click on the **Layer 1** coverage and select the *Coverage Setup* command.
4. In the *Areal Properties* list, turn ON the following options
  - *Horizontal K*
  - *Vertical anisotropy*.

Because of the sandy and highly permeable nature of the soils the vertical anisotropy is set to “1”.

5. Change the *Default layer range* to go from **1** to **1**.
6. Select the *OK* button.
7. Right click on the **Layer 1** coverage and select the *Duplicate* command from the pop-up menu. Change the name of the new coverage to **Layer 2**.
8. Right click on the **Layer 2** coverage and select the *Coverage Setup* command.
9. Change the *Default layer range* to go from **2** to **2**.
10. Repeat until all 8 layers are defined.
10. Select the *OK* button.

### 3.2.8.1 Assigning properties to layers

First, we will assign a K value for the top layer.

1. Select the **Layer 1** coverage in the *Project Explorer*.
2. Select the *Feature Objects / Build Polygons* command.
3. With the *Select Polygons* tool , double click on the polygon.
4. Change the *Horizontal K* to **7.5** ft<sup>2</sup>/day-ft.
5. Leave the *Vertical anisotropy*. at a value of **1**.
6. Select the *OK* button.
7. Repeat this for all model layers.
8. To make a sources/sinks coverage the active coverage select the coverage in the *Project Explorer window*.

### 3.2.9 Locating the Grid Frame

Now that the coverages are complete, we are ready to create the grid. The first step in creating the grid is to define the location and orientation of the grid using the Grid Frame. The Grid Frame represents the outline of the grid. It can be positioned on top of the site map graphically.

1. In the *Project Explorer* right-click on the empty space and then, from the pop-up menu, select the *New / Grid Frame* command.

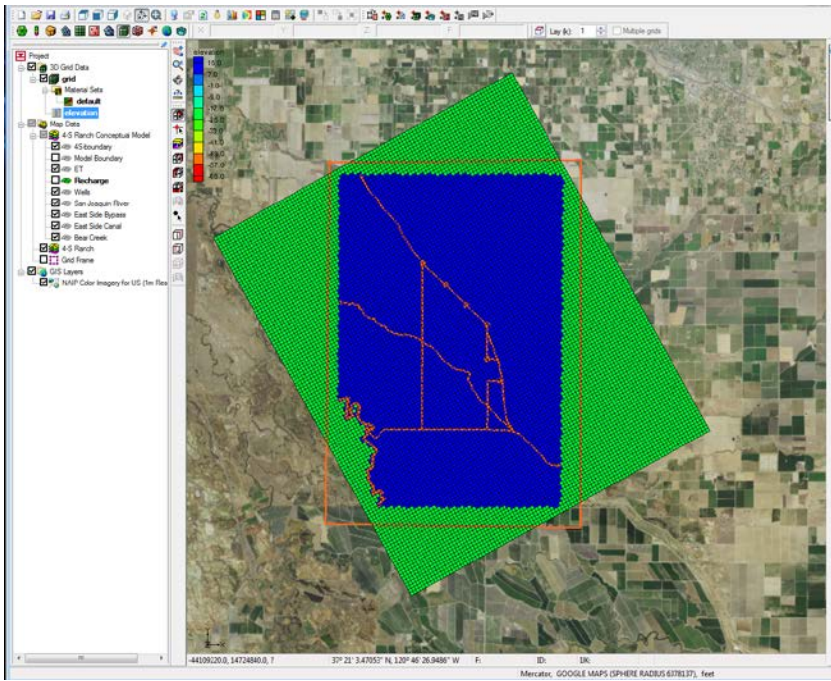


Figure 25. Defining the grid frame and choosing a better model alignment.

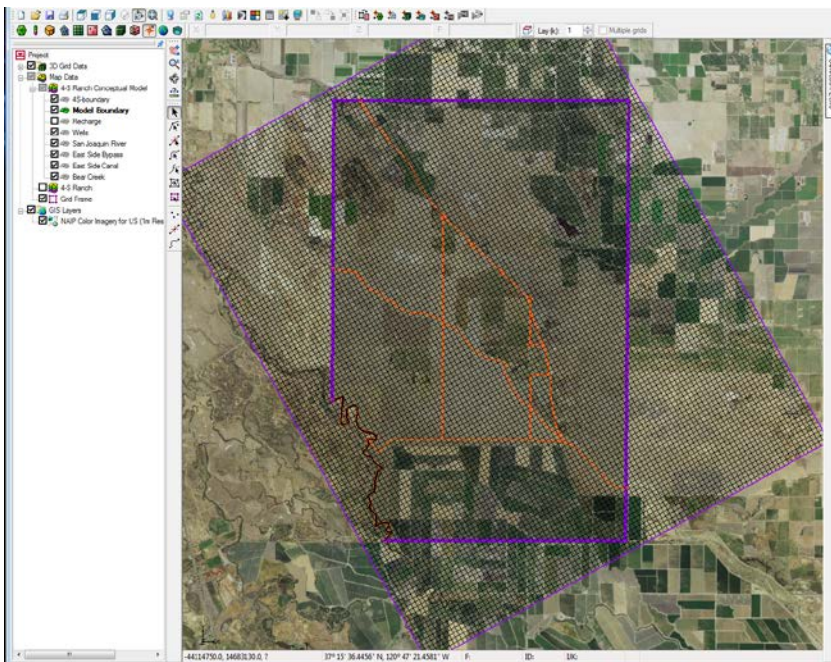


Figure 26. Experimenting with the model mesh configuration to cover the project area. The grid frame was modified to allow surface hydrologic features to be extended to the grid and model boundary. The inactive cells west of the San Joaquin River were eliminated from the final coverage.

2. In the *Project Explorer* right-click on the *Grid Frame* and select the *Fit to Active Coverage* command.
3. Double-click on the grid frame in the *Project Explorer* to bring up the properties dialog.
4. Change the *Origin z:* to **-160** and the *Dimension z:* to **+30**. This provides a set of initial values for the MODFLOW layer elevation arrays. Later, we will interpolate the layer elevations. Initially the elevation of the land surface in the vicinity of 4-S Ranch was set at +30ft using the thalweg of the San Joaquin River as an approximate datum. At a later date the vertical reference can be changed for all boundary heads and layers with reference to sea level. The nearby town of Stevenson is at an elevation of 85ft above sea level.
5. Select the *OK* button to exit the *Grid Frame* dialog.

### 3.2.10 Creating the Grid

Now that the coverages and the Grid Frame are created, we are now ready to create the grid mesh.

1. Select the *Feature Objects / Map*  *3D Grid* command. Note that the grid is dimensioned using the data from the Grid Frame. If a Grid Frame does not exist, the grid is defaulted to surround the model with approximately 5% overlap on the sides. Also note that the number of cells in the x and y dimensions cannot be altered after initial selection. The number of rows and columns and the locations of the cell boundaries is controlled by the refine point data entered at the wells – however in this case the wells have not been defined yet. The model mesh is given an x-y dimension of **80** (width) by **100** (length).
2. In the *Z-Dimension* change *Number cells* to **8**.
3. Select the *OK* button.
4. For numerical efficiency it is common to align the axis of the major hydrologic features – in this case the San Joaquin River, which lies along the axis of the Basin – with the model mesh. The model mesh is therefore rotated counter-clockwise using the grid frame properties menu to an angle of **61.1004** which improves its alignment with the River. The boundary node elevations are left as is and not adjusted.
5. The boundary arcs were extended to the new model boundary as defined by the model mesh using the technique described in Section 3.2.7. The inactive region to the west of the San Joaquin River on the lower left corner of the model mesh was eliminated by re-defining the model boundary and deleting the inactive cells from the coverage.

#### 3.2.10.1 Defining the Active/Inactive Zones

Once the grid is created, the next step is to define the active and inactive zones of the model. This is accomplished automatically using the information in the local sources/sinks coverage.

1. Select the *Map Data* folder in the *Project Explorer*.
2. Select the *Select Polygons* tool .
3. Select *Properties* button .
4. Confirm that the layer assignment is 1 to 8 and click *OK*.
5. Select the *Feature Objects / Activate Cells in Coverage(s)* command. Each of the cells in the interior of any polygon in the local sources/sinks coverage is designated as active and each cell which is outside of all of the polygons is designated as inactive. Notice that the cells on the boundary are activated such that the no-flow boundary at the top of the model approximately

coincides with the outer cell edges of the cells on the perimeter while the specified head boundaries approximately coincide with the cell centers of the cells on the perimeter.

6. Delete inactive cells from the model coverage.

### 3.2.11 Creating the Wells

The next step in creating the local sources/sinks coverage is to define the wells. Wells are defined as point type objects. Ten numbered active pumped wells were created within the 4-S Ranch coverage as previously shown in Figure 16 .

1. Select the *Create Point* tool .
2. Move the cursor to the approximate location of Well #1 shown in Figure 1 and click once with the mouse to create the point.
3. Select the *Properties* button .
4. For the *Type*, select the **well** option. Wells can be labelled using by right-clicking the point and defining the well number in the *Attribute* table.

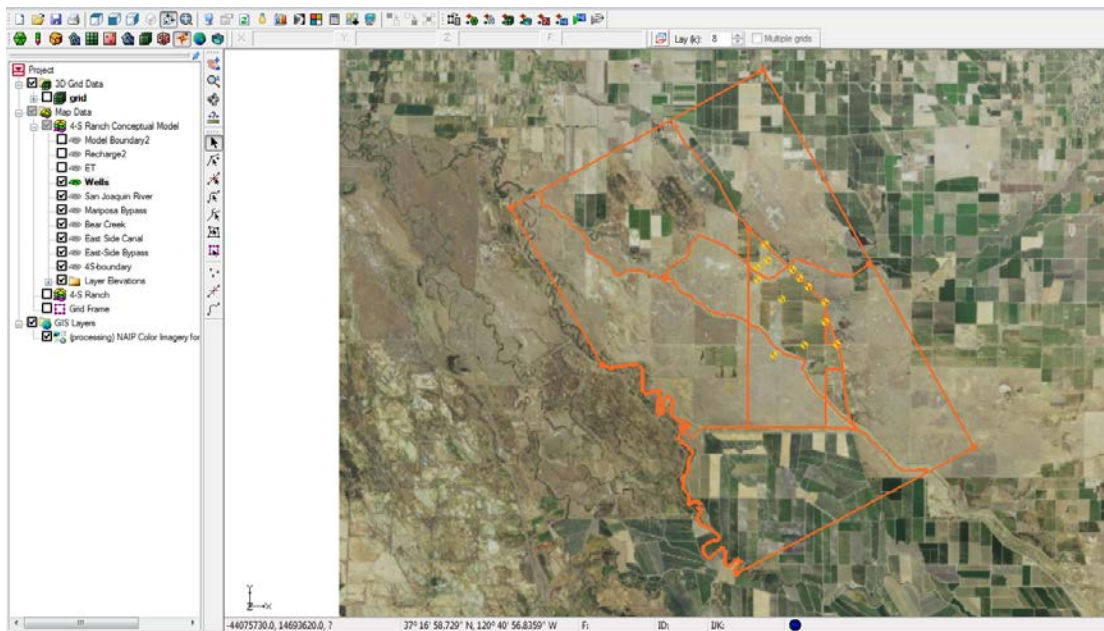


Figure 27. Final model mesh showing the revised model boundary and new alignment.

5. For the *Flow rate*, enter a constant value of **-5775** ft<sup>3</sup>/day – this is equivalent to an annual pumping rate of 30 gallons/minute. In a second scenario run made using the steady state conceptual model the annual average pumping rate was increased to 90 gals/min or approximately 17,000 ft<sup>3</sup>/day.
6. Change the *From layer* and *To layer* properties to be **3 and 4**. This means the well will only actively pump from layers 3 and 4 of the model 3-D mesh – equivalent to depths (z direction) of -20 ft to – 40ft (20 ft screened interval).
7. Select the *OK* button.

### 3.2.12 Building the polygons

With the local sources/sinks type coverage, the entire region to be modeled must be covered with non-overlapping polygons. This defines the active region of the grid. These polygons are of type “NONE” by default but may be converted to other types by selecting the polygons and using the *Properties* command. Now that all of the arcs in the coverage have been created, we are ready to construct polygons representing recharge and evapotranspiration.

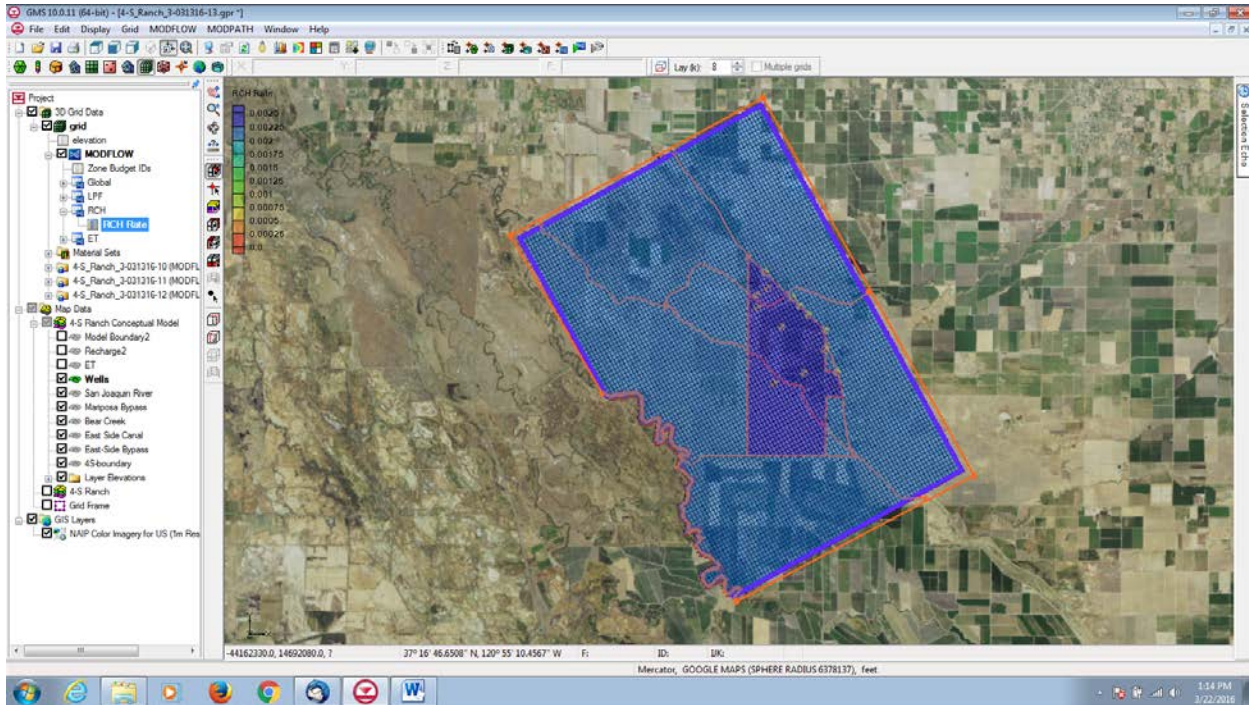


Figure 28. Two polygons were defined for the 4-S Ranch project area and the region outside from the 4-S Ranch boundary to the model boundary. These were used in assignment of ET and recharge rates.

#### 3.2.12.1 Delineating the Recharge Zones

The next step in constructing the conceptual model is to construct the coverage which defines the recharge zones. We will assume that the recharge over the area being modeled is uniform except for the 4-S ranch project area which has a slightly higher recharge rate – given that the land use is mostly irrigated pasture.

#### 3.2.12.2 Assigning the Recharge Values

Now that the recharge zones are defined, we can assign the recharge values. We will assign one value to the **4-S Ranch** polygon, and another value to the remaining polygon.

1. Select the *Select Polygons* tool .
2. Double click on the **4-S Ranch** polygon.
3. Change the *Recharge rate* to **0.007** ft/day.

4. Select the *OK* button.
5. Double click on the outer polygon.
6. Change the *Recharge rate* to **0.0065** ft/day.
7. Select the *OK* button.

### 3.2.12.3 Assigning the Evapotranspiration Values

We now assign the evapotranspiration values. We assign a single value to both the **4-S Ranch** polygon, and another value to the remaining polygon.

1. Select the *Select Polygons* tool .
2. Double click on the **4-S Ranch** polygon.
3. Change the *Evapotranspiration rate* to **0.006** ft/day
4. Select the *OK* button.

### 3.2.13 Defining the Hydraulic Conductivity

Next we will enter the hydraulic conductivity for each layer. For the sake of simplicity, we will use a constant value of **7.5** ft<sup>2</sup>/day-ft for each layer.

### 3.2.14 Initializing the MODFLOW Data

Now that the grid is constructed and the active/inactive zones are delineated, the next step is to convert the conceptual model to a grid-based numerical model. Before doing this, however, we must first initialize the MODFLOW data:

1. Right click on the *grid (1)* item in the *Project Explorer* and select the *New MODFLOW* command.
2. Select the *OK* button

### 3.2.15 Interpolating Layer Elevations

Now we need to define the layer elevations and the starting head. Since we are using the LPF package, top and bottom elevations are defined for each layer regardless of the layer type. For an 8 layer model, we need to define a layer elevation array for the top of layer one (the ground surface), the bottom of layer one, and the bottom of layer two. It is assumed that the top of layer two is equal to the bottom of layer one. We continue this layer assignment until we arrive at the bottom of layer 8. In the model we define the first layer as having a thickness of 30ft – mostly to avoid having the vadose zone appear below layer 1 at the start of the simulation. All other layer except layer 8 are assignment an elevation of 10ft. Layer 8 is given an elevation of 100 ft. The bottom of layer 8 is assigned an elevation of -80ft. The total depth of the model is 190ft (-160 ft to +30 ft).

#### 3.2.15.1 Setting the Heads and Elevations

We define the ground surface elevations and starting heads to the MODFLOW grid.

1. Highlight the **ground\_elev** data set and the **Starting Heads** array, and click the *Map* button.
2. Highlight the **ground\_elev** data set and the **Top Elevations Layer 1** array, and click the *Map* button.
3. Assign all starting heads to +30 ft. Select the *OK* button to perform the operation.

### 3.2.15.2 Viewing the Model Cross Sections

To check the interpolation, we will view a cross section.

1. Select the *3D Grid Data* folder in the *Project Explorer*.
2. Select a cell somewhere near the center of the model.
3. Select the *Side View* button. To get a better view of the cross section, we will increase the z magnification
4. Select the *Display Options* command .
5. Enter a value of **15** for the *Z magnification* factor.
6. Select the *OK* button.
7. Select the *Frame* button. You can use the arrow buttons in the *Tool Palette* to view different columns in the grid.

### 3.2.16 Converting the Conceptual Model

We are now ready to convert the conceptual model from the feature object-based definition to a grid-based MODFLOW numerical model.

1. Right-click on the *4-S Ranch* conceptual model and select the *Map To | MODFLOW / MODPATH* command.
2. Make sure the *All applicable coverages* option is selected and select *OK*. Notice that the cells underlying wells, and general head boundaries were all identified and assigned the appropriate sources/sinks. The heads and elevations of the cells were determined by linearly interpolating along the head arcs. Recharge, ET and hydraulic conductivity values were assigned to the appropriate cells.

### 3.2.17 Checking the Simulation

At this point, we have completely defined the MODFLOW data and we are ready to run the simulation. Let's run the *Model Checker* to see if GMS can identify any mistakes we may have made.

1. Select the *3D Grid Data* folder in the *Project Explorer*.
2. Select the *MODFLOW | Check Simulation* command.
3. Select the *Run Check* button. There should be no errors.
4. Select the *Done* button to exit the *Model Checker*.

### 3.2.18 Saving the Project

Now we are ready to save the project and run MODFLOW.

1. Select the *Save* button . Note: Saving the project not only saves the MODFLOW files but it saves all data associated with the project including the feature objects and scatter points.

### 3.2.19 Running MODFLOW

We are now ready to run MODFLOW.

1. Select the *MODFLOW | Run MODFLOW* command. At this point MODFLOW is launched and the *Model Wrapper* appears.
2. When the solution is finished, select the *Close* button.

### 3.2.20 Viewing the Head Contours

A set of contours should appear. To get better contrast between the contours and the background image, we will change the contour color to blue.

1. Select *Contour Options* from the main toolbar.
2. Click on the *Color Ramp* button and select the down arrow on the *Color* item.
3. Select a dark blue color.
4. Select the *OK* button twice to exit the dialogs. To view the contours for the second layer:
5. Select the down arrow in the mini-grid display.
6. After viewing the contours, return to the top layer by selecting the up arrow.

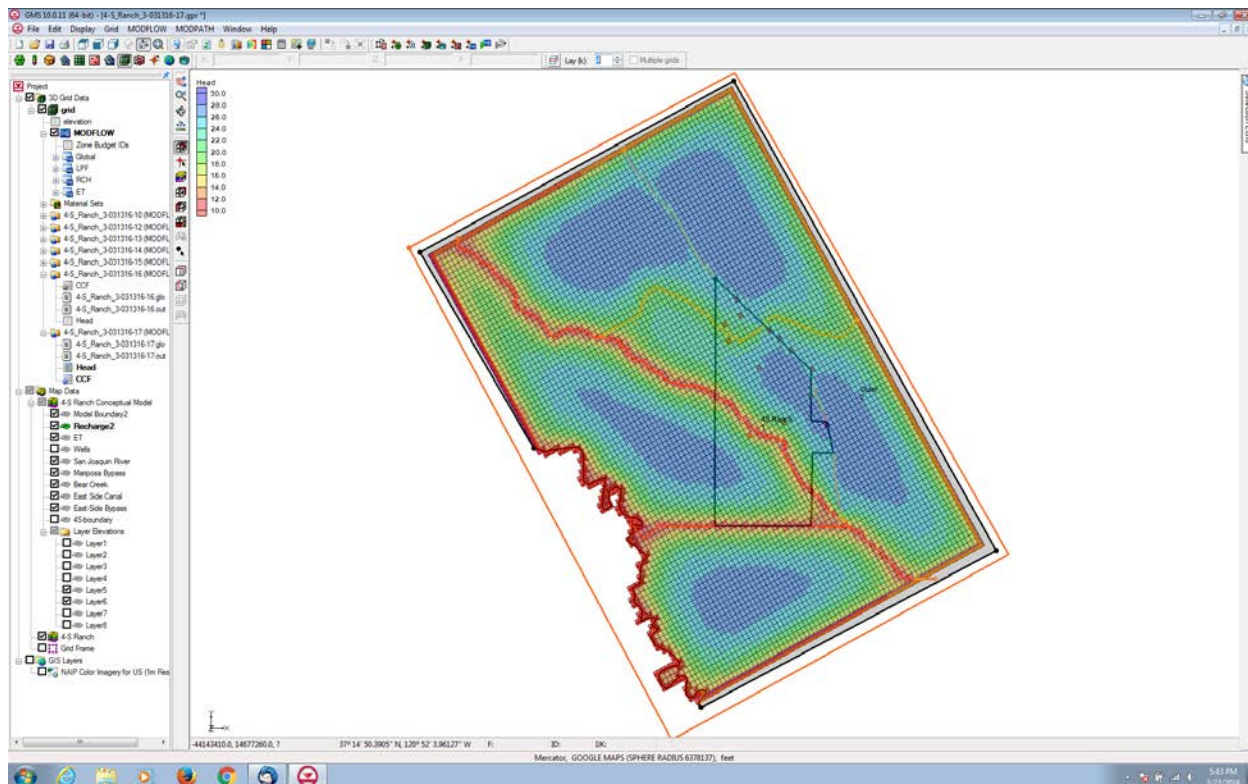


Figure 29. Plan view of 4-S Ranch project area showing higher water tables away from the major conveyances which act as open drains. Water tables are generally high along the alignment of the East-side Canal except in the section where wells are concentrated.

Figure 29 shows the model output from the steady-state conceptual model. The model output reflects the fact that the elevation of the major conveyances, with the exception of the East-side canal, were given water elevations between 10ft and 20 ft below ground surface, whereas the elevation of the East-side Canal was set about 5 ft below land surface. Recall this table provided earlier. Note that these are estimates (guesses) for the purpose of developing the conceptual model. Developing a realistic model would require field reconnaissance and measurement.

Upper elevation      Lower elevation      Depth to canal bottom

Bear Creek	18ft	18ft	10ft
East-side Bypass	10ft	9ft	2ft
East-side Canal	26ft	25ft	10ft
Mariposa Bypass	10ft	9ft	2ft

Water tables are highest away from the East-side Bypass and the Mariposa Bypass which both act as open drains – pulling down the water table. Water tables are lower than the highest water table elevations (shown as dark blue) close to the alignment of the East-side canal owing to the influence of pumping. This is shown in more detail in Figure 29.

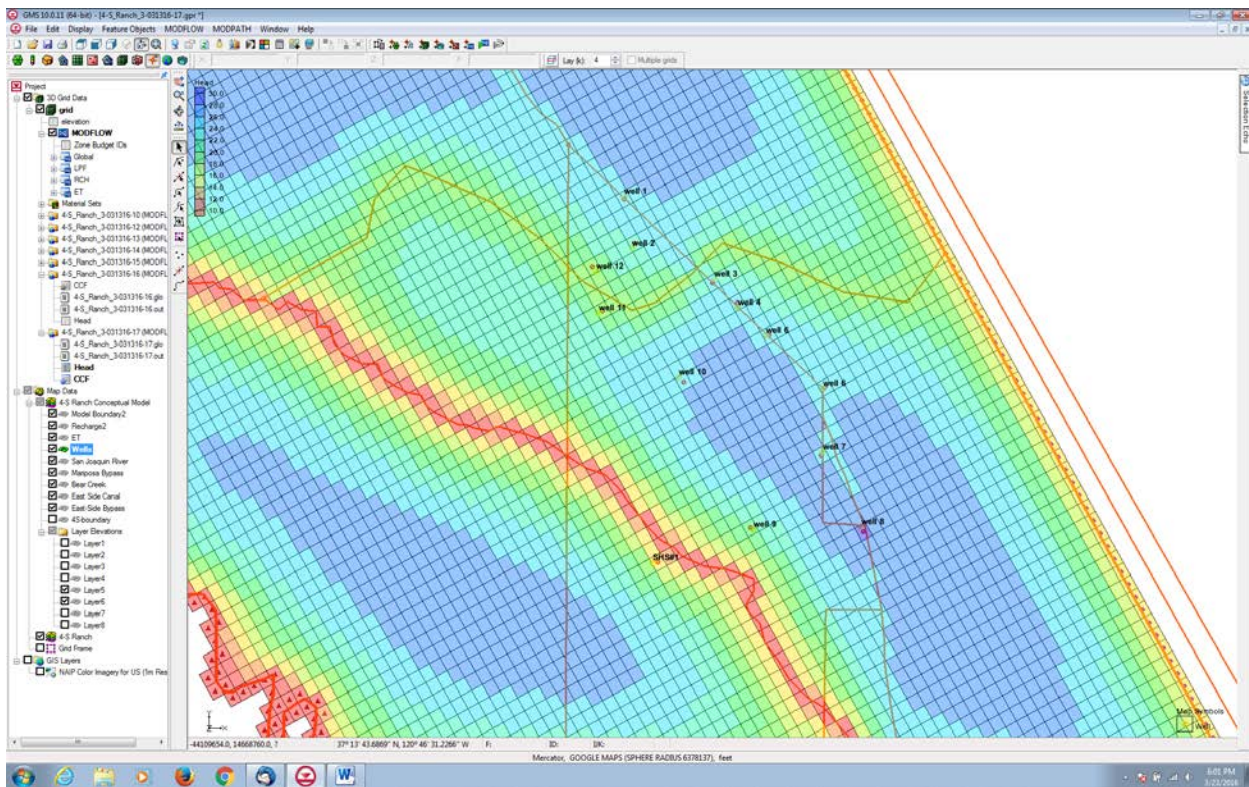


Figure 30. Head contour map output of the steady-state conceptual model showing the influence of the pumped wells mostly along the alignment of the East-side canal. The East-side Bypass acts as a large open drain lowering water tables in it’s vicinity.

In Figure 31 the head contour map depicts the impact of increasing the rate of pumping at all of the wells located along the alignment of the East-side Canal. Pumping was increased 3 times to an average annual pumping rate of 90 gals/min. Making allowance for the fact that the vertical scale has changed (as has the assigned color ramp) from a maximum of 30ft to a maximum of 28ft in Figure 30 – the contour map shows a more pronounced decline in average water tables in Layer 4 along the alignment of the East-side Bypass. Additional scenarios that might be explored might be the potential lining of the East-side Canal which would reduce the recharge from the Canal into

the underlying aquifer. If simulated with the current conceptual model – this would show much more severe water table declines in the surrounding aquifer centered on the location of each of the pumped wells.

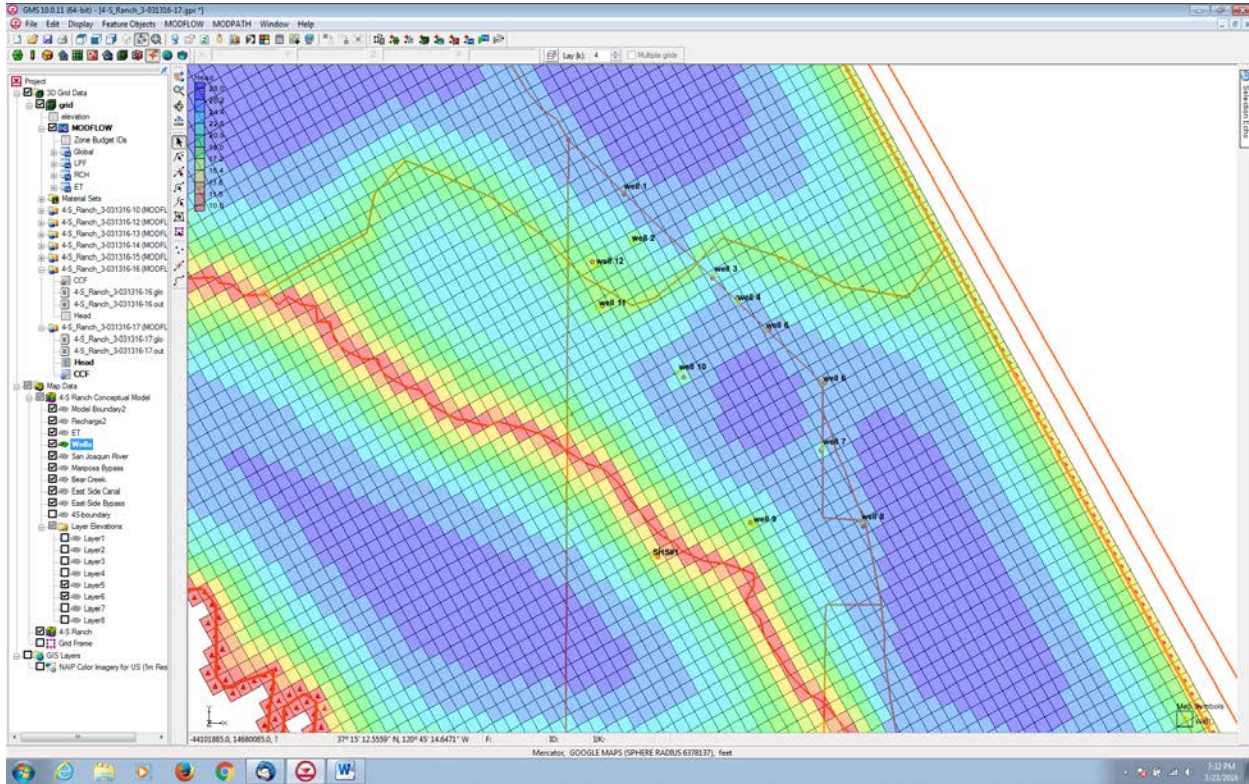


Figure 31. Average annual pumping was increased from 30 gal/min to 90 gal/min at the wells in 4-S Ranch that are mostly along the alignment of the East-side Canal. Note that the vertical scale has changed – so the dark blue color now represents the prior condition and light blue areas where water tables are diminished.

### 3.2.21 Viewing the Water Table in Side View

Another way of viewing the model output is in side view and 3-D projection mode.

For side view :

1. Select the *Select Cell* tool .
2. Select a cell somewhere near the well on the right side of the model.
3. Select the *Side View* button. Notice that the computed head values are used to plot a water table profile. Use the left and right arrow buttons in the mini-grid display to move back and forth through the grid. You should see a cone of depression close to each pumped well. As pumping at each well increases the cone of depression
4. When finished - select the *Plan View* button.

For 3-D projection mode (Figure 32):

1. Select the model frame in the main window.

2. On the top toolbar select *ortho mode*
3. In the center toolbar select *rotate*
4. The image may now be rotated to the best oblique angle to show the features the analyst wants to show.
5. As with the side-view mode – select an appropriate Z-magnification using the *Display* pull-down menu and *Display Options* to exaggerate the width of the layers in the z-direction.

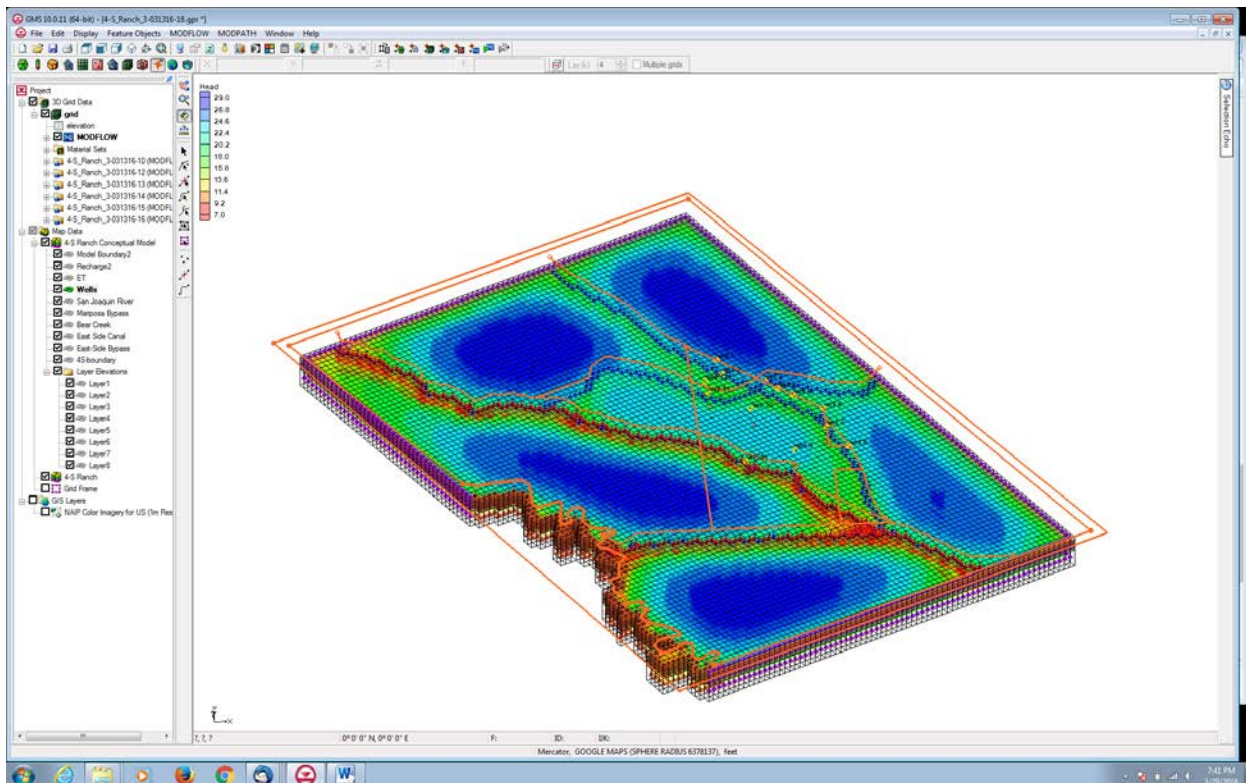


Figure 32. Visualization of the project area using GMS 3-D projection tools. The model frame can be rotated and viewed from a variety of angles to improve conceptual model understanding and reveal features that are not easily visualized in a plan projection mode. In addition 2-D slices of the model can be made to look in more detail at pump drawdown,

### 3.3. Summary

This section of the report has provided an overview of the use of GMS to develop a highly visual conceptual model that can be used as a first step to analyze the water resource problem at hand in a methodical and science-based manner. The methodology prompts the user to make assumptions about aspects of the hydrology that are important in ultimately coming up with a solution or medley of solutions from which the analyst must select from. In this way it can also guide data collection

and assimilation of essential information. For example, in the case of 4-S Ranch chosen for illustrative purposes in this exercise – source-sink arcs (rivers and other conveyances) are shown to play a very significant part in defining the hydrology of the project area. Hence, without spending large sums of money undertaking a fully-fledged modeling study – the analyst can conduct simple sensitivity experiments to ascertain the effect of certain hydrologic features such as Bear Creek, the East-side Canal and East-side Bypass on local hydrology and the ability of achieving sustainable pumping. The conceptual model approach can help set up the problem properly and act as a guide for an eventual modelling study.

Readers should note that this study was conducted without the necessary data and information reconnaissance of the project area that would be needed for development of a realistic model – hence any conceptual model results should be used appropriately.

## **4. Comparison of conceptual models of wetland hydrology using WARMF-SJR and CVHM**

### **4.1 Introduction**

In order to meet the needs of the agricultural industry, water and power companies dammed and diverted rivers in order to provide irrigation water and to drain wetlands, making space for farmland. This resulted in a loss of more than 95% of the wetlands and disruption of the natural cycle of seasonal wetlands in the valley (Igler, 2001). Historically, the wetlands would flood in the autumn and drain during the spring and summer. In order to reestablish the natural cycle, irrigation water is being pumped from the Sacramento – San Joaquin Delta and supplied to these seasonally managed wetlands (Quinn and Hanna, 2002; Quinn, 2004). Weirs control outflow from the wetlands into drainage channels and ultimately the San Joaquin River by varying weir board height. Water resource managers must vary irrigation inflow and outflow rates depending on time of year to meet flood up, maintenance, and drawdown schedules, while taking care not to overload the capacity of the canal systems that drain the wetlands. Wetland drawdown must occur slowly enough to allow a gradual exposure of seeds over time, which constitute a major protein source for waterfowl (Rahilly et al., 2010). Migratory birds traversing the Pacific Flyway overwinter in the wetlands and depend on these seeds as a source of protein (Quinn and Hanna, 2002; Quinn, 2006).

Managers must also monitor and control water salinity. Water pumped from the Delta and diverted into the wetlands contains salt. Evaporation of water from the wetlands increases salt concentration even further (Quinn, 2006). The wetlands are the source of 10 – 15% of the salt load in the San Joaquin River (Quinn and Hanna, 2002; Quinn, 2004).

The Watershed Assessment and Risk Management Framework (WARMF) and Central Valley Hydrologic Model 2 (CVHM2) are models that include the San Joaquin Basin wetlands. Water resource managers can use model output to make informed decisions about the timing and quantity of outflow from the wetlands. However, these models should be proven to be credible. Previous research found that the flow and salinity outputs for wetland drainage from the WARMF model were unrealistic – outflows did not match typical drawdown hydrology. In some cases, water mass balance output would be negative during wet years or positive during dry years, which is the opposite of expected values (Bergstrom, 2013, unpublished). The previous wetland conceptual sub-model treated the wetlands as if they were slow moving rivers. The new wetland conceptual sub-model treats wetland ponds as rectangular impoundments that are filled and drained. Model makers built in allowances to account for water mass balance losses due to evapotranspiration, seepage, and recharge.

The CVHM2 model calculates regional water flow. Surface inflow and outflow, including that to and from seasonally managed wetlands, is calculated using a subroutine called the farm process package that takes into account the differing evapotranspiration rates of various crops. The wetlands were simulated using the evapotranspiration rate of phreatophytes, which are plants typical to the wetlands. Using phreatophytes in these areas of the model also allows the model to simulate ponding of surface water. There is no input parameter time series, however, that allows the user to control the depth of the ponds over the flooded season. There is also no input parameter time series control file to account for a scheduled and controlled-rate outflow from these ponds

using weirs in the outlets. It remains to be seen how this model simulates the managed wetlands in the San Joaquin Valley.

## **4.2 Hypothesis**

The upgraded WARMF model should accurately calculate the flow and salinity of the wetlands. The model must be tested to ascertain whether it can account for the variations of quantity and timing of irrigation inflow and controlled releases of outflow that are used to maintain the flood up and drawdown schedule. In addition, it must be able to accurately account for the need to fully saturate the soil before water depth can accumulate, as well as losses thereafter due to seepage. The model also needs to accurately account for evapotranspiration. Wetland evapotranspiration differs from that of dry land. Wetland depth varies with time. As depth decreases, more land surface area is exposed, which allows vegetation to contribute to evapotranspiration. Wetland vegetation differs from dry land vegetation in that the evapotranspiration rates are higher. This effect is caused by a saturated root zone as well as motive flow, which is water drawn upward along the hollow plant stems by wind-induced low pressure at the top of the stems. Crop coefficients applied to wetland vegetation may require adjustment to allow for differences in evapotranspiration rate (Hall, 2007). My working hypothesis is that the upgraded WARMF model will more accurately reflect actual wetland flow than the CVHM2 model. I also hypothesize that the current WARMF model will produce a more accurate calculation of flow and salinity than the previous version.

## **4.3 Model Theory**

### **4.3.1 Central Valley Hydrologic Model(II)**

The CVHM2 model is the second iteration of the Central Valley Hydrologic Model (CVHM). It was developed using the United States Geological Survey (USGS) FORTRAN hydrologic code, Modflow-OWHM. The CVHM2 model was created and calibrated using historic observations, calculations, and measurements of the factors affecting hydrology, including geological and meteorological data from April 1961 until December 2013. The model divides the valley into one-mile by one-mile cells, which form a grid 98 cells wide and 441 cells long (Figure 1). The cells are grouped into zones that correspond to geographic areas of interest. The grid is also 13 layers deep in the vertical dimension, enabling the user to analyze subsurface water flow separately from surface water flow.

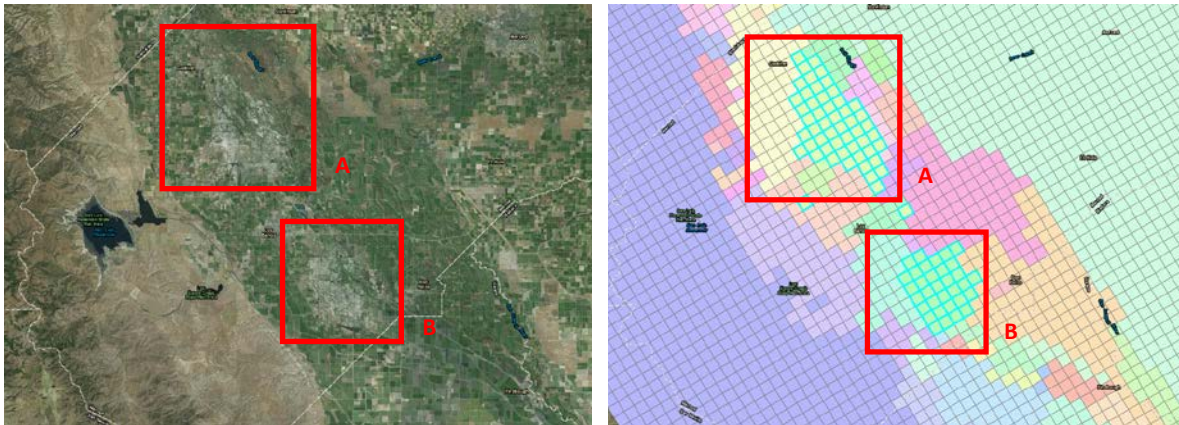


Figure 1: Satellite imagery of the North (A) and South (B) Grassland Water Districts. The districts are enclosed in red boxes (left). The CVHM grid overlay, as depicted in ArcGIS. Different colors represent different zones. The two zones representing the North and South Grassland Water Districts are enclosed in red boxes (right).

The model uses the farm process package (FMP) to simulate surface flow (Hanson et al., 2014). The output from this simulation results in a water budget, which accounts for all water mass into and out of the surface of each zone. The output time series is divided into monthly stress periods (calendar months). Each stress period is divided into two time steps of half a month each. Sources of water flow into the zone surface are precipitation, piped irrigation from external sources (non-routed deliveries), open-channel irrigation diverted from streams (semi-routed deliveries), wells, and evaporation/transpiration from ground water moving up to the surface from the aquifer (groundwater) (Figure 2). Water leaves the zone surface via evaporation/ transpiration of precipitation, open-channel irrigation water, and groundwater. It returns to streams by forming runoff over the ground or being channeled via open-channel drains (semi-routed delivery). Water may get pumped via wells or percolate down into the aquifer (deep percolation). Unused piped irrigation also will leave the zone (non-routed delivery). The only surface flows not accounted for by the FMP are streams (routed deliveries). Stream/river flow is calculated separately by the stream flow routing package (SFR). Stream flow into and out of each cell is calculated. Water flows into cell streams from neighboring cells located upstream, precipitation, runoff and drains (from FMP), and upflux from the underlying aquifer. Water leaves the stream via flow to cells downstream, diversions for irrigation (to FMP), evapotranspiration, and seepage down to aquifer. Horizontal and vertical subsurface (groundwater or aquifer) flow is calculated by the unsaturated zone flow package (UZF) and the groundwater flow process (GWP).

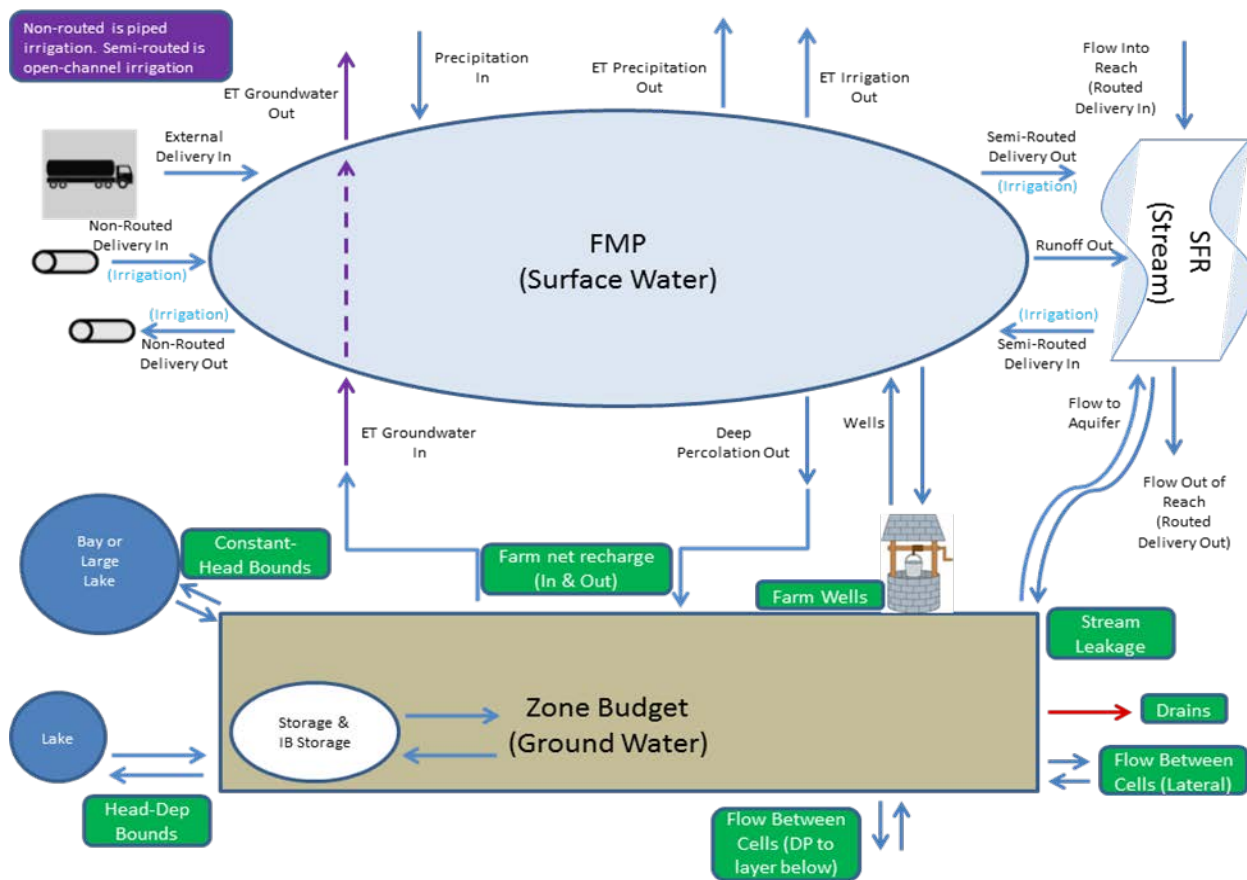


Figure 2: Relationships between Farm Process package (FMP), Stream Flow Routing package (SFR), and ZoneBudget.

CVHM2 model users utilize a tool called Zonebudget to divide CVHM2 model groundwater output into three dimensional, user-defined volumes or “zones” (Harbaugh, 1990). These zones can be further divided using vertical layers, allowing the user to analyze water flow passing between various layers in the groundwater system. The output time is divided into the same monthly stress periods as the CVHM2 model. As in the CVHM2 model, there are also two time steps per stress period, but the output only expresses the second time step each month. Zonebudget calculates groundwater budgets for each zone by summing groundwater stresses, change in storage, and flow to/from other zones. Stresses include recharge, stream leakage, rivers, lakes, neighboring cells, wells, drains, stream leakage, and deep percolation. Change in storage is total inflow minus total outflow and represents water added to or subtracted from storage. The limitation of Zonebudget, however, is that it only accounts for groundwater, thereby excluding surface water and streams.

#### 4.3.2 Watershed Analysis Risk Management Framework

The Watershed Analysis Risk Management Framework (WARMF) model was developed by Systech and is a GIS-based hydrologic model that calculates water flow and quality of a river basin (Goldstein, 2001; Herr et al., 2001). It was created and calibrated using historic meteorological, flow, and water quality data. The WARMF model divides watersheds into land catchments, stream segments, and reservoirs (Figure 3). Each catchment is assigned an averaged slope, orientation, surface roughness (Manning's number), and detention storage (ponds) for surface water.

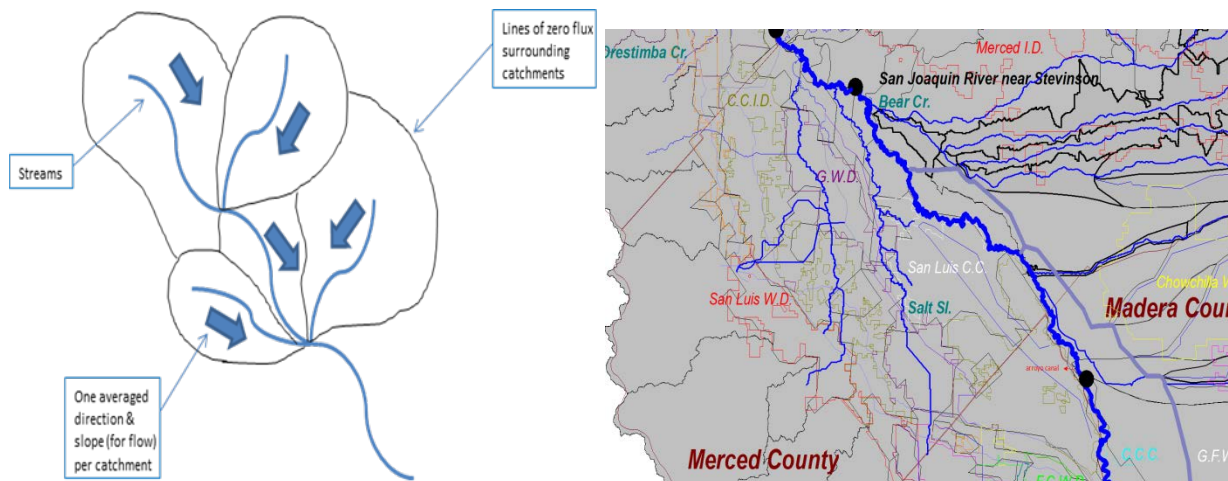


Figure 3: WARMF model flow (left). The watershed is divided into catchments, from which flows water into streams. WARMF interface (right). Catchments and streams can be selected using the interface in order to adjust input parameters or to acquire flow and salinity outputs.

There are also a variety of land uses that can be assigned to each catchment to reflect the various evapotranspiration rates of differing vegetation. Soil properties are divided into multiple layers and include hydraulic conductivity, saturated moisture content, and field capacity. Water drains from the land catchments to streams segments, which subsequently drain into reservoirs or other stream segments (figure 4). Chemical initial conditions and properties are also input into the model. This includes initial conditions for soil and stream segments, air and rain quality, fertilizer application, point sources of pollutants, and chemical reactions occurring within the plants, soil, and streams (Figure 5).

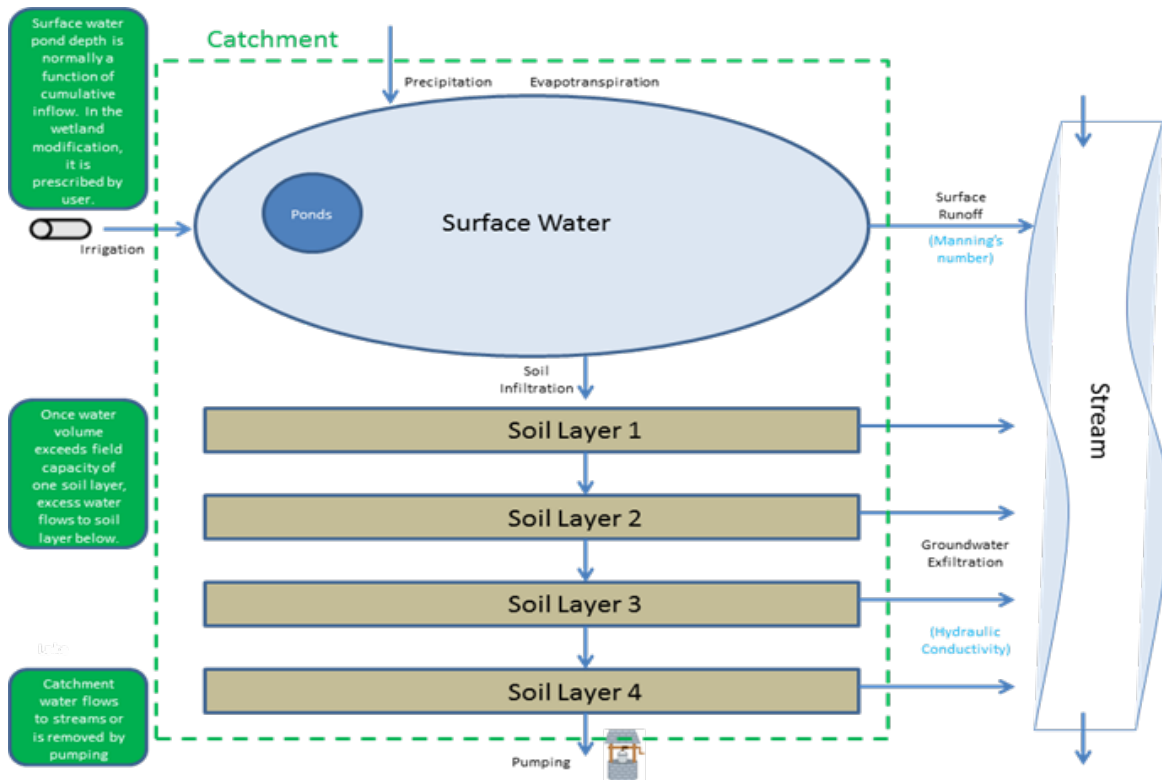


Figure 4: Water flow in the WARMF model through catchment to stream. Surface ponding used to be calculated as a fraction of cumulative inflow. In the wetland modification, pond depth can be prescribed by the user.

The latest model includes a sub-model for wetland simulation, which was formerly accomplished by treating wetlands as a wide stream slowly moving across the landscape. This worked for annual water balances but is not capable of producing the hydrology of a wetland drawdown where a considerable volume of water is introduced to the San Joaquin River of a period of 1 – 2 months. The new wetland sub-model was created and calibrated using historic observed water depth data for given land areas representing the wetlands, from which it can derive outflow necessary to maintain these depths (figure 6) (vanWerkhoven, 2015). It treats the wetlands as rectangular impoundments capable of holding a volume of stationary surface water and allows for the timed inflow and outflow of water according to the prescribed schedule for flood up, maintenance, and drawdown. The user can select the output time step. Output is provided separately for catchments and streams, and includes flow, velocity, sediment, and electrical conductivity data.

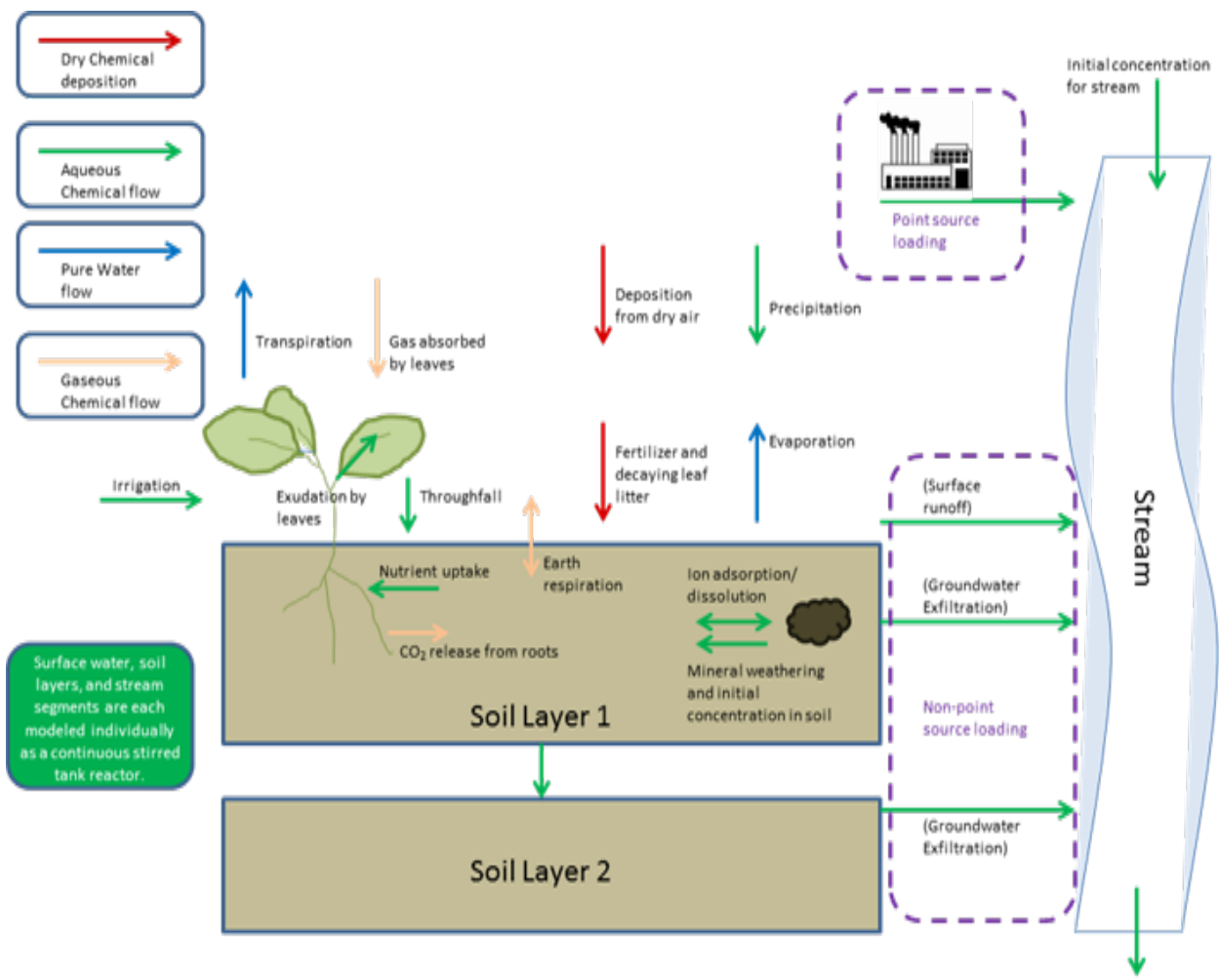


Figure 5: Chemical flow and processes in the WARMF model. Chemistry is incorporated with hydrology. Ions move with irrigation, precipitation, surface runoff, infiltration, and exfiltration water flows.

### 4.4 Procedure

Daily averaged observed water flow in cubic feet per second (cfs) and electrical conductivity (EC) data in microsiemens per centimeter ( $\mu\text{S}/\text{cm}$ ) covering the time period from May 2009 until April 2014 was collected from five stations located at wetland outlets (Figure B1). The flow data represents surface outflow from the wetlands to areas downstream. The EC data is directly related to the salinity of the water. Daily flow data was averaged over the course of a month in order to compare to CVHM2 model output.

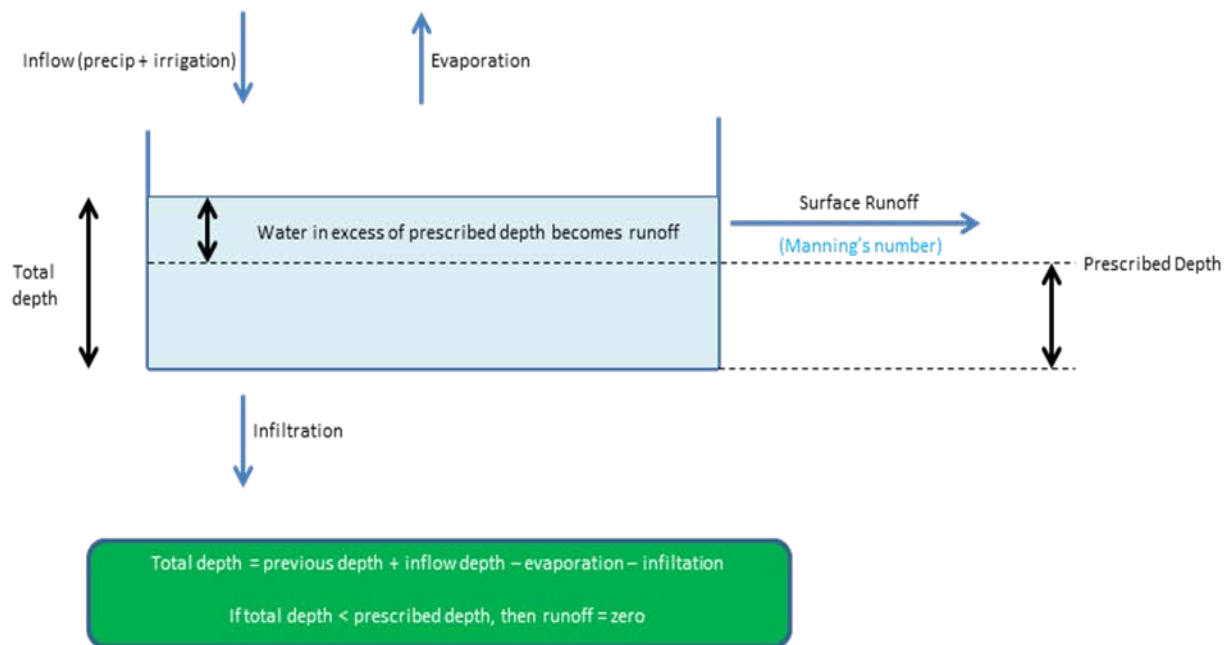


Figure 6: The wetland modification of the WARMF model. Outflow from the wetlands results from ponded water that is in excess of the user-prescribed depths.

SFR output from the CVHM2 simulation includes one stream that correlates to one of the five wetland outlet stations and a second stream that correlates to the other four wetland outlet stations. Flow data from this output is in average cubic meters per day for a month and was converted into cubic feet per second in order to be compared to observed flow at the corresponding stations. FMP output includes semi-routed and runoff data that represents the remainder of the outlets, however, the CVHM2 zone encompassing the wetlands includes large, diverse parcels of land that are not included in the study.

WARMF model simulations of both versions (new and old) of model were performed. Flow was divided into surface flow and subsurface flow, with the subsurface soil structure divided into 4 to 5 layers and totaling up to 15 feet in thickness. Wetland catchment surface and subsurface outflow, EC, and TDS output is in daily time steps, with flow in cubic feet per second, EC in  $\mu\text{mho}/\text{cm}$ , and TDS in  $\text{mg}/\text{L}$ . (The “ $\mu\text{mho}$ ” is equivalent to “ $\mu\text{S}$ ”; therefore no unit conversion is required.) Surface water and some subsurface water from catchments flow into streams. Stream flow, EC, and TDS data was also output. The stream flow and EC data were compared to observed flow and EC from the five stations. Simulated flows and EC were compared with observed flows and EC and a percent error was calculated using observations as references.

## 4.5 Results

The percent error tolerance used to compare simulated values to observed values was  $\leq 25\%$ . Percent error was calculated by computing the difference between cumulative simulated water volume and cumulative observed water volume, then dividing this by cumulative observed volume. Cumulative volumes were calculated for the entire study period.

### 4.5.1 Central Valley Hydrologic Model(II)

In order to compare simulated stream flow to observed stream flow, the CVHM2 model was run and output analyzed from the SFR (Stream Flow Routing) package. The period of study was from June 2009 to February 2012 for Los Baños Creek and from May 2009 to September 2013 for Mud Slough. (There was no observed data during May 2009 for Los Baños Creek.) The SFR package simulates streams that form due to overland runoff and precipitation while accounting for water mass losses due to evapotranspiration and percolation into the soil (flow to aquifer). Inflows and outflows were calculated for every “reach” of a stream in cubic meters per day. A “reach” represents the section of the stream within one model cell. SFR Stream #58 corresponds to Los Baños Creek, with Reach #29 corresponding to the location of the flow monitoring station. At certain points in time, the simulated outflow for Los Baños Creek (LBC) substantially exceeded observed outflow. At one point during the study period the simulated value was 91 times the observed value (Figure B2). This error was caused by an incorrect initial inflow into the creek, which at several points in time exceeds the maximum possible inflow of  $\sim 200$  cfs. This error occurs throughout the simulation time period, which extends beyond the study time period (Figure B3). According to the USGS, Los Baños Creek initial inflow was estimated using flow for Los Gatos Creek. This data was multiplied by 100 (an unrealistic assumption). In order to correct this, the outflow was manually recalculated using inflow without the multiplier. Flow to aquifer, which is dependent on water volume, was also readjusted. As a result of this correction, the error was reduced to 0.98% (Table A1 and Figure B4).

The CVHM2 model treats Mud Slough, Fremont Canal, Hollow Tree Drain, and S Lake as one stream (Stream #582); therefore, observed data from these four drains were added together and compared to SFR output for Stream #582. Reach #5 corresponds to the locations of the flow monitoring stations of Mud Slough, Fremont Canal, Hollow Tree Drain, and S Lake. When cumulative simulated flow volume was compared to cumulative observed flow volume, the error of 61.67% was found (Table A2). This higher level of accuracy when compared to flow for Los Baños Creek is attributed to the fact that there was no estimated initial inflow for Stream #582 in the simulation. The simulated flow is six months out of phase with observed flow (figure B5). The reason simulated volume in Mud Slough exceeded observed volume is that the combined flow of Los Baños Creek, Mud Slough, Fremont Canal, Hollow Tree Drain, and S Lake accounts for only roughly 85% of actual flow from the Grassland Water District, with most of the unaccountable flow occurring in the area of Mud Slough, Fremont Canal, Hollow Tree Drain, and S Lake. This rough percentage was estimated by Grassland Water District personnel. When station observations for Mud Slough, Fremont Canal, Hollow Tree Drain, and S Lake are adjusted to account for this,

the error between simulated and corrected observed flow was reduced to 34.29% (Table A3 and Figure B6).

In order to locate other possible sources of error, observed precipitation was compared to input precipitation in the Farm Process package (FMP) package, from May 2005 to September 2013. FMP input precipitation was consistent with observed precipitation from May 2005 until January 2010, with little discrepancy. After January 2010, however, FMP input precipitation diverges significantly from observed precipitation, with precipitation input maxima averaging over 3 times observed precipitation maxima (Figure B7). The input data is also 6 months out of phase with the observed data. Precipitation input affects many of the simulation outputs, including surface and ground water flow.

#### **4.5.2 Watershed Analysis Risk Management Framework**

In order to compare simulated stream flow to observed stream flow, the WARMF model simulation was run. The period of study was from June 2009 to April 2014 for Los Baños Creek and from May 2009 to April 2014 for Mud Slough. When cumulative simulated flow volume for Los Baños Creek (LBC) was compared to cumulative observed flow volume, an error of 19.68% was found (Table A4). This seems to be due to increased model error at high flow rates. When the first five months and the last three months of observed data were dropped due to suspected anomalies, the error decreased to 11.19% (Table A5). The timing of the simulated flow was in phase with observed flow (Figure B8).

The WARMF model treats Mud Slough, Fremont Canal, Hollow Tree Drain, and S Lake as one stream (Mud Slough), therefore, observed data from these four drains were added together and compared to WARMF model output for Mud Slough. When the cumulative simulated flow volume was compared to the cumulative observed flow volume, simulated volume was 2.5 times observed volume (Table A6 and Figure B9). Once again, the reason simulated volume in Mud Slough exceeded observed volume is that the combined flow of Los Baños Creek, Mud Slough, Fremont Canal, Hollow Tree Drain, and S Lake accounts for only roughly 85% of actual flow from the Grassland Water District, with most of the unaccountable flow occurring in the area of Mud Slough, Fremont Canal, Hollow Tree Drain, and S Lake. When station observations for Mud Slough, Fremont Canal, Hollow Tree Drain, and S Lake were adjusted to account for this, the error between simulated and corrected observed flow was reduced to 1.21% (Table A7 and Figure B10). The timing of the simulated flow was in phase with observed flow.

Analyzing the WARMF model EC output vs. observed output revealed some interesting information. When simulated EC was compared to observed EC in Los Baños Creek, it was found that observed values often decreased to zero (Figure B11). This is likely due to a limitation in the monitoring instruments. When observed flow was compared to observed EC, it was found that when the stream flow decreases to zero, the EC readout becomes zero (Figure B12). Observed values were then corrected to average out any readings less than 500  $\mu\text{S}/\text{cm}$ . There was also found to be a direct relationship between observed flow and observed EC in Los Baños Creek, which is not the norm. Normally in large rivers such as the San Joaquin River, flow and EC have an inverse

relationship. This is to be expected, because a higher flow results in greater dilution of salts. The WARMF model simulated EC in Los Baños Creek using this norm, which can be seen when comparing simulated flow with simulated EC (Figure B13). As a result, when the WARMF model simulated EC was compared to corrected observed EC, there remained a discrepancy (Figure B14). The error across the entire study period was at 40.90% (Table A8). During periods of initially increasing observed EC, however, the WARMF model output had greater correlation, and the error of 14.71% during these time periods was within tolerance. This is due the fact that the WARMF model simulates an initial rise in EC concurrent with an initial large spike in flow after an extended period of low flow. During the spike, flow and EC have a direct relationship. After the initial spike, however, the inverse relationship between flow and EC takes effect in the simulation, causing the subsequent discrepancy.

When simulated EC was compared to observed EC at Mud Slough, the findings were similar to those as Los Baños Creek, except that EC did not often become unrealistically low. The observed data, therefore, was not adjusted. There was once again better correlation between simulated EC and observed EC during periods of initially increasing EC, with an error of 21.73% compared to an error of 78.47% for the entire study period (Table A9 and Figure B15). This is once again due to observed flow and EC having a direct relationship (Figure B16) while the WARMF model simulated flow and EC with a mostly indirect relationship, with some periods of direct relationship during initial flow spikes (Figure B17). The direct relationship during initial flow spikes seems to be less pronounced in the Mud Slough simulation when compared to the Los Baños Creek simulation. This may explain the greater error in Mud Slough vs. Los Baños Creek.

In order to compare the latest version of the WARMF model output with the previous version of the model, errors between simulated and observed values from the older model were compared to errors between simulated and observed values from the newer model. When cumulative simulated flow volume for Los Baños Creek (LBC) was compared to cumulative observed flow volume, an error of 18.62% was found in the older version of the model (Table A10), which is almost the same as the error in the newer version (19.68%). This is to be expected, because in the simulation, Los Baños Creek does not draw upon the wetlands as a water source. Only the wetland flow was altered in the new version of the WARMF model, therefore, LBC flow in the older model was almost identical to flow in the newer model.

When analyzing Mud Slough, however, the alterations to the wetland flow calculations in the new model were evident. In the simulation, Mud Slough is partly fed by water flowing from the wetlands. As in the study of the new version of the model, the observed flow at Mud Slough was corrected to account for the roughly 15% of flow that bypasses monitoring stations. When cumulative simulated flow volume for Mud Slough was compared to the corrected cumulative observed flow volume, an error of 66.93% was found in the old version of the WARMF model (Table A11). This error was greater than the error in the newer model (1.21%). Also, in the older version of the model, the duration of periods of increased outflow was shorter than observed, while in the newer version, the duration of increased outflows was in sync with observed (Figure B18). This indicates improved model flow calculations in the newer version of the model.

The old model version's EC output was similar to the newer version's output, for both Los Baños Creek and Mud Slough (Figure B19). As with the newer version of the model, simulated EC did not correlate well with observed EC. When comparing the CVHM model flow output with the WARMF model flow output, it can be seen that the WARMF model flow output correlates better to observed values than the CVHM flow output. This is the case for both Los Baños Creek and Mud Slough (figure 20A).

## 4.6 Discussion

The WARMF model more accurately reflects actual wetland flow than the CVHM2 model. The CVHM2 simulated flow for Los Baños Creek exceeded observed flow by up to 91 times observed flow due to incorrect input for initial inflow; whereas the WARMF model simulation error for Los Baños Creek was within tolerance at 19.68%. For Mud Slough, the error between CVHM2 simulated flow and observed flow was 34.29%, and simulated values were about six months out of phase with observed values. It was subsequently found that output during the last forty-five months of the simulation time period (January 2010 – September 2013) was unreliable due to incorrect precipitation input. This input was also about six months out of phase with observed precipitation, as well as in excess of observed precipitation by three times observed values. The precipitation input prior to January 2010, however, matches weather station readings, but there was not enough observed data prior to January 2010 to make a valid comparison. The incorrect precipitation input may be part of the reason for the inaccurate flow output, given that both of them were six months out of phase. In the WARMF model, the cumulative volume of simulated flow was 2.5 times that of observed flow at Mud Slough, however, according to Grassland Water District personnel, roughly 15% of the total outflow from the wetlands bypasses the monitoring stations at Mud Slough. When observed values were corrected to account for this, using the rough estimate of 15%, the error was reduced to 1.21%. Also, the WARMF model flows were in phase with observed flows.

In comparison with the previous version of the WARMF model, the current version produces a more accurate calculation of flow, with an error of only 1.21%, compared to an error of 66.93% found in the older version of the model. The newer version's EC output, however, is not better than EC output from the older version. This is not surprising, given that both versions of the WARMF model assume a mostly inverse relationship between flow and EC, which is usually an accurate assumption for larger rivers like the San Joaquin River. Masses of a variety of salts are used as initial inputs into the WARMF model. Greater flow leads to greater dilution of these salts and lower EC. The unexpected reality, however, is that in the canals and sloughs of the Grassland Water District wetlands, there is a more direct relationship between flow and EC, as evidenced by observed values. This is caused by water being kept in shallow ponds with large surface areas for an extended period of time. During this time, EC increases as salts become more concentrated due to evaporation. The water is then released, causing a large, simultaneous increase in both flow and EC. This led to the lack of correlation between the simulated and observed EC values. Since this is a deviation from the accepted norm, a new method of relating flow and EC needs to be created for wetland streams, sloughs, and canals. This new method could then be employed by models such as WARMF to create more accurate calculations of EC. Another limitation to the WARMF

model is the need to account for the flow that bypasses the monitoring stations when comparing simulated flow to observed flow in Mud Slough. The WARMF model assumes that all of the water flows out of the catchments via a limited number of streams. The untested assumption, however, is that ~15% of the water bypasses the main outlet conveyances flowing out of Grassland Water District. Observed values in Mud Slough have to be adjusted to account for this. In addition, the WARMF model's simulated flow accuracy decreases during periods of unusually high observed flow in Los Baños Creek.

Sources of error in this study include occasional gaps in observed data due to equipment malfunction. Other sources of error are the unrealistically low observed EC readings during periods of low flow. A reading of less than 500  $\mu\text{S}/\text{cm}$  was used as the cutoff for unreliable data. Finally, 15% is a rough estimate of how much wetland outflow is unaccounted for by the monitoring stations.

## **4.7 Conclusions**

Provided the limitations of the model are accounted for, the current version of the WARMF model provides a more accurate conceptual model of wetland flow than both the CVHM2 model and the previous version of the WARMF model. The WARMF model EC output, however, is still inaccurate. A new method of calculating EC for wetland canals, sloughs, and streams should be created to improve the WARMF model EC output accuracy. The findings also imply that research on the relationship between monitoring station readings of flow and EC in the wetlands could be useful in correcting station EC readings during periods of low flow. Once these improvements are made, it may become possible for wetland managers to use the WARMF model as a decision-making tool. Forecast weather could even be input into the model to simulate flow and EC in the future in order to help determine how to allocate water resources to the benefit of both the wildlife and the agricultural industry.

## **5. References**

- Argent, R.M., 2009. Components of Adaptive Management, In: Allan, C., Stankey, G.H. (Eds.), Adaptive Environmental Management. Springer Science and Business Media, pp. 11-38.
- Aragues, R., K.K. Tanji and J. Faci, 1990. Conceptual irrigation return flow hydrosalinity model, in Agricultural Salinity assessment and Management, K.K. Tanji (Editor), Amer. Soc. Civil Eng., Manuals and Reports of Engineering Practice, No. 71
- Axelrod, R., 1976. The structure of decision: The cognitive maps of political elite, Princeton University Press, Princeton, NJ.
- Belitz, K., 1988. Character and evolution of the ground water flow system in the central part of the western San Joaquin Valley, California. United States Geol. Surv., Open File Report 87-573. 34 p.
- Belitz, K., 1990. Character and evolution of the ground water flow system in the central part of the western San Joaquin Valley, California. United States Geol. Surv., Water Supply Paper, 2348, 28 p.
- Belitz, K. and S.P. Phillips, 1993. Simulation of water table response to management alternatives, central part of the western San Joaquin Valley, California, United States Geol. Surv., Water Resources Investigation Report, 91-4193, 41 p.
- Belitz, K. and S.P. Phillips, 1995. Alternatives to agricultural drains in California's San Joaquin Valley: Results of regional scale hydrogeologic approach, *Water Resources Res.*, 31 (8), 1845-1862.
- Belitz, K., S.P. Phillips and J.M. Gronberg, 1991, Numerical Simulation of Groundwater Flow in the Central Part of the Western San Joaquin Valley, California, United States Geol. Surv. Open File Rept., 91-535, 71 p.
- Belitz, K., S.P. Phillips and J.M. Gronberg, 1993, Numerical Simulation of Groundwater Flow in the Central Part of the Western San Joaquin Valley, California, United States Geol. Surv. Water Supply Paper 2396, 69 p.
- Ben-Asher, J. and J.E. Ayars, 1990. Deep seepage under non-uniform sprinkler irrigation, *Amer. Soc. Civil Eng., Jour. Irr. and Drainage Div.*, 116(3), 354-362.
- Cardon, G.E. and J. Letey, 1992b. Soil-based irrigation and salinity management model, 1. Plant water uptake calculations, *Soil Sci. Soc. Amer. Jour.*, 56 (6), 1881-1886.
- Cardon, G.E. and J. Letey, 1992c. Soil-based irrigation and salinity management model, 2. water and solute movement calculations, *Soil Sci. Soc., Amer. Jour.*, 56 (6), 1887-1892.
- Carlson, G.A., D. Zilberman and J.A. Miranowski, 1993. Agricultural and Environmental Resource Economics, Oxford University Press, New York, 523 p.
- Davis, G.H. and T.B. Copen, 1989, Late Cenozoic plaeohydrogeology of the Western San Joaquin Valley, as related to structural movements in the Central Coast Ranges, Special Paper 234, Geological Society of America, 40 p.
- Deverel, S.J. and J. Fio, 1991, Groundwater flow and solute movement to drain laterals, Western San Joaquin Valley, California, 1. Geochemical assessment, *Water Resources Res.*, 27 (9), 2233-2246.
- Dinar, A., M.D. Aillery and M.R. Moore, 1993. A dynamic model of soil salinity and drainage generation in irrigated agriculture: A framework for analysis, *Water Resources Res.*, 29 (6), 1527-1537.
- Doneen, L.D., 1967, Quality of percolating waters, I. properties of deep substrata materials in the west side of the San Joaquin Valley, California, *Hilgardia*, 38 (9), 285-305.

- Dubrovski, N.M., J.M. Neil, R. Fujii and R.S. Orelan, 1990. Influence of redox potential on selenium distribution in ground water, Mendota, western San Joaquin Valley, California. United States Geol. Surv., Open File Rept., 90-138.
- Dutt, G.R., 1962, Prediction of the concentration of solutes in soil solutions for soil systems containing gypsum and exchangeable Ca and Mg, *Soil Sci. Soc. Amer., Proc.*, 26, 341-343.
- Dutt G.R. and K.K. Tanji, 1962, Prediction of concentrations of solutes in water percolated through a column of soil, *Jour. Geophys. Res.*, 67 (9), 3437-3439.
- Felmy, A.R., D.C. Girvin and E.A. Jenne, 1984. MINTEQ: A computer program for calculating aqueous geochemical equilibria, NIIS PB84-157148 National Technical Information Service, Springfield Virginia.
- Fio, J.L., 1994. Calculation of water budget and delineation of sources to drain-flow in western San Joaquin Valley, California, United States Geological Survey, Open File Rept., 94-35. 28 p.
- Fio, J.L. and S.J. Deverel, 1991, Groundwater flow and solute movement to drain laterals, Western San Joaquin Valley, California, 2. Quantitative hydrologic assessment, *Water Resources Res.*, 27 (9), 2247-2257.
- Forrester, J. (1973). World Dynamics. Waltham, MA: Pegasus Communications.
- Funtowicz S.O. and Ravetz J.R. ,1993. Science for the Post-normal Age, *Futures* 25, 739-755.
- Giupponi, C. and Sgobbi, A., 2007. Models and decision support systems for participatory decision making in integrated water resource management, In: Koundouri, P. (ed.), *Coping with water deficiency. From research to policy making*, Springer, 165-186.
- Goldstein, R.A. 2001. Watershed Analysis Risk Management Framework (WARMF): Update One.
- Grismer, M.E, 1989. Drainage efficiency and drain water quality, In *Land and Water Use*, Editors Dodd and Grace, Balkens, Rotterdam, 285-290.
- Grismer, M.E, 1993. Subsurface drainage system design and drain water quality, *Amer. Soc. Civil Eng., Jour. Irr. and Drain. Eng.*, 119(3), 537-543.
- Grismer, M.E, 1993. Subsurface drainage system distribution and drain water quality, *Amer. Soc. Civil Eng., Jour. Irr. and Drain. Eng.*, 119 (3), 537-543.
- Grismer, M.E. and R.C. Woodring, 1987. Assessment of lateral groundwater flows in the SJV., *California Agriculture*, March-April, 22-23.
- Gronberg, J.M., K. Belitz and S.P. Phillips, 1990. Distribution of wells in the central part of the western San Joaquin Valley, California. United States Geol. Surv., Water Resources Investigations Rept., 89-4158.
- Hall, A. 2007. Estimating Evaporative Transpiration of Wetlands in the San Joaquin Valley.
- Hanson, R.T, S.E. Boyce, W. Schmid, J.D. Hughs, S.M. Mehl, S.A. Leake, T. Maddock III, and R.G. Niswonger. 2014. One-Water Hydrologic Flow Model (MODFLOW-OWHM)
- Hanson, B.R., Grattan, S.R., Fulton, A., 2006. Agricultural Salinity and Drainage. Division of Agriculture and Natural Resource Publication 3375, University of California Irrigation program, University of California, Davis
- Harbaugh, A.W. 1990. A Computer Program for Calculating Subregional Water Budgets Using Results from the U.S. Geological Survey Modular Three-dimensional Finite-difference Ground-water Flow Model

- Hatchett, S.A., Quinn, N.W.T., Horner, G.L., Howitt, R.E., 1989. A drainage economics model to evaluate policy options for management of selenium contaminated drainage. Toxic Substances in Agricultural Water Supply and Drainage. Proceedings of the Second Pan American Regional Conference on Irrigation and Drainage, Ottawa, Ontario, June 8-9.
- Hatchett, S.A., N.W.T. Quinn, G.L. Horner and R.E. Howitt, 1989. Drainage Economics Model to Evaluate Policy Options for Managing Selenium Contaminated Drainage. Proc. of the International Committee on Irrigation and Drainage. Toxic Substances in Agricultural water Supply and Drainage - An International Perspective, Ottawa, Canada.
- Herr, J., Weintraub, L., Chen, C.W., 2001. User's Guide to WARMF-documentation of Graphical User Interface. Electrical power research institute.
- Igler, David. 2001. Industrial cowboys: Miller & Lux and the transformation of the Far West, 1850-1920.
- Keller, A.A., 2007. User's Guide for Developing a WARMF 6.2 Watershed Model Using BASINS 4.0.
- Knapp, K.C., 1992a, Irrigation management and investment under saline limited drainage conditions, 1. Model formulation, *Water Resources Res.*, 3085-3090.
- Knapp, K.C., 1992b, Irrigation management and investment under saline limited drainage conditions, 2. Characterization of optimal decision rules, *Water Resources Res.*, 3091-3097.
- Knapp, K.C., 1992c, Irrigation management and investment under saline limited drainage conditions, 3. Policy analysis and extensions, *Water Resources Res.*, 3099-3109.
- Knapp, K.C. and D. Wichelns, 1990. Dynamic optimization models for salinity and drainage management, in *Agricultural Salinity Assessment and Management*, K.K. Tanji (Editor) Amer. Soc. Civil Eng., Manuals and Reports of Engineering Practice, No. 71.
- Kok, K., 2009. The potential of Fuzzy Cognitive Maps for semi-quantitative scenario development, with an example from Brazil, *Global Environmental Change* 19 122–133.
- Kosko, B. 1986. Fuzzy cognitive maps, *International Journal of Man-Machine Studies* 24 (1) 65–75
- Lempert, R.J., 2003. Shaping the next one hundred years: new methods for quantitative, long-term policy analysis. Rand Corporation.
- León, Elizabeth., and Ferré, Ty., 2003. “A Conceptual Model of Groundwater Flow in the Upper Agua Fria”, Rural Watersheds Initiative Grant from the Arizona Department of Water Resources.
- Mattigod, S.V. and G. Sposito, 1979. Chemical modeling of trace metal equilibria in contaminated soil solutions using the computer program GEOCHEM, in *Chemical Modeling in Aqueous Systems*, Amer. Chem. Soc. Symp. Ser., Editor E.A. Jenne, 93, 837-856
- Minns, S.A., 1993. Conceptual Model Ground-Water Flow in the Eastern Kentucky Coal Field, Kentucky Geological Survey 0075-5621
- Nimah, M.N. and R.J. Hanks, 1973. Model for estimating soil, water, plant and atmospheric interrelations: I. Description and sensitivity. *Soil Sci. Soc. Amer. Jour.*, 37, 522-527.
- Orlob, G.T, 1991. San Joaquin salt balance: Future prospects and possible solutions, in *The Economics and Management of Water and Drainage in Agriculture*, A. Dinar and D. Zilberman (Editors) Kluwer Publishing Co., 143-167.

- Özesmi, U. and Özesmi, S. L., 2004. Ecological models based on people's knowledge: a multi-step fuzzy cognitive mapping approach, *Ecological modelling* 176, pp 43-64.
- Parkhurst, D.L., D.C. Thorstensen and L.N. Plummer, 1980. PHREEQE: A computer program for geochemical calculations, United States Geol. Surv., Water Resources Investigation Rept., 86-167801.
- Popper, S.W., Lempert, R.J., Bankes, S.C. (2005). Shaping the future. *Scientific American* 292(4) 66-71.
- Presser, T.S., W.C. Swain, R.R. Tidball and R.C. Severson, 1991. Geologic sources, mobilization and transport of selenium from the California coast ranges to the western San Joaquin Valley: A reconnaissance study. United States Geol. Surv., Water Resources Investigations Rept., 90-4070. 66 p.
- Quinn, N.W.T. 2006. Bottom-up, decision support system development: a wetland salinity management application in California's San Joaquin Valley.
- Quinn, N.W.T. 2004. Wetland Plant Guide for Assessing Habitat Impacts of Real-Time Salinity Management.
- Quinn, N.W.T. and W.M. Hanna. 2002. Real-time management of seasonal wetland drainage to satisfy salinity TMDL objectives in California's Grasslands basin.
- Rahilly, P, N.W.T. Quinn, J.A. Beam, D.L. Widell, R. Ortega, W. Cook, L. Sparks, M. O'Dell. 2010. Wetland Response to Modified Hydrology with Respect to Salinity Management: Biological Monitoring.
- Rhoades, J.D., Suarez, D.L., 1977. Reducing water quality degradation through minimized leaching management. *Agriculture water management*, Vol.1, Issue. 2, PP. 127-142.
- Salinity and Drainage Task Force, 1992, Principal Accomplishments, 1985-1990, Division of Batural Resources, University of California, 95 p.
- San Joaquin Valley Drainage Program, 1990. A Management Plan for Agricultural Subsurface Drainage and Related Problems on the Western San Joaquin Valley, 183 p.
- Schoups, G and J.W. Hopmans, C.A. Young, J.A. Vrugt, W.W. Wallender, K.K. Tanji, and S. Panday. 2005. Sustainability of irrigated agriculture in the San Joaquin Valley, California. *PNAS*. 102:43 15352-15356
- Scott, A. C., J. E. Clayton, and E. L. Gibson, 1991. A practical guide to knowledge acquisition. Addison-Wesley Publishing Company. Reading, Massachusetts. 509 pages.
- Simunek, J. and D.L. Suarez, 1993. Modeling of carbon dioxide transport and production in soil, I. Model Development, *Water Resources Res.*, 29(2), 487-497.
- Singhal V. and R. Goyal, 2011. Development of conceptual groundwater flow model for Pali Area, India. *African Journal of Environmental Science and Technology* 5 (12), 1085-1092
- Sojda, R.S., S.H. Chen, S. El Sawah, J.H.A. Guillaume, A.J. Jakeman, S. Lautenbach, B.S. McIntosh, A.E. Rizzoli, R. Seppelt, P. Struss, A.A. Voinov, and M. Volk., 2012. Identifying the decision to be supported: a review of papers from Environmental Modelling and Software. In: Proceedings of the Sixth Biennial Meeting of the International Environmental Modelling and Software Society (iEMSs 2012): Managing Resources of a Limited Planet. R. Seppelt, A.A. Voinov, S. Lange, D. Bankamp, eds. Leipzig, Germany. <http://www.iemss.org/society/index.php/iemss-2012-proceedings>. Argent, R.M. et al. / *Best Practice in Conceptual Modelling*.
- Suarez, D.L. and J. Simunek, 1993. Modeling of carbon dioxide transport and production in soil,

2. Parameter selection, sensitivity analysis and comparison of model prediction to field data, *Water Resources Res.*, 29(2), 499-513.
- Suarez, D.L., 1989. Impact of agricultural practices on groundwater salinity. *Agric. Ecosystems Environ.*, 26: 215-227
- Tanji, K.K., 1990. Nature and extent of agricultural drainage, in *Agricultural Salinity Assessment and Management*, K.K. Tanji (Editor), Amer. Soc. Civil Eng. Manuals and Reports of Engineering Practice, No. 71, 1-17.
- Tanji, K.K., L.D. Doneen, G.V. Ferry and R.S. Ayers, 1972. Computer simulation analysis on reclamation of salt-affected soil in San Joaquin Valley, California, *Soil Sci. Soc. Amer. Proc.*, 36 (1), 127-133.
- Toth, J, 1963. A theoretical analysis of groundwater flow in small drainage basins. *Jour. Geophys Res.*, 68, 4795-4812.
- van Genuchten, M.Th., 1987. A numerical model for water and solute movement in and below the root zone, Research Rep. 121, United States Salinity Laboratory, Riverside, California.
- vanWerkhoven, Katie. 2015. Technical Memorandum: WARMF Model Upgrade to Simulate Managed Wetland Operations
- Voinov, A.A. , 2008. Conceptual Diagrams and Flow Diagrams In *Encyclopedia of Ecology*, Jørgensen, S.E. and Fath, B.D. (eds) 731–7. Elsevier.
- Voinov, A.A. and Bousquet, F., 2010. “Modelling with Stakeholders.” *Environmental Modelling & Software* 25 (May): 1268–1281. doi:10.1016/j.envsoft.2010.03.007. <http://linkinghub.elsevier.com/retrieve/pii/S1364815210000538>.
- Williamson, A.K., D.E. Prudic and L.A. Swain, 1985, Ground-water flow in the Central Valley, California, United States Geol. Surv., Open File Rept., 85-345, 203 p.
- Willis, Robert., 2014, “Conceptual Groundwater Model of Sea Level Rise in the Humboldt Bay Eureka-Arcata Coastal Plain .” Coastal Ecosystems Institute of Northern California. [http://humboldt-bay.org/sites/humboldt-bay2.org/files/Final\\_HBSLR\\_ConceptualGroundwaterModel\\_141209.pdf](http://humboldt-bay.org/sites/humboldt-bay2.org/files/Final_HBSLR_ConceptualGroundwaterModel_141209.pdf)
- Wolery, T.J, 1979. Calculation of Chemical equilibrium between aqueous solutions and minerals: The EQ 3/6 Software Package, UCRL-52658, Lawrence Livermore National Laboratory.
- Yao et al., 2014, “Conceptual and numerical models for groundwater flow in an arid inland river basin” .hydrological processes, Wiley Online Library. DOI: 10.1002/hyp.10276. [https://www.researchgate.net/profile/Chunmiao\\_Zheng/publication/263473747\\_Conceptual\\_and\\_numerical\\_models\\_for\\_groundwater\\_flow\\_in\\_an\\_arid\\_inland\\_river\\_basin/links/53dfa2f50cf2aede4b4918a4.pdf](https://www.researchgate.net/profile/Chunmiao_Zheng/publication/263473747_Conceptual_and_numerical_models_for_groundwater_flow_in_an_arid_inland_river_basin/links/53dfa2f50cf2aede4b4918a4.pdf)

## 5.1 Webography

- Bergstrom, H. 2013. Evaluation of Watershed Models for Simulation of Salt Mass Balance of Seasonally Managed Wetlands in the San Joaquin River Basin. Available at [http://esd1.lbl.gov/FILES/research/projects/heads/Research\\_Report\\_Bergstrom\\_Helen\\_SU\\_LI\\_Summer\\_2013.pdf](http://esd1.lbl.gov/FILES/research/projects/heads/Research_Report_Bergstrom_Helen_SU_LI_Summer_2013.pdf) >

California Department of Water Resources (DWR), 2015. Statewide integrated water Management, California water plan, San Joaquin River Region. Available at < <http://www.waterplan.water.ca.gov/previous/b160-93/b160-93v2/SJRR.cfm> > Consulted on May 11, 2015

## 6.0 Annexes

### Annex 1

#### Water unit

**1 hectare**= 2.47105 acre

**1 acre** = an area of land that is 43560 ft<sup>2</sup>

**1 acre-foot** = 43560 ft<sup>2</sup> x 1 foot water depth = a volume that is 43560 ft<sup>3</sup>

**1m<sup>3</sup>**= 35.31467ft<sup>3</sup>

English Unit			
0.3 to 3.2 tons of salt ha <sup>-1</sup>		0.12 to 1.29 tons of salts acre <sup>-1</sup>	
6200 to 9300 m <sup>3</sup> ha <sup>-1</sup>	2509.05 to 3763.58 m <sup>3</sup> acre <sup>-1</sup>	2.03 to 3.05 acre-ft/acre	
1000m <sup>3</sup>	35314.67 ft <sup>3</sup>	0.81 acre-ft	0.06 to 3.95 tons per acre-ft

### Annex 2

#### Unit conversation

1 m = 100 cm

Load= flow \* concentration → Concentration= Load/flow

**1 sq.m** = 10.76 sq.ft

**1 m<sup>3</sup>** = 35.313 ft<sup>3</sup>

**1hour** = 3600 second

**1day** = 24 hours

**1day** = 86400 second

**1 year** = 365 day

**1 year** = 31536000 second

**1cubic water**= 1000 Litter

**1 Kilogram**= 10<sup>6</sup> milligram

**1 acre** = 4046.85 m<sup>2</sup>

**1 hectare**= 10000 m<sup>2</sup>

## 6.1 List of Abbreviations and Acronyms

cft: Cubic foot

cm = Centimeter

CVP: Central Valley Project

DSS: Decision Support System

EC: Electrical Conductivity  
ESD: Earth Science Division  
ETo= Evapotranspiration  
Ft: foot  
GIS: Geographic Information System  
GUI: Graphical User Interface  
ha: Hectare  
HEADS: Hydro Ecological Engineering Advanced Decision Support  
In= Inch  
LBNL: Lawrence Berkeley National Laboratory  
m = Meter  
m<sup>3</sup>:Cubic meter  
mg<sup>l</sup><sup>-1</sup>: Milligram per liter  
mS/cm: Micro Siemens per centimeter  
my<sup>-1</sup>: Meter per year  
NAS: National Academy of Science  
ppm: part per million  
SJB: San Joaquin Basin  
SJV: San Joaquin Valley  
sq.ft: Square foot  
sq.m: Square meter  
SWP: California Water Plan  
TDS: Total Dissolved Solid  
TMDLs: Total Maximum Daily Loads  
U.S: United States  
UCB: University of California Berkeley  
USEPA: United States Environmental Protection Agency  
USGS: United States Geological Survey  
WADE: Westside Agriculture Drainage Model  
WARMF: Watershed Analysis Risk Management Framework

# APPENDIX A

## Tables A1- A11

Table A1: Corrected CVHM Los Baños Creek flow volume per month (calculated with more realistic inflows) compared to observed flow volume per month at Los Baños Creek. Cumulative volume and percent error were calculated.

	Stress Period	Month	Corrected SFR (LBC) - 10 <sup>6</sup> ft <sup>3</sup>	Observed (LBC) - 10 <sup>6</sup> ft <sup>3</sup>
2	579	Jun-09	7.83	20.44
3	580	Jul-09	14.50	6.97
4	581	Aug-09	12.25	11.37
5	582	Sep-09	5.22	11.89
6	583	Oct-09	5.75	177.84
7	584	Nov-09	1.59	33.02
8	585	Dec-09	44.60	34.83
9	586	Jan-10	71.91	109.03
10	587	Feb-10	60.09	180.13
11	588	Mar-10	78.39	167.73
12	589	Apr-10	89.01	109.21
13	590	May-10	97.02	53.98
14	591	Jun-10	98.60	77.22
15	592	Jul-10	103.00	55.42
16	593	Aug-10	92.74	25.16
17	594	Sep-10	75.06	7.37
18	595	Oct-10	62.44	53.62
19	596	Nov-10	43.97	53.21
20	597	Dec-10	44.80	85.99
21	598	Jan-11	56.30	71.82
22	599	Feb-11	77.51	52.24
23	600	Mar-11	230.59	157.48
24	601	Apr-11	151.05	94.84
25	602	May-11	130.05	46.13
26	603	Jun-11	111.67	91.06
27	604	Jul-11	112.02	63.89
28	605	Aug-11	102.53	44.71
29	606	Sep-11	81.04	33.79
30	607	Oct-11	64.61	49.46
31	608	Nov-11	44.16	83.42
32	609	Dec-11	30.25	92.76

33	610	Jan-12	27.38	52.46
34	611	Feb-12	30.88	28.29
		Sum:	2258.81	2236.81
		Percent Error:	$100\% \times \frac{ \text{output sum} - \text{observed sum} }{\text{observed sum}} =$	0.98%

Table A2: CVHM flow volume per month compared to observed flow volume per month at Mud Slough, Fremont Canal, Hollow Tree Drain, S Lake. Cumulative volume and percent error were calculated.

	Stress Period	Month	SFR (Stream #582) - 10 <sup>6</sup> ft <sup>3</sup>	Observed (Mud, Frem, HT, S) - 10 <sup>6</sup> ft <sup>3</sup>
1	578	May-09	0.11	31.62
2	579	Jun-09	0.00	13.42
3	580	Jul-09	0.00	0.00
4	581	Aug-09	0.00	0.00
5	582	Sep-09	0.00	28.87
6	583	Oct-09	0.00	119.42
7	584	Nov-09	0.00	72.30
8	585	Dec-09	0.00	103.02
9	586	Jan-10	6.91	144.46
10	587	Feb-10	17.25	95.53
11	588	Mar-10	51.52	134.57
12	589	Apr-10	72.59	71.12
13	590	May-10	91.72	44.89
14	591	Jun-10	109.66	69.84
15	592	Jul-10	132.45	32.44
16	593	Aug-10	149.69	22.42
17	594	Sep-10	144.23	22.45
18	595	Oct-10	145.81	175.63
19	596	Nov-10	129.64	209.72
20	597	Dec-10	129.06	258.84
21	598	Jan-11	128.11	230.38
22	599	Feb-11	120.66	169.34
23	600	Mar-11	156.76	209.97
24	601	Apr-11	176.16	151.68
25	602	May-11	206.00	67.78
26	603	Jun-11	217.17	68.70
27	604	Jul-11	246.66	2.98

28	605	Aug-11	245.10	2.86
29	606	Sep-11	232.76	16.31
30	607	Oct-11	231.79	178.10
31	608	Nov-11	207.27	234.53
32	609	Dec-11	200.06	198.91
33	610	Jan-12	184.70	226.70
34	611	Feb-12	168.71	150.78
35	612	Mar-12	186.96	104.73
36	613	Apr-12	190.68	46.05
37	614	May-12	211.34	3.68
38	615	Jun-12	213.75	23.84
39	616	Jul-12	231.78	4.09
40	617	Aug-12	239.89	3.63
41	618	Sep-12	224.34	12.99
42	619	Oct-12	223.58	124.63
43	620	Nov-12	204.09	158.53
44	621	Dec-12	197.82	227.08
45	622	Jan-13	184.69	192.44
46	623	Feb-13	164.12	166.21
47	624	Mar-13	193.01	156.06
48	625	Apr-13	197.08	42.64
49	626	May-13	218.87	31.03
50	627	Jun-13	223.08	21.40
51	628	Jul-13	242.71	3.20
52	629	Aug-13	249.06	0.11
53	630	Sep-13	233.27	24.64
		Sum:	7932.69	4906.58
		Percent Error:	$100\% \times \frac{ \text{output sum} - \text{observed sum} }{\text{observed sum}} =$	61.67%

Table A3: CVHM flow volume per month compared to corrected observed flow volume per month at Mud Slough, Fremont Canal, Hollow Tree Drain, S Lake. Cumulative volume and percent error were calculated.

	Stress Period	Month	SFR (Stream #582) - 10 <sup>6</sup> ft <sup>3</sup>	Corrected Observed (Mud, Frem, HT, S) - 10 <sup>6</sup> ft <sup>3</sup>
1	578	May-09	0.11	77.80
2	579	Jun-09	0.00	33.01
3	580	Jul-09	0.00	0.00
4	581	Aug-09	0.00	0.01
5	582	Sep-09	0.00	71.04
6	583	Oct-09	0.00	293.81
7	584	Nov-09	0.00	177.88
8	585	Dec-09	0.00	253.46
9	586	Jan-10	6.91	355.42
10	587	Feb-10	17.25	235.04
11	588	Mar-10	51.52	331.08
12	589	Apr-10	72.59	174.97
13	590	May-10	91.72	110.45
14	591	Jun-10	109.66	171.82
15	592	Jul-10	132.45	79.82
16	593	Aug-10	149.69	55.15
17	594	Sep-10	144.23	55.24
18	595	Oct-10	145.81	432.10
19	596	Nov-10	129.64	515.97
20	597	Dec-10	129.06	636.83
21	598	Jan-11	128.11	566.82
22	599	Feb-11	120.66	416.64
23	600	Mar-11	156.76	516.59
24	601	Apr-11	176.16	373.18
25	602	May-11	206.00	166.77
26	603	Jun-11	217.17	169.03
27	604	Jul-11	246.66	7.33
28	605	Aug-11	245.10	7.03
29	606	Sep-11	232.76	40.14
30	607	Oct-11	231.79	438.18
31	608	Nov-11	207.27	577.01
32	609	Dec-11	200.06	489.40
33	610	Jan-12	184.70	557.75
34	611	Feb-12	168.71	370.97
35	612	Mar-12	186.96	257.68

36	613	Apr-12	190.68	113.29
37	614	May-12	211.34	9.06
38	615	Jun-12	213.75	58.64
39	616	Jul-12	231.78	10.07
40	617	Aug-12	239.89	8.93
41	618	Sep-12	224.34	31.95
42	619	Oct-12	223.58	306.62
43	620	Nov-12	204.09	390.05
44	621	Dec-12	197.82	558.69
45	622	Jan-13	184.69	473.47
46	623	Feb-13	164.12	408.94
47	624	Mar-13	193.01	383.96
48	625	Apr-13	197.08	104.91
49	626	May-13	218.87	76.36
50	627	Jun-13	223.08	52.64
51	628	Jul-13	242.71	7.88
52	629	Aug-13	249.06	0.27
53	630	Sep-13	233.27	60.61
		Sum:	7932.69	12071.77
		Percent Error:	$100\% \times \frac{ \text{output sum} - \text{observed sum} }{\text{observed sum}} =$	34.29%

Table A4: WARMF flow volume per month compared to observed flow volume per month at Los Baños Creek. Total volume and percent error were calculated.

Year	WARMF Volume (LBC) – 10 <sup>6</sup> ft <sup>3</sup>	Observed Volume (LBC) – 10 <sup>6</sup> ft <sup>3</sup>
2009	48.06	294.32
2010	938.42	978.08
2011	1079.89	881.60
2012	211.40	444.11
2013	221.17	409.50
2014	31.62	143.11
Sum:	2530.56	3150.73
Percent Error:	$100\% \times \frac{ \text{output sum} - \text{observed sum} }{\text{observed sum}} =$	19.68%

Table A5: WARMF flow volume per month compared to observed flow volume per month at Los Baños Creek. Total volume and percent error were calculated. Time periods of abnormally high flow were excluded.

Year	WARMF Volume (LBC) – 10 <sup>6</sup> ft <sup>3</sup>	Observed Volume (LBC) – 10 <sup>6</sup> ft <sup>3</sup>
2009	16.46	65.12
2010	938.42	978.08
2011	1079.89	881.60
2012	211.40	444.11
2013	221.17	409.50
2014	0.14	0.00
Sum:	2467.48	2778.42
Percent Error:	$100\% \times \frac{ \text{output sum} - \text{observed sum} }{\text{observed sum}} =$	11.19%

Table A6: WARMF flow volume per month compared to observed flow volume per month at Mud Slough, Fremont Canal, Hollow Tree Drain, S Lake. Total volume and percent error were calculated.

Year	WARMF Volume (Mud) – 10 <sup>9</sup> ft <sup>3</sup>	Observed Volume (Mud, Fremont, HT, S Lake) – 10 <sup>9</sup> ft <sup>3</sup>
2009	1.41	0.37
2010	3.84	1.28
2011	4.17	1.53
2012	2.70	1.09
2013	1.89	1.15
2014	0.33	0.34
Sum:	14.33	5.76
Percent Error:	$100\% \times \frac{ \text{output sum} - \text{observed sum} }{\text{observed sum}} =$	149.00%

Table A7: WARMF flow volume per month compared to corrected observed flow volume per month at Mud Slough, Fremont Canal, Hollow Tree Drain, S Lake. Observed flow was corrected to account for water bypassing monitoring stations. Total volume and percent error were calculated.

Year	WARMF Volume (Mud) – 10 <sup>9</sup> ft <sup>3</sup>	Corrected Observed Volume (Mud, Fremont, HT, S Lake) – 10 <sup>9</sup> ft <sup>3</sup>
2009	1.41	0.91
2010	3.84	3.15
2011	4.17	3.77
2012	2.70	2.67
2013	1.89	2.83
2014	0.33	0.83
Sum:	14.33	14.16
Percent Error:	$100\% \times \frac{ \text{output sum} - \text{observed sum} }{\text{observed sum}} =$	1.21%

Table A8: WARMF EC compared to corrected observed EC at Los Baños Creek. In order to allow for daily variations, total EC and percent error were calculated.

Year	WARMF EC (LBC) – 10 <sup>6</sup> μS/cm	Corrected Observed EC (LBC) – 10 <sup>6</sup> μS/cm
2009	0.24	0.27
2010	0.67	0.57
2011	0.75	0.49
2012	0.77	0.42
2013	0.81	0.48
2014	0.20	0.20
Sum:	3.43	2.44
Percent Error:	$100\% \times \frac{ \text{output sum} - \text{observed sum} }{\text{observed sum}} =$	
		40.90%

Table A9: WARMF EC compared to observed EC at Mud Slough. In order to allow for daily variations, total EC and percent error were calculated.

Year	WARMF EC (Mud) – 10 <sup>6</sup> μS/cm	Observed EC (Mud) – 10 <sup>6</sup> μS/cm
2009	0.54	0.38
2010	0.86	0.63
2011	1.44	0.55
2012	1.06	0.49
2013	1.06	0.55
2014	0.19	0.28
Sum:	5.15	2.89
Percent Error:	$100\% \times \frac{ \text{output sum} - \text{observed sum} }{\text{observed sum}} =$	
		78.47%

Table A10: WARMF (old version) flow volume per month compared to observed flow volume per month at Los Baños Creek. Total volume and percent error were calculated. The output is almost identical to the new model version output.

Year	WARMF Volume (LBC) – 10 <sup>6</sup> ft <sup>3</sup>	Observed Volume (LBC) – 10 <sup>6</sup> ft <sup>3</sup>
2009	49.92	294.32
2010	941.74	978.08
2011	1066.31	881.60
2012	227.05	444.11
2013	244.28	409.50
2014	34.91	143.11
Sum:	2564.20	3150.73
Percent Error:	100% ×  output sum – observed sum  ÷ observed sum = 18.62%	

Table A11: WARMF (old version) flow volume per month compared to observed flow volume per month at Mud Slough. Total volume and percent error were calculated. The percent error is higher than that produced by the newer version of the model (1.21%).

Year	WARMF Volume (Mud) – 10 <sup>9</sup> ft <sup>3</sup>	Corrected Observed Volume (Mud, Fremont, HT, S Lake) – 10 <sup>9</sup> ft <sup>3</sup>
2009	0.45	0.91
2010	1.27	3.15
2011	1.66	3.77
2012	0.66	2.67
2013	0.53	2.83
2014	0.12	0.83
Sum:	4.68	14.16
Percent Error:	100% ×  output sum – observed sum  ÷ observed sum = 66.93%	

# APPENDIX B

## Figures B1- B20

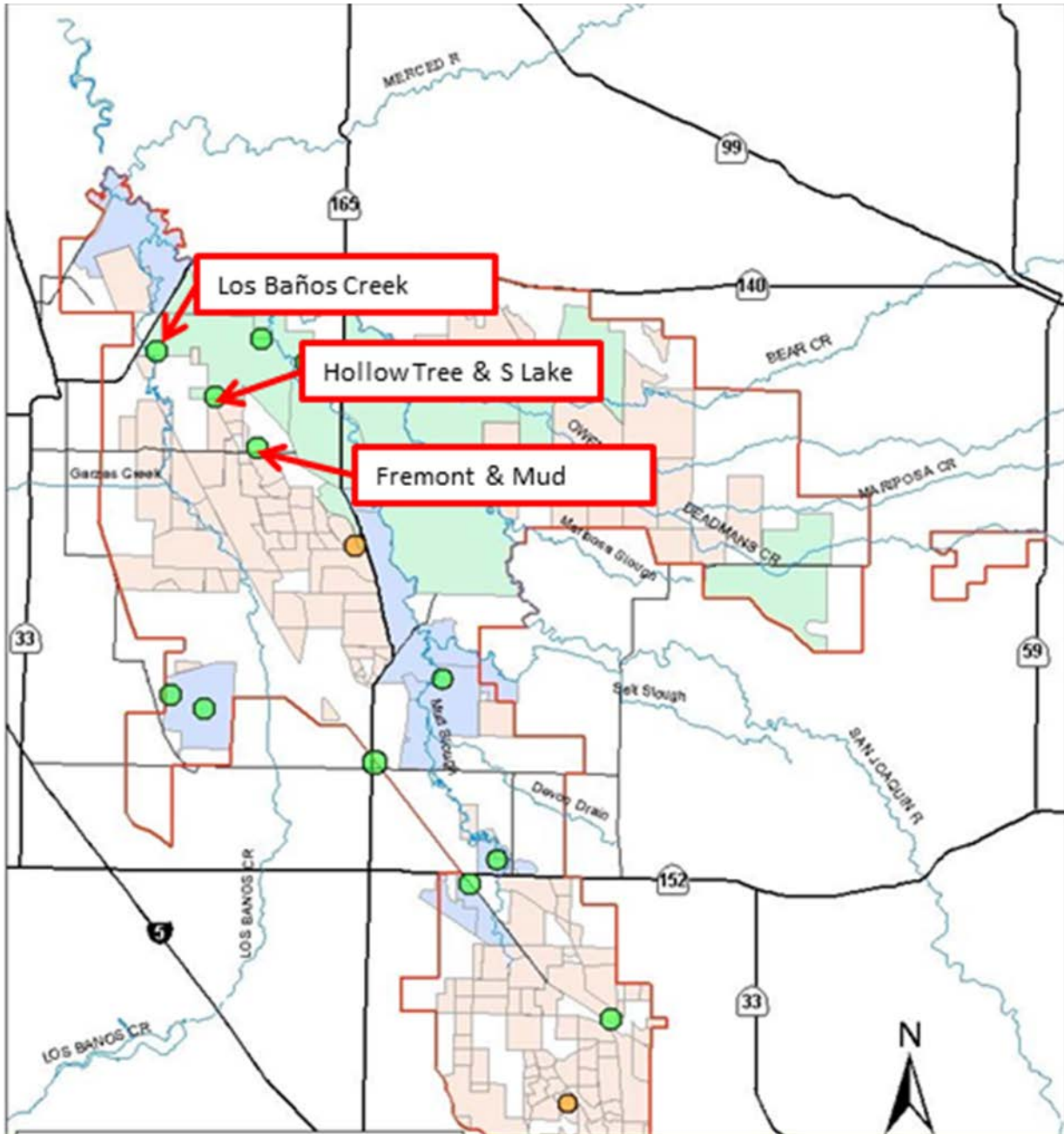


Figure B1: Stream monitoring stations. Stations record observed data, including flow and electrical conductivity.

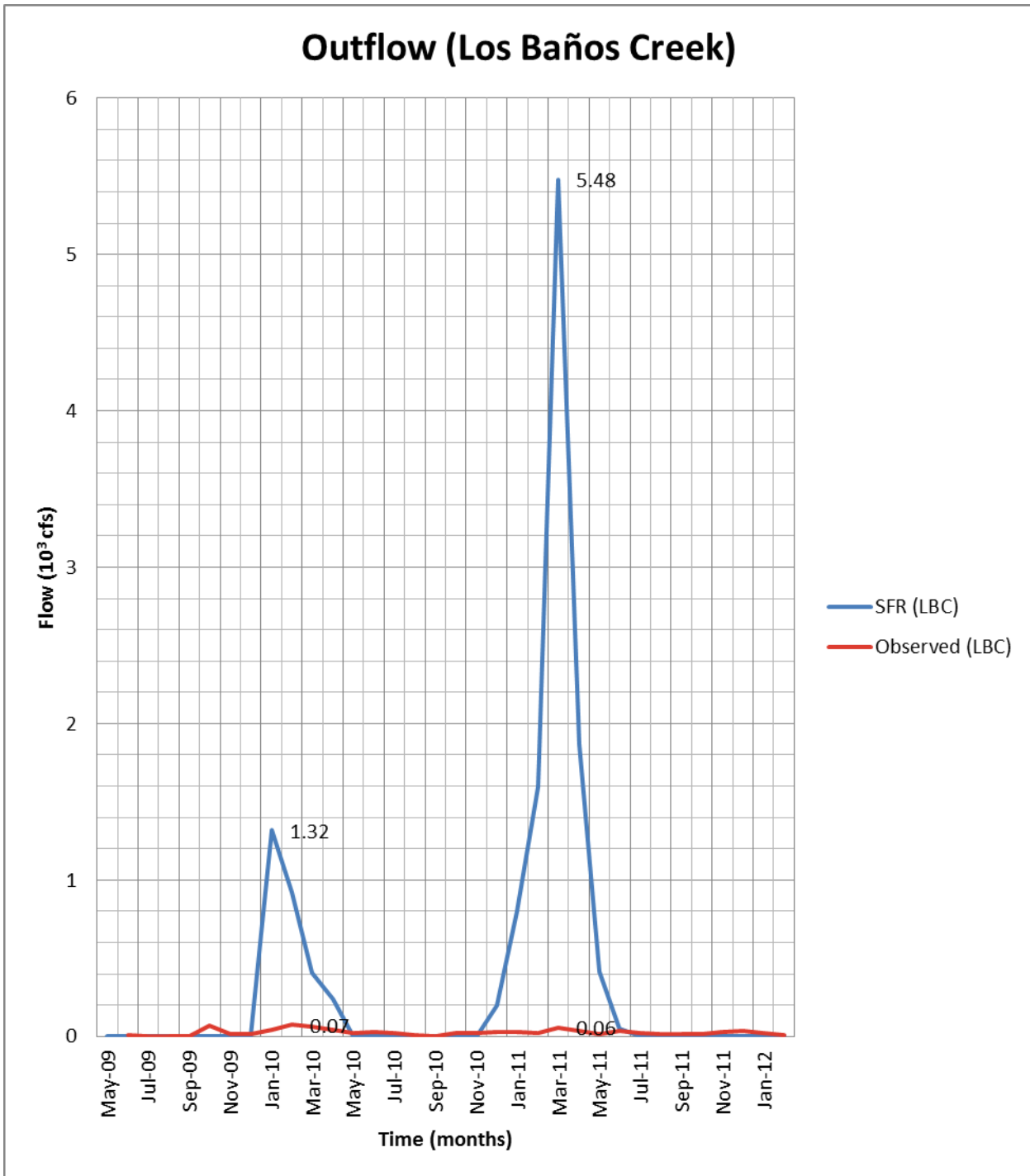


Figure B2: CVHM flow compared to observed flow at Los Baños Creek. During January 2010 and March 2011, simulated flow greatly exceeds observed flow.

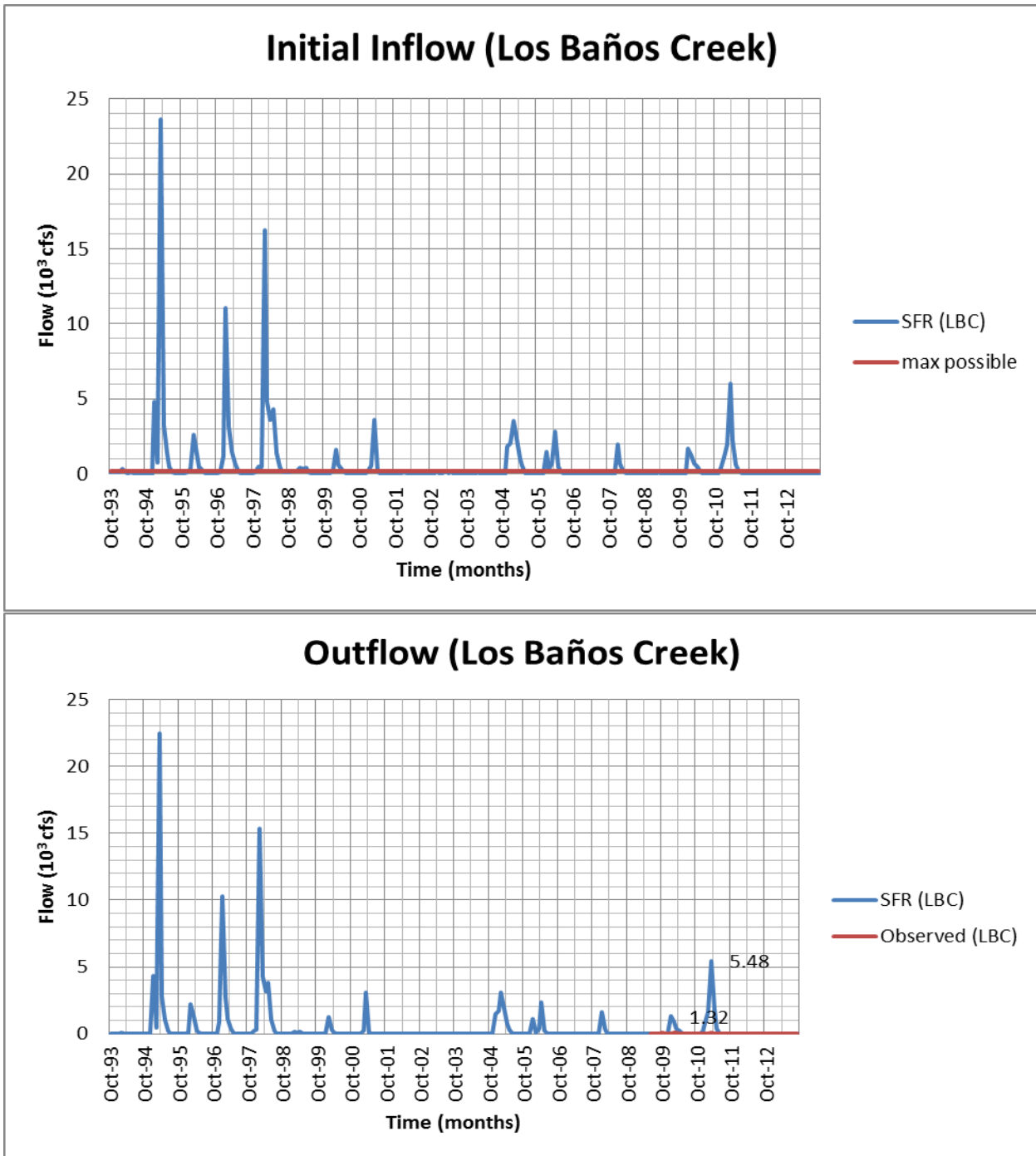


Figure B3: Simulated Initial Inflow into Los Baños Creek compared to maximum possible inflow, showing inflow used in simulation exceeded maximum possible inflow over a 20-year period (top). Simulated outflow from Los Baños Creek over the same 20-year period, showing a correlation between initial inflow input and simulated outflow (bottom).

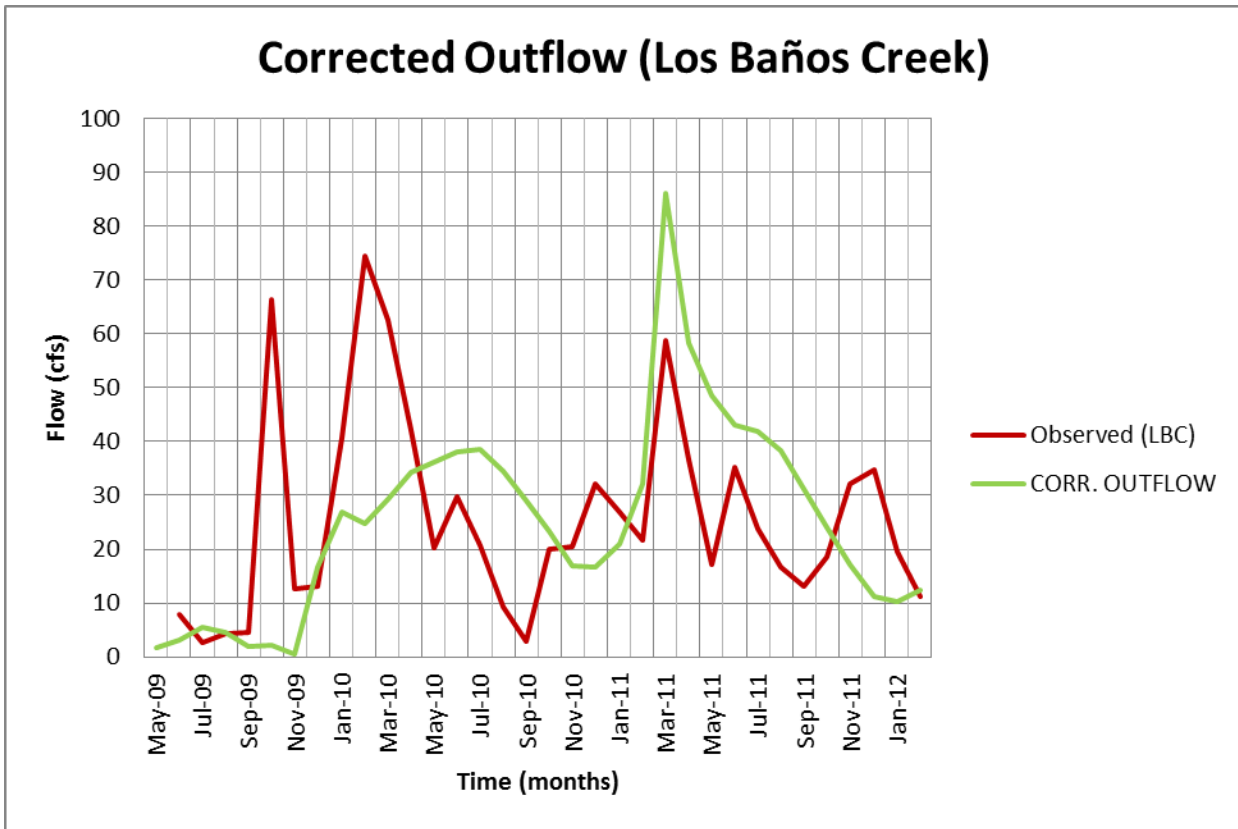


Figure B4: Corrected CVHM flow compared to observed flow at Los Baños Creek. Observed flow corresponds better to corrected CVHM flow than uncorrected CVHM flow. Drawdown occurs February – April each year when weirs are removed to allow unrestricted outflow in order to drain the wetlands.

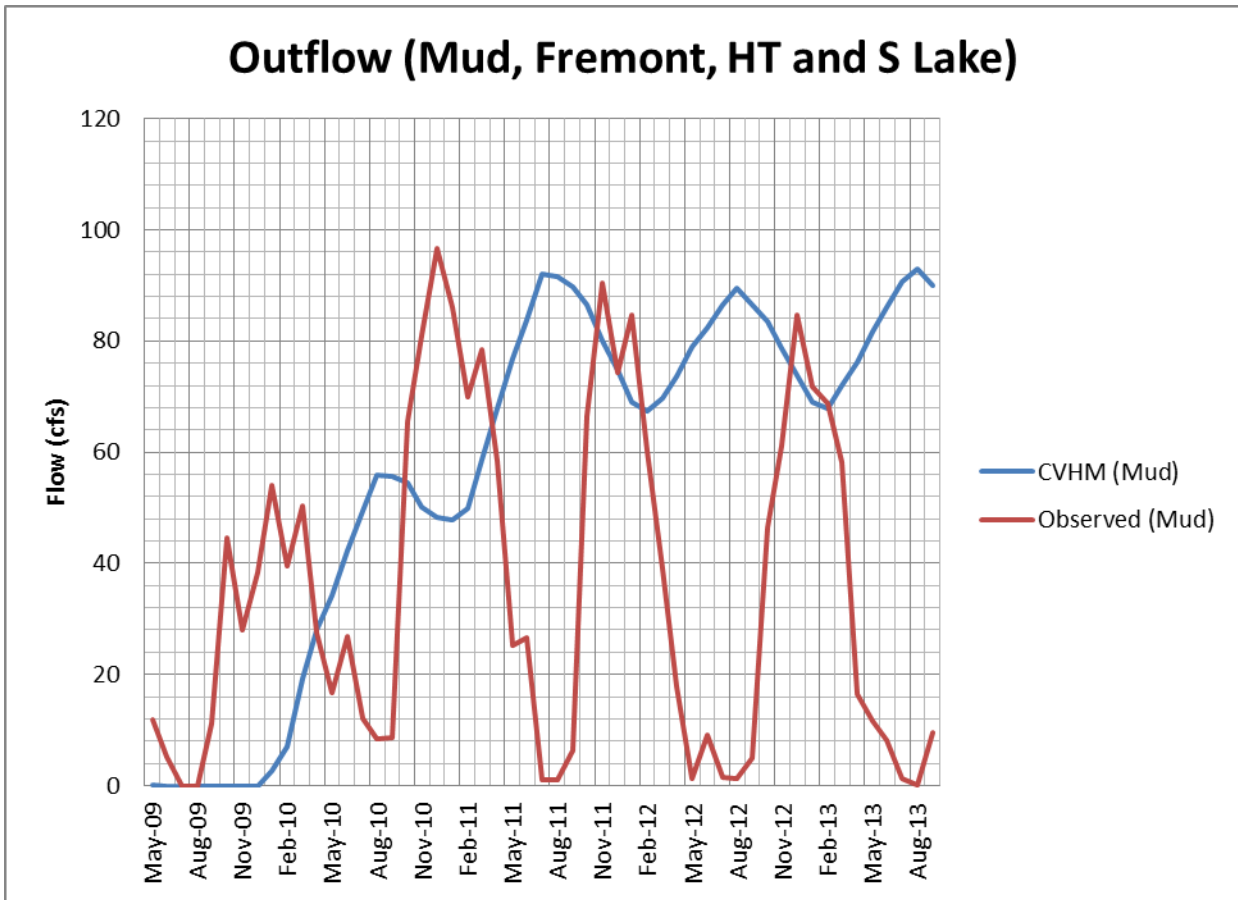


Figure B5: CVHM flow compared to observed flow at Mud Slough, Fremont Canal, Hollow Tree Drain, S Lake. The simulated outflow is out of phase with observed values.

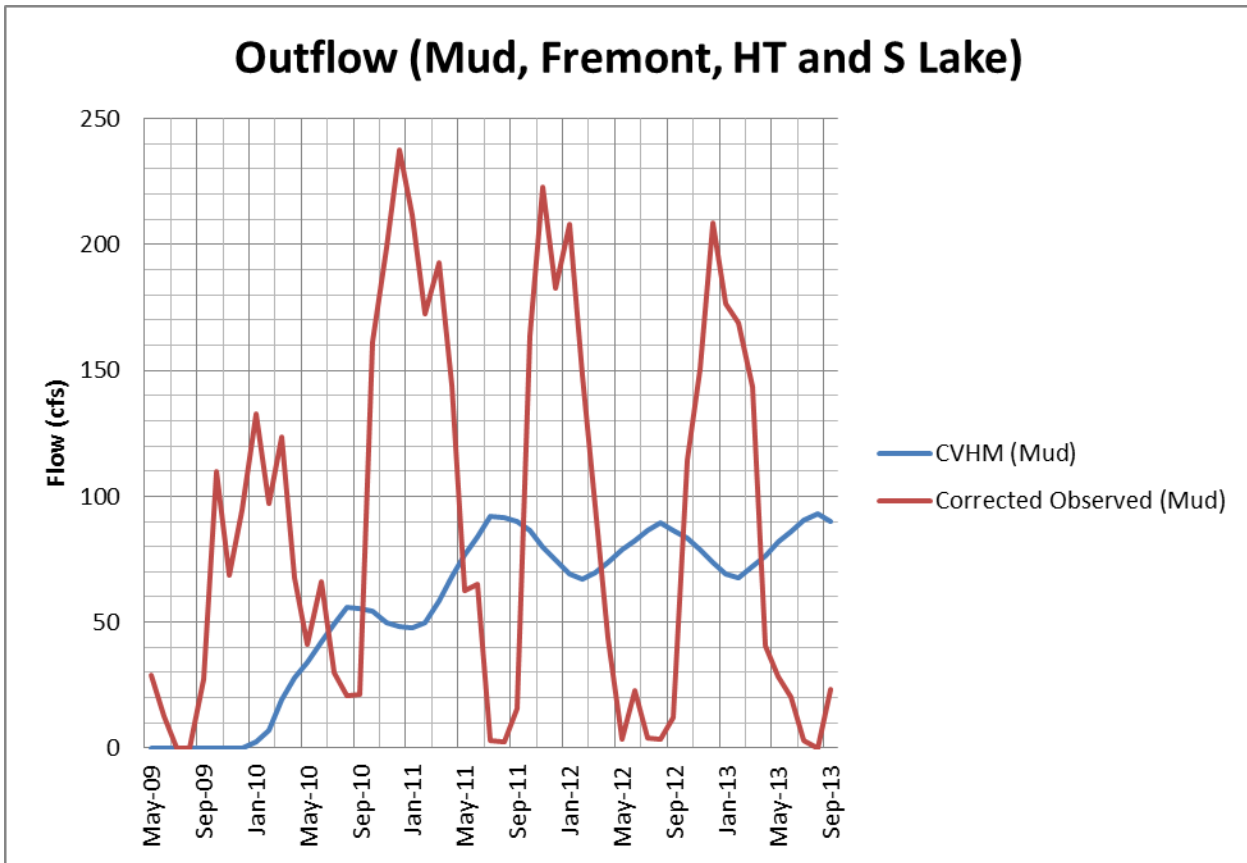


Figure B6: CVHM flow compared to corrected observed flow at Mud Slough, Fremont Canal, Hollow Tree Drain, S Lake. The simulated outflow is out of phase with observed values. When observed values are corrected to account for the discrepancy between actual flow and monitoring station observed flow, simulation values correlate to corrected observed values better than uncorrected observed values.

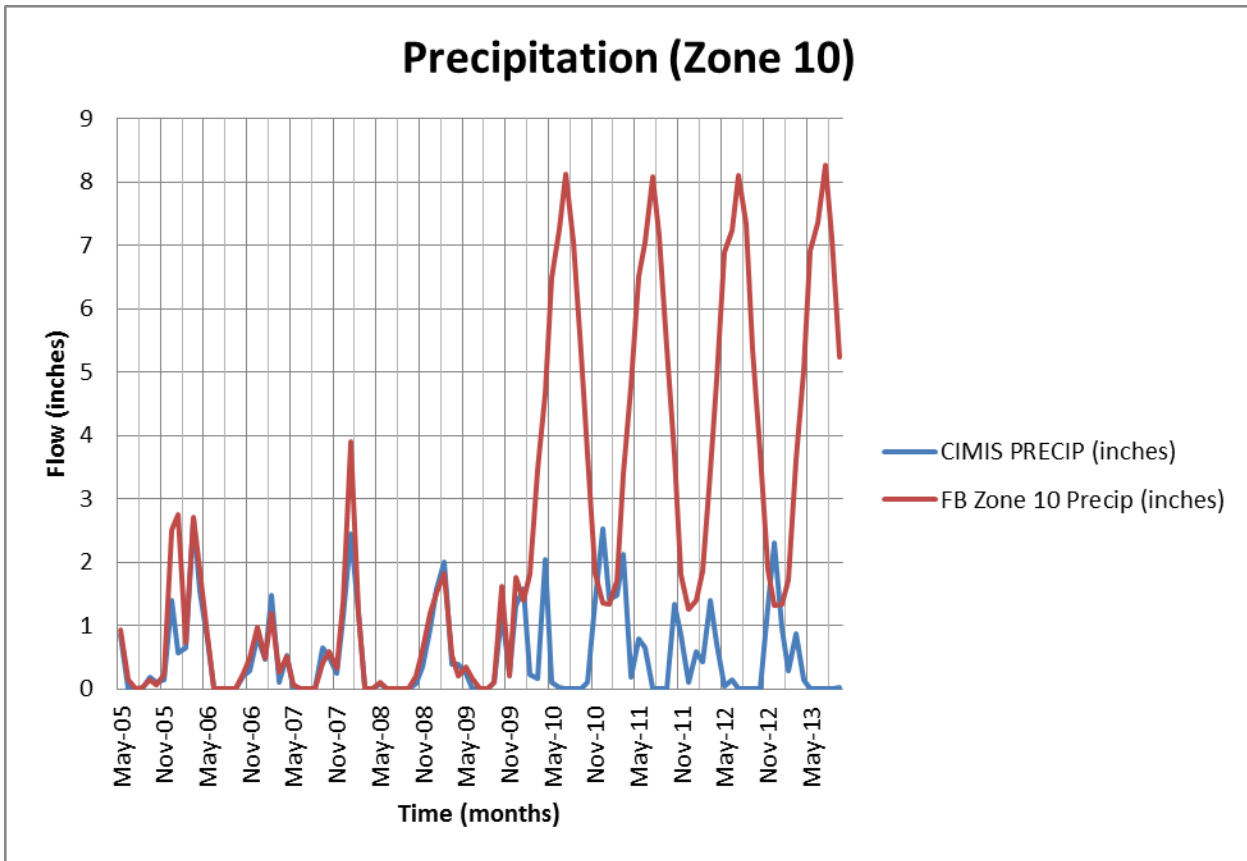


Figure B7: CVHM precipitation compared to observed precipitation in Grasslands Water District. Model input for precipitation is consistent with observed precipitation until month 57 (January 2010), at which point it does not correlate well with observed data. Model input maxima are more than 3 times observed maxima, and are out of phase with the observed data.

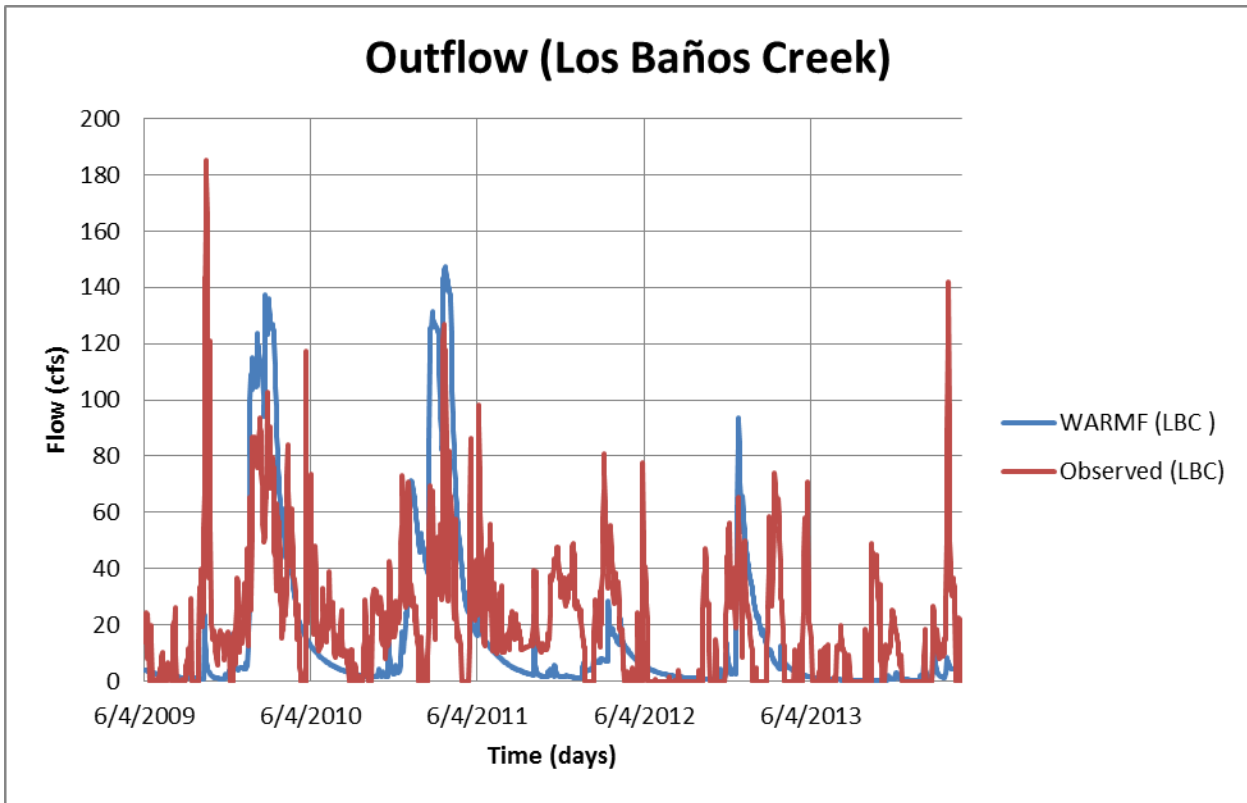


Figure B8: WARMF flow compared to observed flow at Los Baños Creek. The model does not accurately calculate flow during periods of high observed flow.

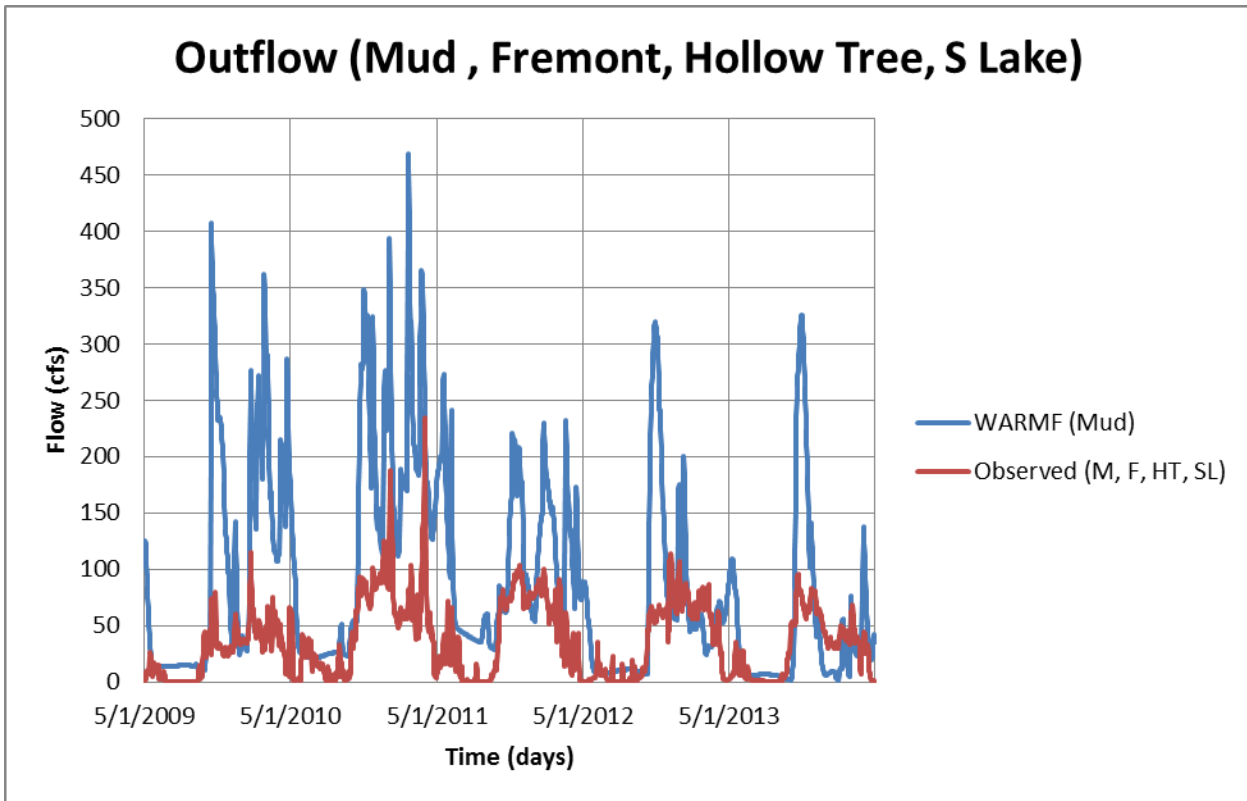


Figure B9: WARMF flow compared to observed flow at Mud Slough, Fremont Canal, Hollow Tree Drain, S Lake. The simulated flow is much larger than uncorrected observed flow.

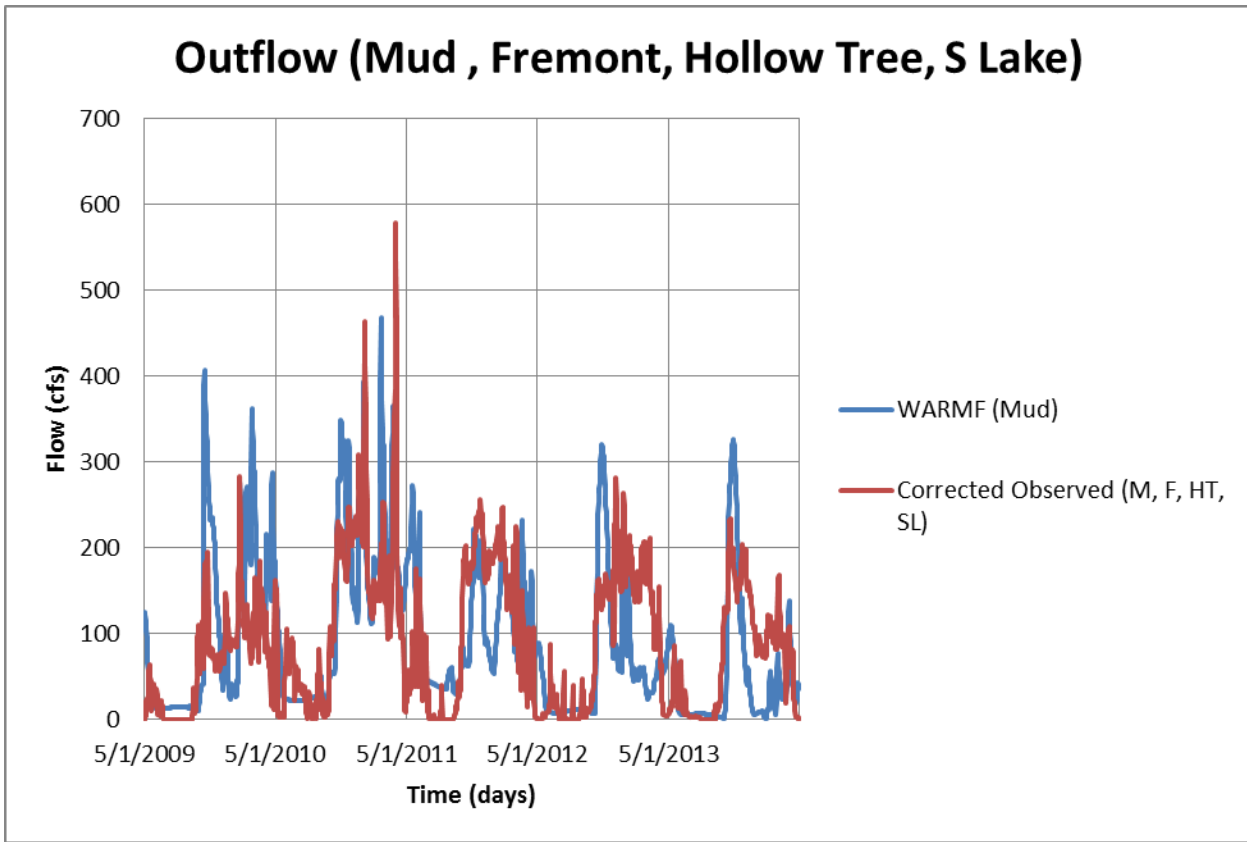


Figure B10: WARMF flow compared to corrected observed flow at Mud Slough, Fremont Canal, Hollow Tree Drain, S Lake. When observed values are corrected to account for the discrepancy between actual flow and monitoring station observed flow, simulation values correlate to corrected observed values better than uncorrected observed values.

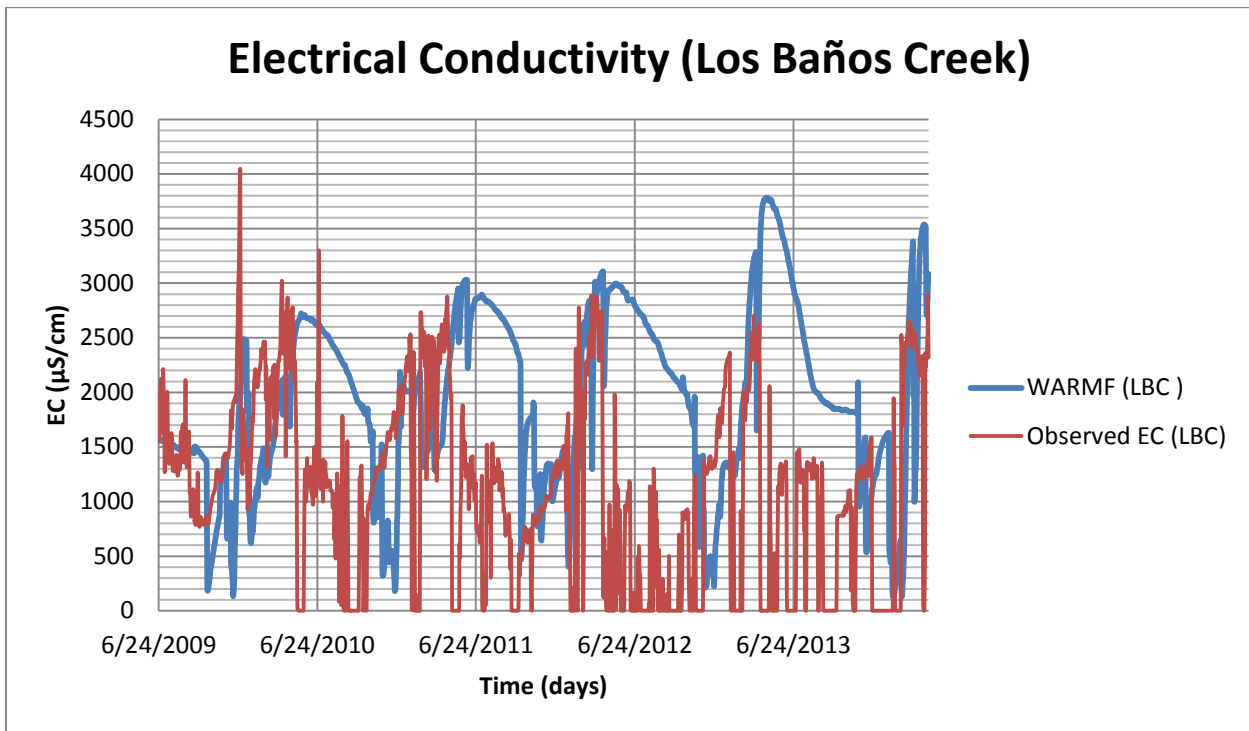


Figure B11: WARMF EC compared to observed EC at Los Baños Creek. Observed EC repeatedly reads zero, which is unrealistic since this indicates pure water.

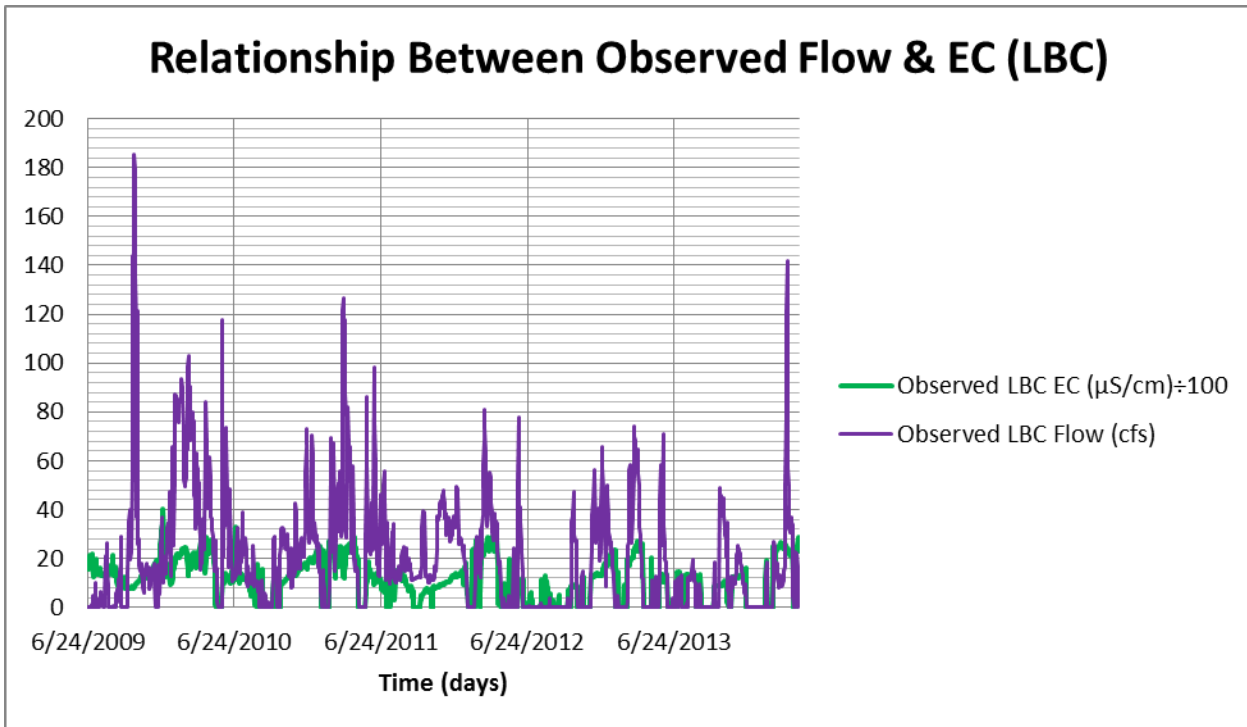


Figure B12: Observed flow compared to observed EC at Los Baños Creek. There is evident direct relationship between the two.

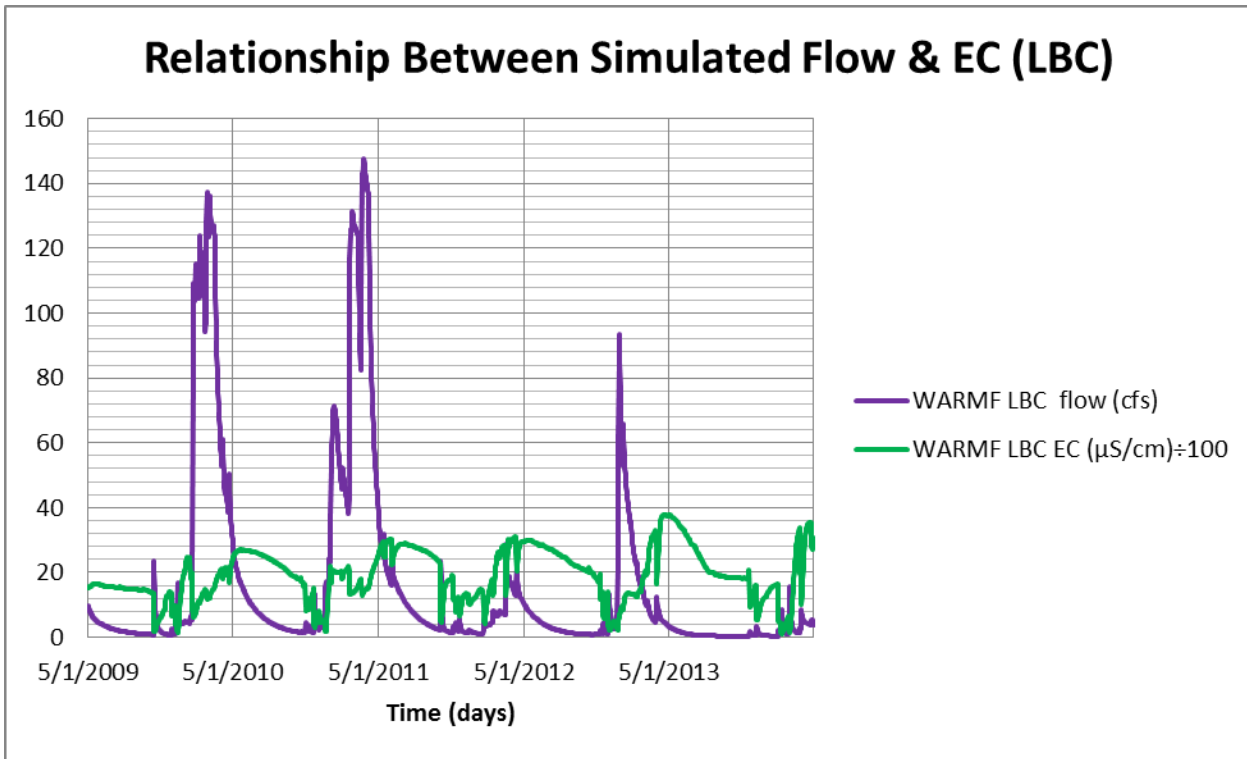


Figure B13: WARMF flow compared to WARMF EC at Los Baños Creek. There is a direct relationship between the two during the initial spike in flow. After the initial flow spike, it becomes an inverse relationship.

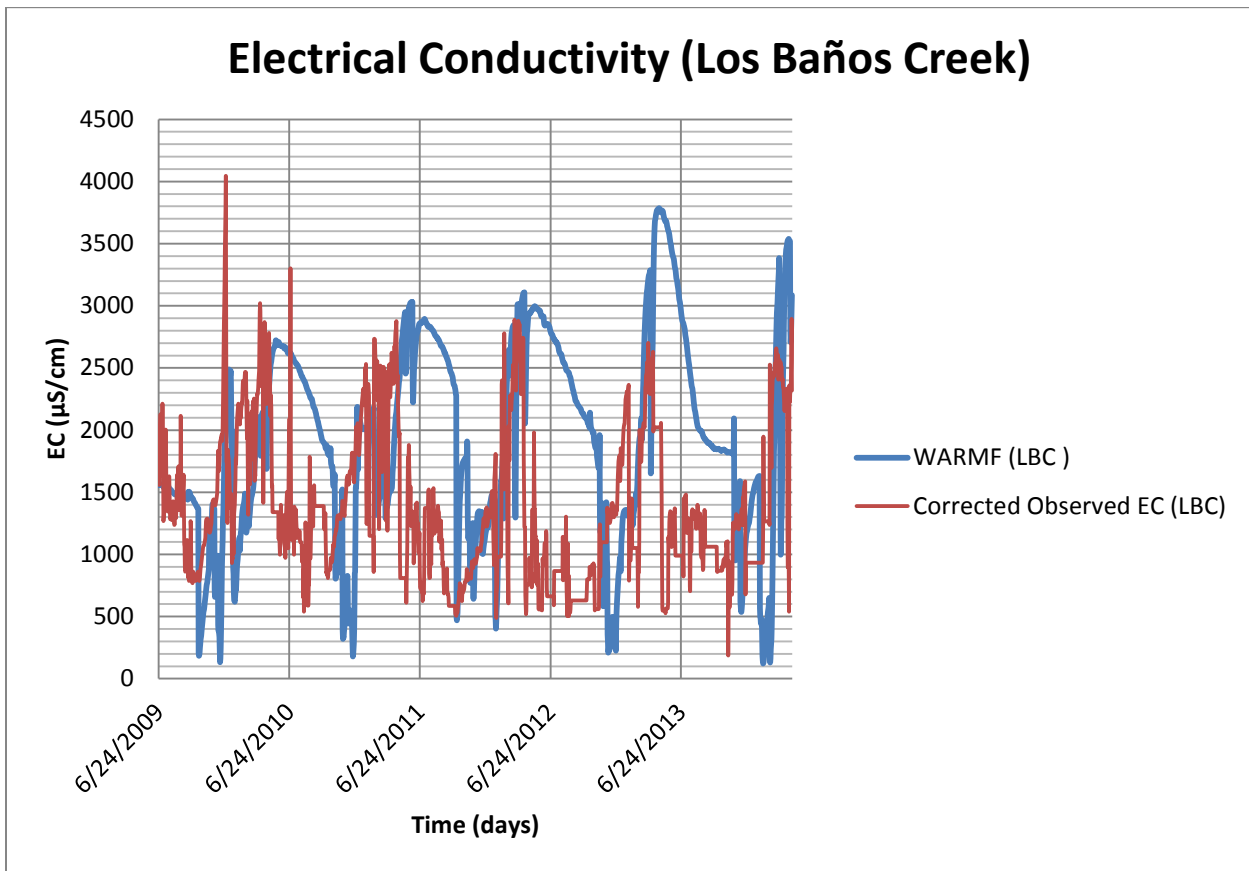


Figure B14: WARMF EC compared to corrected observed EC at Los Baños Creek. There is good correlation between the two during periods of initial EC increase, but an inverse relationship for the remainder of the time.

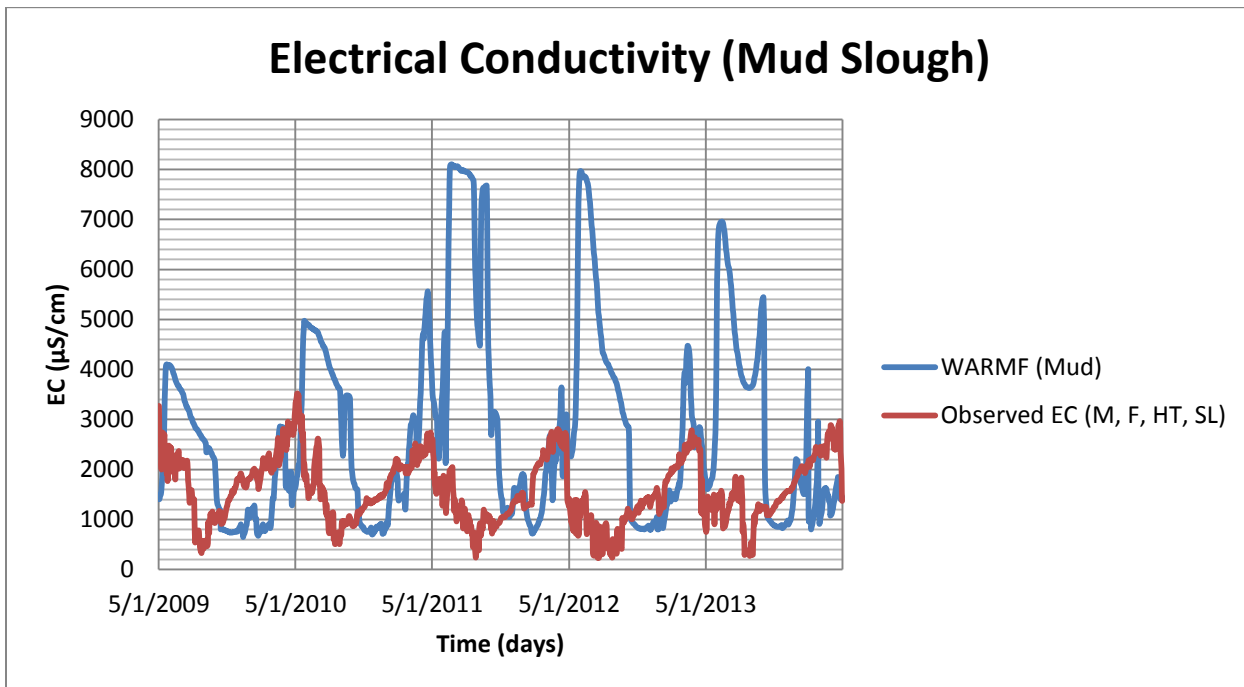


Figure B15: WARMF EC compared to observed EC at Mud Slough. There is correlation between the two during periods of initial EC increase, but an inverse relationship for the remainder of the time. The spike in EC may be due to a sudden large influx of highly concentrated saline fluid near the monitor.

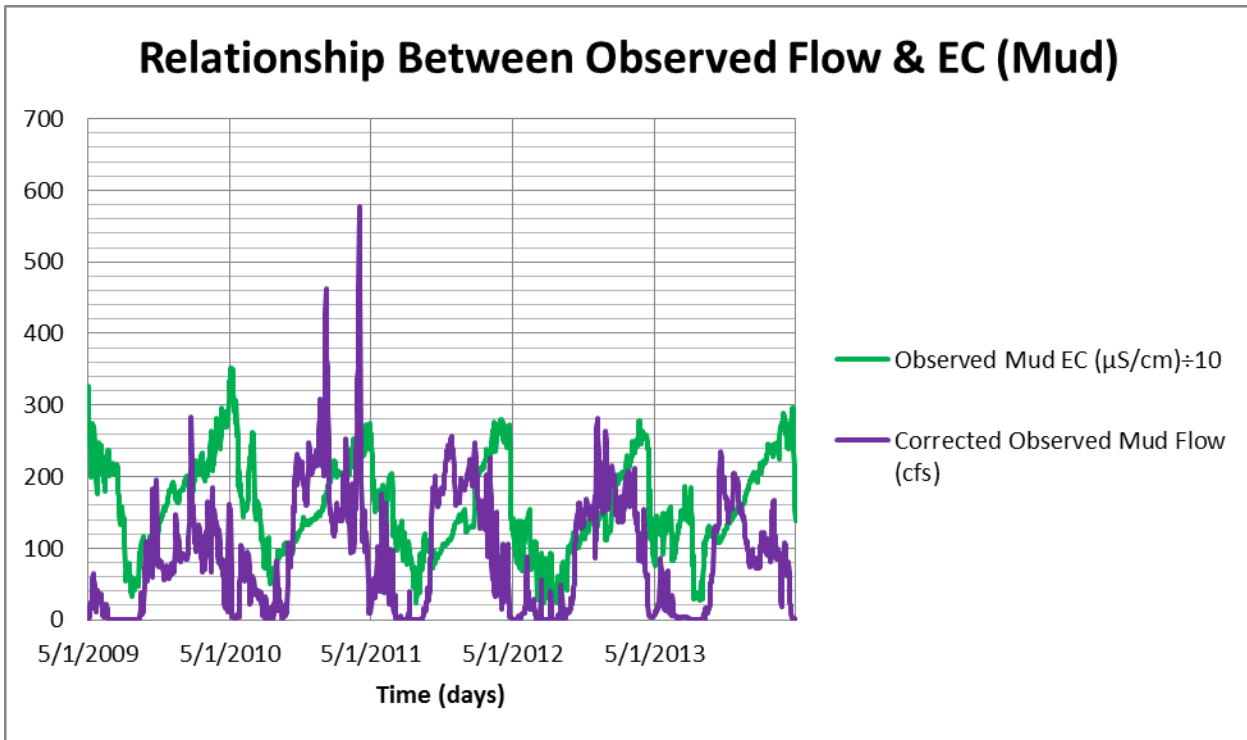


Figure B16: Observed flow compared to observed EC at Mud Slough. There is evident direct relationship between the two.

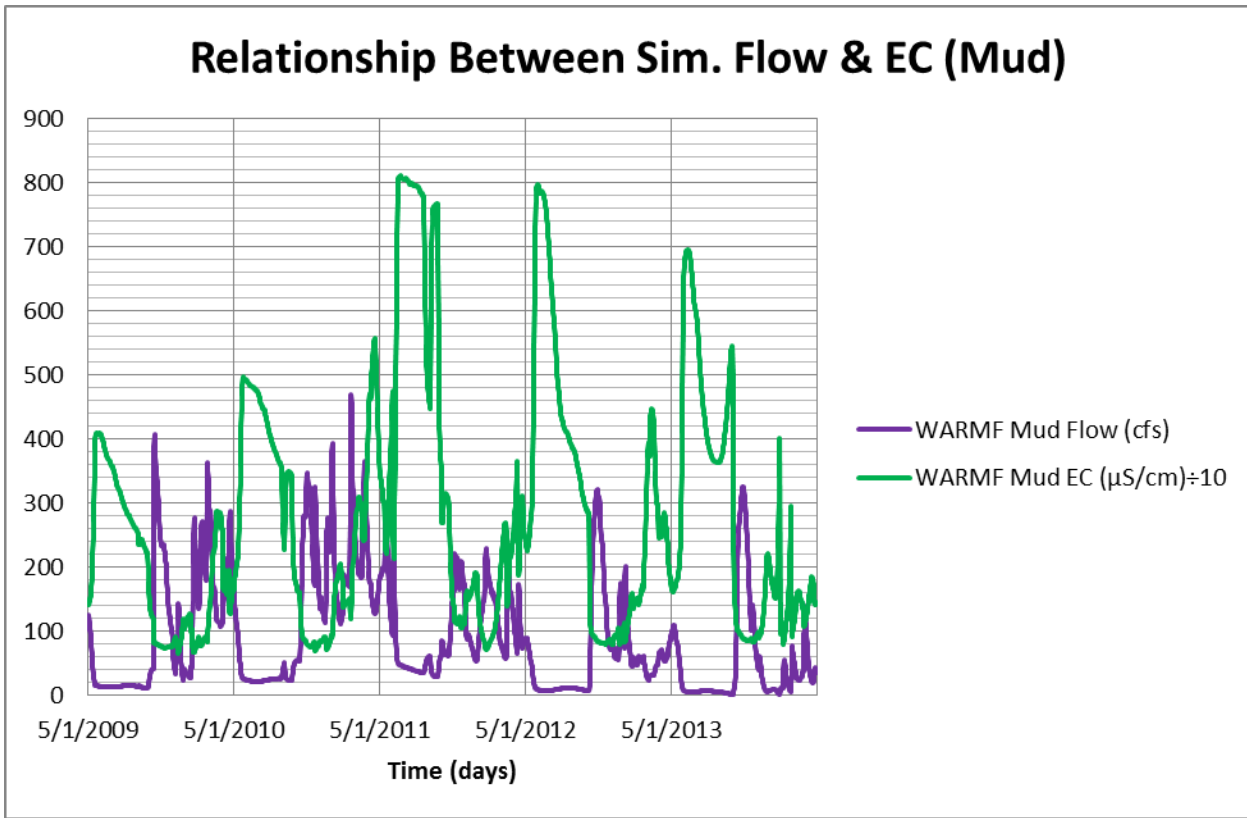


Figure B17: WARMF flow compared to WARMF EC at Mud Slough. There is a direct relationship between the two during the initial spike in flow, but it is less pronounced than in the Los Baños Creek simulation. After the initial flow spike, it becomes an inverse relationship.

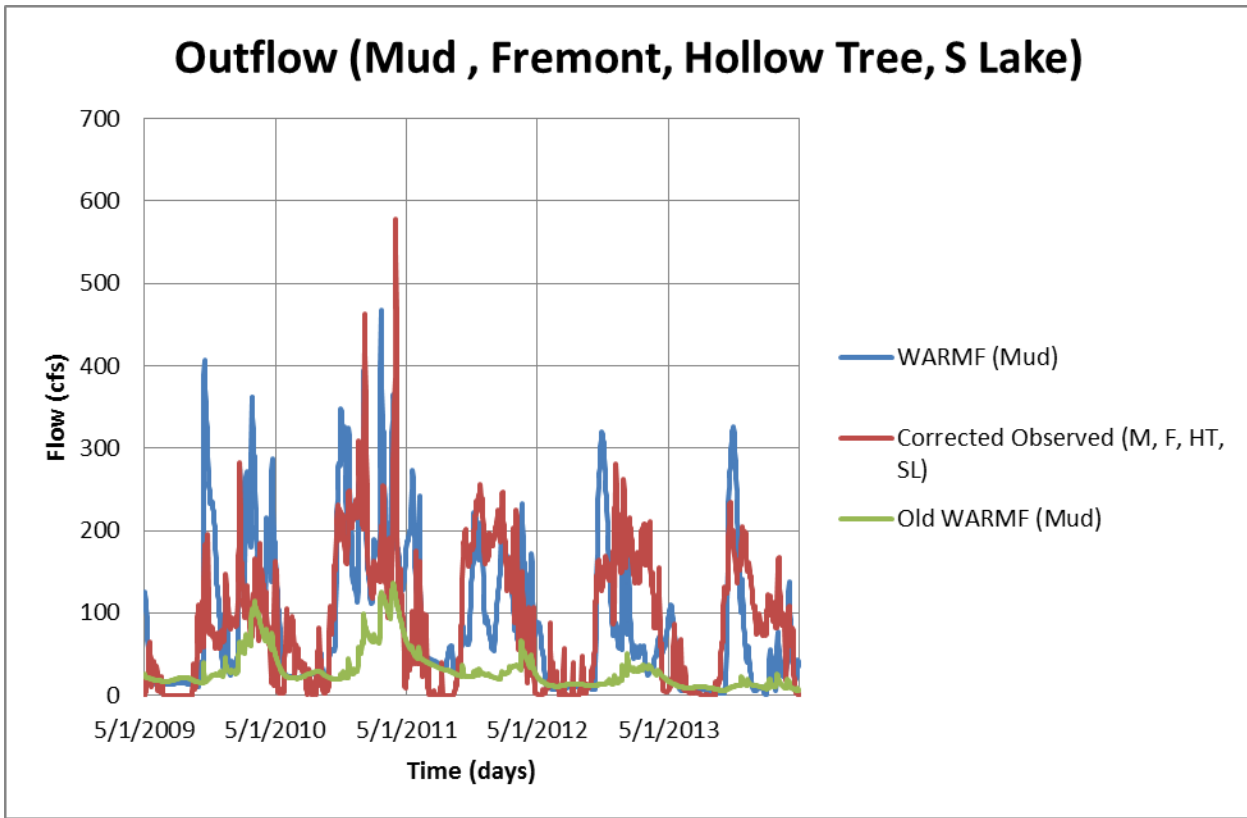


Figure B18: Old and new version WARMF flow compared to corrected observed flow at Mud Slough, Fremont Canal, Hollow Tree Drain, S Lake. Quantity and timing of new model version simulated flow correspond better to observed values than simulated flow from the older version of the model.

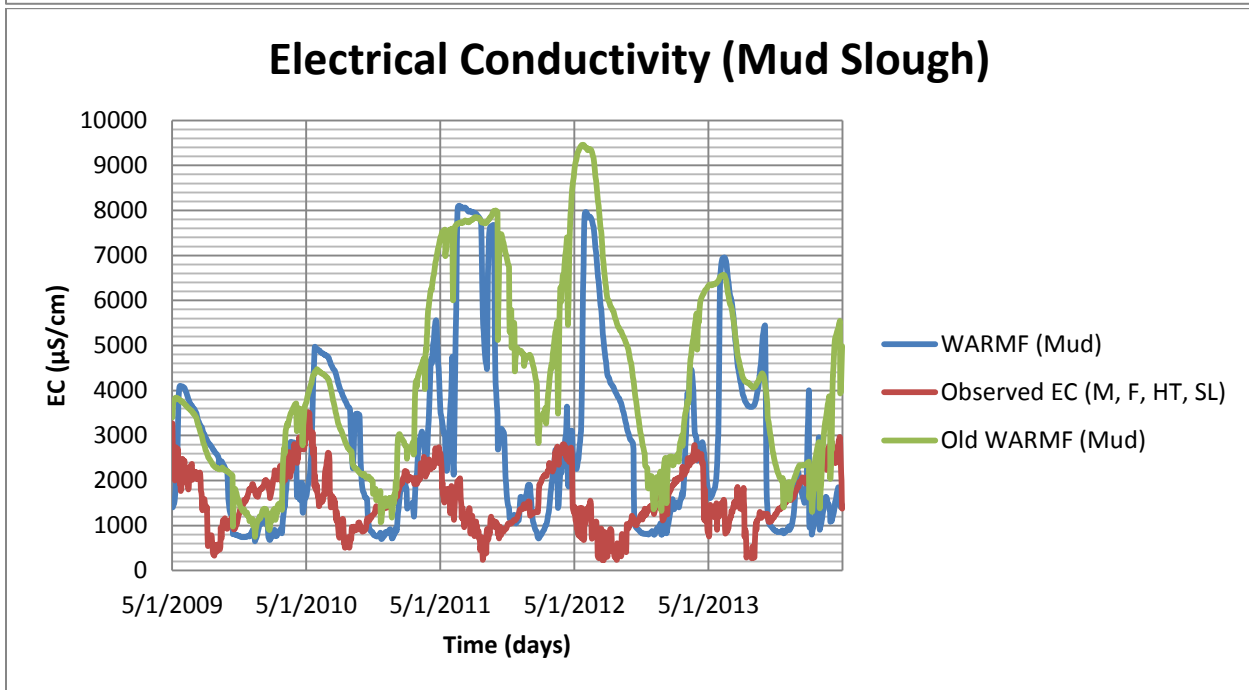
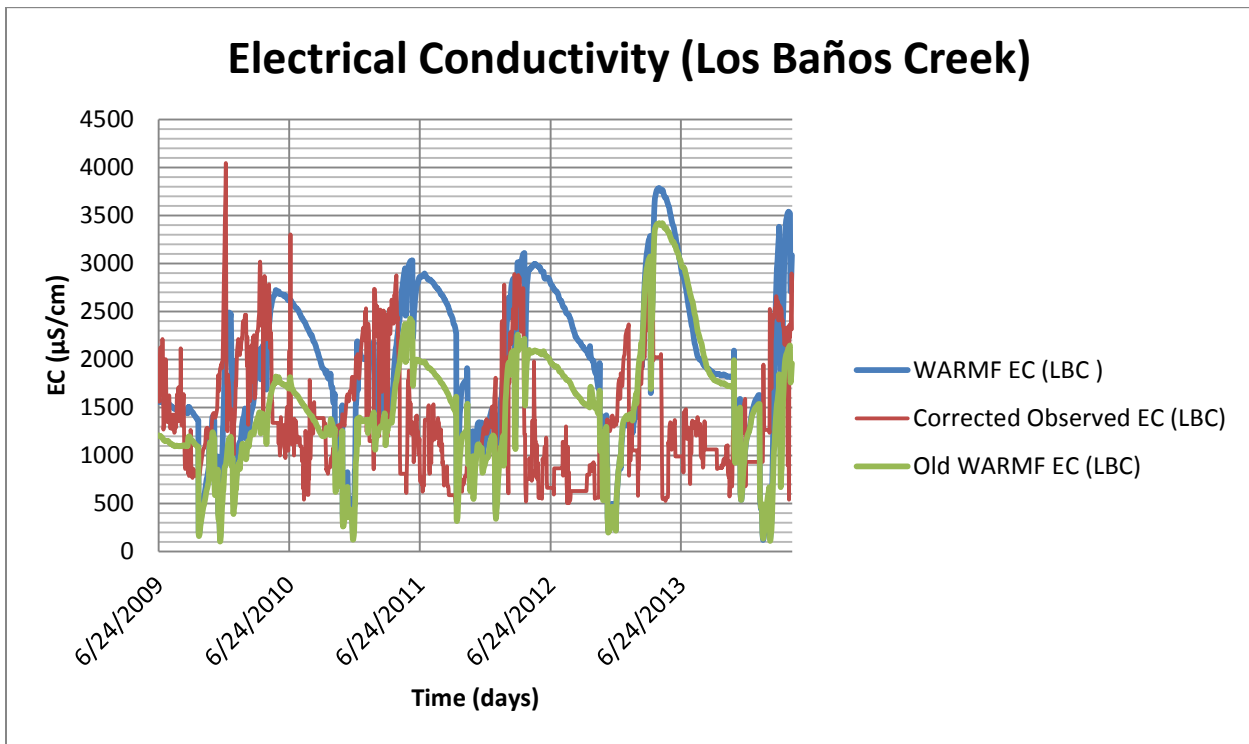


Figure B19: WARMF EC compared to observed EC at Los Baños Creek (top) and Mud Slough (bottom). The output from the older version of the WARMF model is similar to the output from the newer version, and neither version’s output correlates well to observed values.

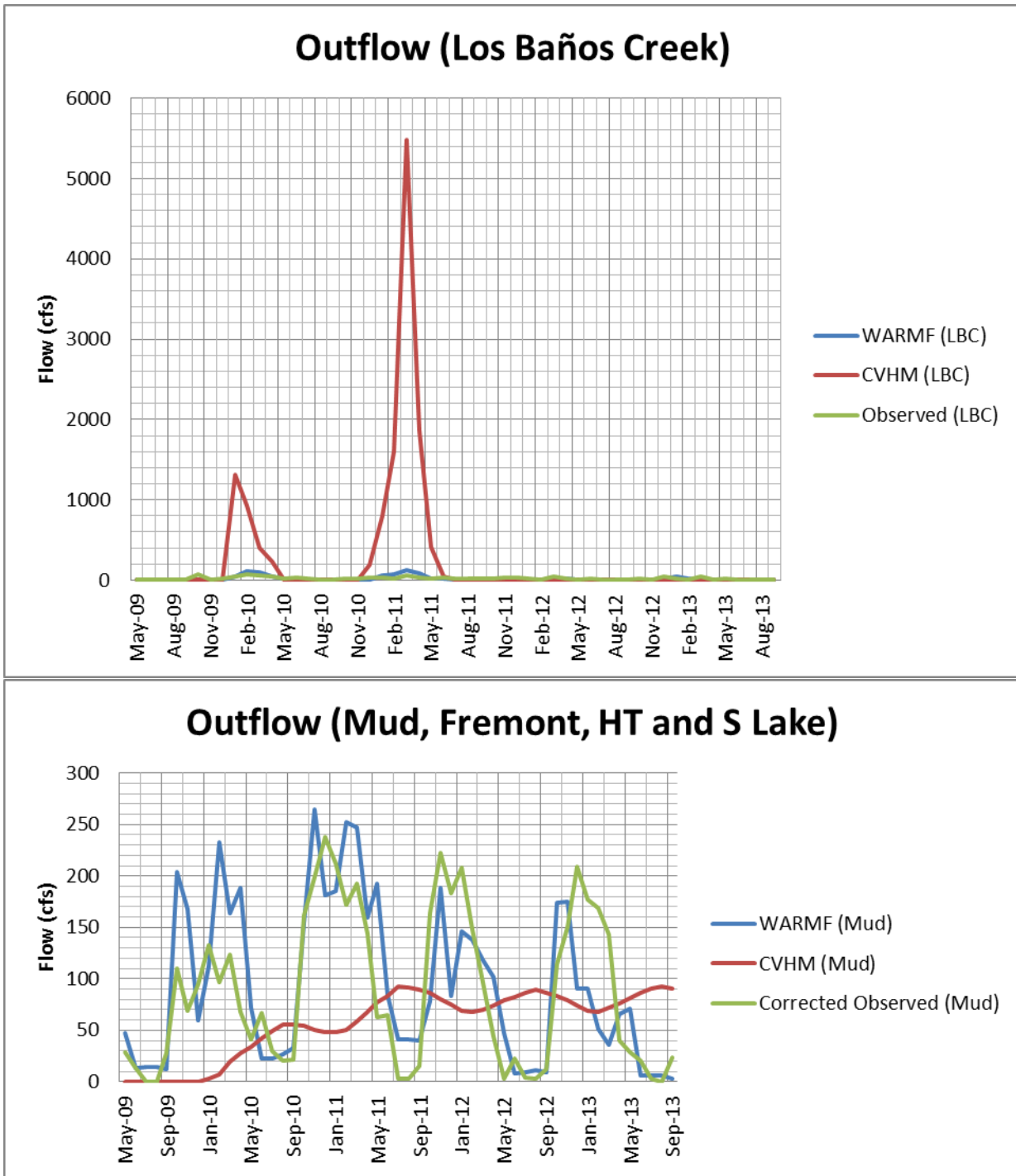


Figure B20: CVHM flow and WARMF flow compared to observed flow in Los Baños Creek (top) and Mud Slough (bottom). In both cases, the WARMF simulated flow correlates better to observed values.

